



NTNU – Trondheim
Norwegian University of
Science and Technology

Engineering geological evaluation of the applicability of Drill & Split in tunnels at the Follo line project

Jens Anders Brenne Volden

Geotechnology

Submission date: June 2015

Supervisor: Bjørn Nilsen, IGB

Co-supervisor: Lise Backer, Jernbaneverket

Norwegian University of Science and Technology
Department of Geology and Mineral Resources Engineering



MASTEROPPGAVEN

Kandidatens navn: Jens Anders Volden

Oppgavens tittel: Ingeniørgeologisk vurdering av anvendbarheten for «Drill & Split» i tunneler på Follobanen

English title: Engineering geological evaluation of the applicability of «Drill & Split» in tunnels at the Follo Line project

Utfyllende tekst:

1.

Mechanical excavation based on the “Drill & Split” method is planned to be used for tunnels at the Follo line project close to existing underground structures. In December 2014 this MSc-candidate completed his project assignment comprising a general assessment of possibilities and limitations for “Drill & Split” and other non-explosive excavation methods. This master thesis represents a following-up of the project assignment with more detailed study of the applicability of Drill & Split for the relevant sections of tunnels in Follo line. Key issues of this thesis work include:

- On site inspection for supplementary engineering geological mapping and collecting rock samples.
- Laboratory testing of rock properties, including input parameters for numerical analysis.
- Numerical analysis using Phase2, with special emphasis on the analysis of fracture development and propagation from splitting of different rock qualities.
- Evaluation and discussion of Drill & Split at the Follo line project (with respect to borehole spacing, distance to the free face, design of free face, etc.).
- Overall evaluation and discussion of Drill & Split method applicability in sections where the method is planned to be used at the Follo line project

2.

The study is to be conducted in collaboration with the Norwegian National Rail Administration (Jernbaneverket), with Construction Manager Lise Backer as primary contact person and Project manager Adler Enoksen as a cooperation partner.

Studieretning: Ingeniør- og miljøgeologi

Hovedprofil: Ingeniørgeologi og bergmekanikk

Tidsrom: 14.01.-10.06.2015

Bjørn Nilsen, Professor/hovedveileder

Abstract

As a part of major upgrading of regional railway lines around Oslo, The Follo line project comprises the construction of new twin-tube tunnels connecting Oslo central city to the new Ski mass transit station. Due to the tunnel alignments' close proximity to existing underground structures, vibrations limits is set upon parts of the tunnel excavation work. Consequently, The Norwegian National Rail Administration has suggested mechanical excavation by "Drill & Split" as their preferred excavation method for subjected sections.

Q-values assessed by the author suggests that the rock mass quality ranges from 13-40, which is classified as good quality rock. Laboratory testing of intact rock enhances the impression of good quality rock, as it presents high compressive strength. The measurements undergone corresponds well with previous assessments, and are therefore assumed to reflect the rock masses for most part of the area subjected to "Drill & Split" reasonably well.

The main scope of this study is to analyze the applicability of D&S under the assessed geological situation in finite element code *Phase*². This excavation method was modelled by applying staged loading that were ranging from 10-50 MPa inside the borehole at the tunnel face. When splitting against a free face, this was found to replicate the initial splitting process reasonably well. With this basic configuration set up, it was possible to model the influence of various aspects such as individual and accumulated rock parameter and assess different stress field situations by varying input parameters in *Phase*². Their respective influence were evaluated in terms of easiness of yielding.

The results from this study suggests that lowering the *GSI*-parameter has the most impact upon easiness of splitting, while the elastic properties of the rock mass (ν and *E-modulus*) has no practical influence. The intact *UCS* has also a noticeable influence and Hoek-Brown parameter *mi* has a slight influence. In general terms, easiness of splitting is dependent of the overall rock quality in such a manner that stronger and more massive rock mass is considered harder to split. The stress analysis suggests that easiness of splitting may benefit greatly from altering the free face design according to the in-situ stress field in such a manner that the most anisotropic stress state is induced. This creates de-tensioned zones around the periphery of the free face that can be exploit for easier splitting at the tunnel face. Based on numerical analysis and assumptions, the author considers the method as the best choice available under the given conditions at the Follo line project.

Sammendrag

Som et ledd av arbeidet med å oppgradere regionale jernbanelinjer omkring Oslo omhandler Follobanen utbygging av nye to-løps tunneler som forbinder Oslo sentralstasjon til nye Ski kollektivtrafikkstasjon. På grunn av de prosjekterte tunnelforløpene nærhet til eksisterende underjordkonstruksjoner er det satt vibrasjonsbegrensinger for tunneldrivingen på enkelte deler av traseene. Jernbaneverket har tatt konsekvensene av dette ved å introdusere mekanisk driving ved hjelp av metoden "Drill & Split" som deres foretrukne drivemetode for de utsatte strekningene.

Basert på forfatterens vurderinger er de lokale Q -verdiene estimert mellom 13-40, noe som kvalifiserer til bra bergkvalitet. Laboratorieundersøkelser av intakte bergartsprøver forsterker inntrykket av bra bergkvalitet, med gjennomgående høye målinger av bergartens trykkfasthet. Sammenlignet med tidligere undersøkelser av eksterne aktører samsvarer forfatterens målinger generelt godt. Det er derfor antatt at gjennomførte tester og vurderinger reflekterer faktiske forhold godt.

Hovedfokuset til oppgaven går ut på å utføre numeriske analyser av anvendelsen av D&S under de anslåtte geologiske forholdene i endelig-elementkode *Phase²*. Drivemetoden er modellert ved å pålaste stegvis økende, ekspanderende last fra 10-50 MPa radielt inne i utborede borehull i tunnelprofilet. Ved å splitte opp mot en fri flate ble det funnet at den modellerte situasjonen gjenspeiler den første fasen av splitteprosessen rimelig godt. Ved å ha denne grunnleggende konfigurasjonen på plass var det mulig å foreta sensitivitetsanalyser av ulike bergartsparametere og spenningsforhold for å undersøke deres innflytelse på splitteprosessen. Innflytelsen ble vurdert ut ifra antallet elementer som gikk i brudd.

Resultatene fra studien tyder på at lavere GSI verdi gir lettere splitting, mens bergartens elastiske egenskaper (ν og E -modul) har ingen praktisk innflytelse. Bergartens trykkfasthet (UCS) har også en merkbar innflytelse, mens Hoek-Brown parameteren mi har noe innflytelse. På generelt grunnlag oppnås det dårligere splitteresultat ved bedre bergkvaliteter. Spenningsanalyser tyder på at splitteprosessen kan tjene mye på en gjennomtenkt utforming av fri flate i forhold til in-situ spenningsfelt. Størst gevinst oppnås ved å utforme den frie flaten på en slik måte at en mest mulig anisotrop spenningstilstand induseres. Dette skaper avspente soner langs periferien av den frie flaten som kan utnyttes videre i splitteprosessen. Basert på numeriske analyser og antakelser under de gjeldende forhold vurderes metoden som mest velegnet blant alternativene for bruk på Follobanen.

Preface

This master thesis called “*Engineering geological evaluation of the applicability of “Drill & Split” in tunnels at the Follo line project*” is conducted at the Department of Geology and Mineral Resources Engineering at Norwegian University of Science and Technology (NTNU). The thesis was written in the spring of 2015, and completes a 5-year Master of Science program within Engineering Geology and Rock Mechanics at NTNU.

I would like to express my gratitude to my supervisor, Professor Bjørn Nilsen at NTNU for lending his professional expertise in times of need. Your excellent guidance and our productive discussions are greatly appreciated. I would also thank construction manager Lise Backer and other employees at the Norwegian National Rail Administration for their insight into the Follo line project and for supplying background material. Without their insight and productive discussions, this thesis would be a lot shorter.

Jens Anders Volden

NTNU, Trondheim

June 2015

Table of contents

ABSTRACT	I
SAMMENDRAG	III
PREFACE	V
TABLE OF CONTENTS	VII
LIST OF ABBREVIATIONS	IX
1 INTRODUCTION	1
1.1 BACKGROUND FOR THESIS	1
1.2 AIM OF STUDY	1
1.3 STRUCTURE AND METHODOLOGY OF THE STUDY	2
1.4 LIMITATIONS	3
2 FOLLO LINE PROJECT	5
2.1 GENERAL INFORMATION	5
2.2 NEARBY STRUCTURES	7
2.2.1 ALNA RIVER TUNNEL	7
2.2.2 EKEBERG OIL STORAGE	8
2.2.3 EKEBERG ROAD TUNNELS AND GRØNLIA TUNNEL	9
3 GEOLOGICAL CONDITIONS	11
3.1 BEDROCK	11
3.1.1 MINERALOGY	13
3.1.2 INTACT ROCK STRENGTH	14
3.2 DISCONTINUITIES	15
3.2.1 JOINTS	16
3.2.2 WEAKNESS ZONES	17
3.3 IN-SITU STRESS	19
3.4 ROCK MASS QUALITY	22
4 DRILL AND SPLIT	25
4.1 PRINCIPLE	26
4.2 METHOD	27
4.2.1 WEDGE SPLITTER	27
4.2.2 PISTON SPLITTER	29
4.3 BOREHOLE CONFIGURATION	30
4.3.1 BOREHOLE DRILLING	30
4.3.2 FREE FACE	31
4.4 EXPERIENCE WITH THIS METHOD	33
4.4.1 EVACUATION TUNNEL FOR EXISTING HIGHWAY TUNNEL	33
4.4.2 KAMINIKO TUNNEL	35
4.5 PRELIMINARY CONCLUSION FROM PROJECT WORK	36
5 FIELD MAPPING	37
5.1 CLASSIFICATION SYSTEMS	38
5.1.1 Q-METHOD	38
5.1.2 GSI – GEOLOGICAL STRENGTH INDEX	39
5.2 RESULTS	41
5.3 EVALUATION OF RESULTS FROM FIELD MAPPING	43

6	LABORATORY TESTING	45
6.1	ROCK SAMPLE	46
6.2	SAMPLE PREPARATION	48
6.3	TEST PROCEDURE	51
6.3.1	POISSON'S RATIO	51
6.3.2	E-MODULUS	52
6.3.3	OTHER PARAMETERS AND FEATURES	52
6.4	RESULTS	53
6.5	EVALUATION OF RESULTS FROM LABORATORY TESTING	54
7	NUMERICAL ANALYSIS	55
7.1	GENERAL	56
7.1.1	<i>PHASE</i> ² CODE	57
7.1.2	FAILURE CRITERION	57
7.2	ANALYSIS ASSUMPTIONS	59
7.2.1	ROCK PROPERTIES	59
7.2.2	RESIDUAL ROCK PARAMETERS	60
7.2.3	SPLITTING PROCESS	62
7.3	FREE FACE DESIGN	63
7.3.1	RESULTS FROM CUT CONFIGURATION	65
7.3.2	ALTERNATIVE CIRCULAR CUT	67
7.4	ROCK PARAMETER SENSITIVITY ANALYSIS	70
7.4.1	INDIVIDUAL SENSITIVITY ANALYSIS	70
7.4.2	ACCUMULATED SENSITIVITY ANALYSIS	73
7.5	STRESS ANALYSIS	75
7.5.1	HYDROSTATIC STRESS STATE	75
7.5.2	IN-SITU STRESS CONDITIONS AT FOLLO	76
7.5.3	INDIVIDUAL STRESS SENSITIVITY ANALYSIS	79
7.5.4	ACCUMULATED STRESS SENSITIVITY	81
8	DISCUSSION	83
8.1	GEOLOGICAL	83
8.2	FREE FACE DESIGN	84
8.3	ROCK PARAMETER SENSITIVITY	85
8.4	STRESS SENSITIVITY	86
8.5	APPLICABILITY OF D&S	88
9	CONCLUSION	91
10	FURTHER WORK	93
11	REFERENCES	95
12	APPENDICES	1
12.1	APPENDIX A - THE FOLLO LINE PROJECT	1
12.2	APPENDIX B - GEOLOGY	3
12.3	APPENDIX C - DRILL AND SPLIT METHOD	4
12.4	APPENDIX D - FIELD MAPPING	6
12.5	APPENDIX E - LABORATORY TESTING	13
12.6	APPENDIX F - NUMERICAL ANALYSIS	17
12.6.1	- ANALYSIS ASSUMPTIONS	17
12.6.2	- INDIVIDUAL ROCK PARAMETER SENSITIVITY	19
12.6.3	- INDIVIDUAL STRESS SENSITIVITY ANALYSIS	24

List of abbreviations

NNRA	Norwegian National Rail Administration	
NTNU	Norwegian University of Science and Technology	
NGU	Geological Survey of Norway	
NGI	Norwegian Geotechnical Institute	
ISRM	International Society for Rock Mechanics	
DRI	Drill Rate Index	
UCS	Uniaxial Compressive Strength	[MPa]
D&B	Drill and Blast	
D&S	Drill and Split	
σ_1	Major principal stress	[MPa]
σ_2	Intermediary principal stress	[MPa]
σ_3	Minor principal stress	[MPa]
σ_v	Vertical stress	[MPa]
σ_H	Major horizontal stress	[MPa]
σ_h	Minor horizontal stress	[MPa]
RMR	Rock Mass Rating	
GSI	Geological Strength Index	
TBM	Tunnel Boring Machine	
RQD	Rock Quality Designation	
SRF	Strength Reduction Factor	
SAB	Spinning anti-bend rod	

1 Introduction

1.1 Background for thesis

Areas surrounding the Norwegian capital Oslo have experienced a massive population growth over the past 20 years. In order to comprehend the forthcoming increase in population, major upgrades to the existing infrastructure is necessary. As a part of major development and upgrades to the existing railway network around the city of Oslo in Norway, the Follo line project comprises the construction of new twin-tube tunnels connecting Oslo central city to the new Ski mass transit station.

Due to vibration restrictions and close proximity between the existing underground structures and the new tunnels, the Norwegian National Rail Administration (NNRA) is forced to consider alternative excavation methods in certain part of the tunnels. NNRA has decided that the most viable option for excavating is the “Drill & Split” method. This excavation method is based upon inserting an expanding wedge that initiates tension failure between boreholes at the tunnel face.

This master thesis is the continuation of a project assignment conducted in the autumn of 2014 by the author. It is emphasized that both the project and master thesis are two independent works, so it is not necessary to be familiar with one to understand the other. While the project assignment was purely a theoretical study of the applicability of “Drill & Split” at the Follo line project, this master thesis focuses on providing supplementary rock quality assessments and further investigations of the applicability of the “Drill & Split” excavation method through numerical modelling.

1.2 Aim of study

The scope of this study is to assess the engineering geological applicability and evaluate limitations of the excavation method called “Drill and Split” for use at the Follo line project. This involves identifying on-site rock parameters and numerical modelling of the “Drill and Split” process using finite element program *Phase²*. The main objectives are listed under:

- Supplementary field assessment of rock mass quality, both for comparing against previous investigations, as well as quantifying parameters for numerical analysis
- Supplementary laboratory assessments of rock parameters for comparison and use in numerical modelling
- Numerical modelling with focus on optimizing free face design and surrounding borehole configuration

- Numerical modelling for assessing the influence of various rock qualities towards the splitting process
- Modelling of in-situ stress conditions to investigate the effect of different stress situations on the splitting process
- Discussion and preliminary conclusion of altogether applicability of “Drill and Split” based on the numerical analysis and the given presumptions.

1.3 Structure and methodology of the study

The master thesis is structured into the following sections based on the underlying methodology behind each chapter:

- Literature review of existing material (Chapter 2, 3 and 4):
 - a) Background information of the Follo line project
 - b) Geological review of the area subjected for “Drill and Split”
 - c) General presentation of the “Drill and Split” excavation method
- Field mapping (Chapter 5)
 - a) Comparing the authors own interpretation of rock mass quality against previous assessments
 - b) Discussion of limitations and validity of the assessed rock mass qualities
- Laboratory work (Chapter 6)
 - a) General assessment of rock strength and elastic behaviour – input data for later numerical analysis
 - b) Quantitative comparison toward previously assessed rock properties
 - c) Discussion of limitations and validity of the assessed rock properties
- Numerical analysis (Chapter 7)
 - a) Modelling of the splitting process in order to assess the influence of various rock parameters, free face design and in-situ stress field related to easiness of yielding
 - b) Discussion of assumptions and limitations for the analysis

1.4 Limitations

Because excavation work at the Follo line project were not started at the time of writing, the author was unable to compare results from analysis with actual splitting performance. This is considered a main restraint from being able to optimize the model, as the author was unable to calibrate the numerical model with real life data of actual splitter performance.

This study is also limited to looking at the sections where “Drill & Split” will be used, and focuses only on aspects of the project that influences this process. This excludes a number of features that may be of interest for other purposes.

Little literature exists on performance, encountered challenges and gained experience from earlier projects utilizing “Drill & Split”. Given this limitation, a number of assumptions regarding the method is necessary –which ultimately adds up to the uncertainty in the analysis.

Another concern is the applicability of a finite element code such as *Phase²* for modelling a splitting operation at the tunnel face. Given that the initial purpose of the software is to assess stress distributions around underground excavations, it is assumed that the splitting process can be reasonably modelled. A more thorough evaluation of the program applicability for this problem will be presented later in the analysis.

2 Follo line project

2.1 General information

The Follo line is the railroad connecting Ski to Oslo central station, and it is a part of the InterCity project. The InterCity project comprises of upgrading existing railway network into two-track lines on the following sections out of Oslo: north towards Lillehammer, southeast towards Halden and southwest towards Skien (figure 2.1). Predictions undergone by Statistics Norway (SSB, 2015) concludes that these areas will experience a great population growth the coming years, and upgrades to existing railway network is crucial to cope with this.

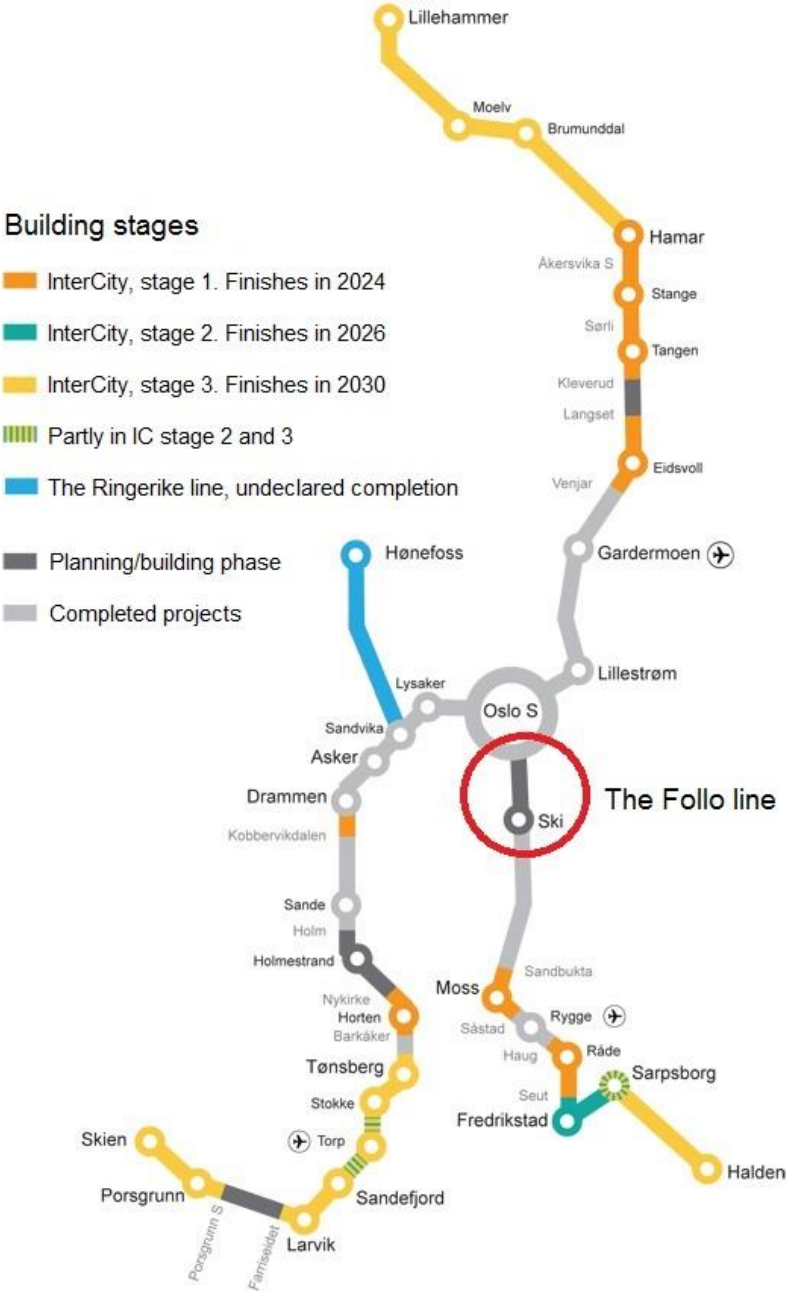


Figure 2.1 - InterCity project and phases (NNRA, 2015)

The Follo line project covers the first stage in constructing the railway southeast out of Oslo towards Ski. The entire project includes construction of 22 km two-track railway, building of a new train station at Ski and necessary reconstruction work at Oslo central station. The two-track railway is designed for speed up to 250 km/h, which in turn halves the travel time between Ski station and Oslo central station (NNRA, 2015).

Due to a densely populated area, roughly 20 kilometres out of the 22-kilometre two-track railway is planned under ground in twin tube tunnels. It is also necessary to divert and upgrade the existing railway (inbound Østfold line) for speed up to 90 km/h to cope with traffic in the construction phase and later to handle cargo trains. The project is set to start in 2015, and prospected completion is in 2021 (NNRA, 2015).

The Follo line project is divided into four enterprises, which can be seen in figure 2.2. In addition to these, there is a separate enterprise for signal work. The enterprise at Oslo central station covers necessary upgrades of existing tracks to handle the increased traffic, while the enterprise at Ski includes construction of a new mass transit station with extended parking capacity and buss connections to handle daily commuters to Oslo (NNRA, 2015). The tunnelling of the railways is divided into two separate enterprises; the longer one, which will utilize tunnel-boring machines, and the shorter, which will excavate using conventional drill and blast. This thesis will focus solely on the drill and blast enterprise.



Figure 2.2 - Follo line project divided into enterprise (NNRA, 2014a)

As shown in figure 2.2, the drill and blast enterprise comprises of tunnelling the northernmost parts of the twin tube tunnels towards the Oslo tunnel entrance before merging with the railway work executed in the Oslo central station enterprise. Necessary upgrades to the inbound Østfold line are also included in this contract.

The different elements included in the drill and blast contract are presented in Appendix A. 1. Tunnelling of the twin tube tunnels and inbound Østfold line makes up major parts of this contract, while some minor tunnelling jobs consists of creating access tunnels and re-routing the Alna river.

2.2 Nearby structures

The Ekeberg hill is very attractive for construction of underground structures due to good rock conditions and its close proximity to Oslo city. Some of the structures lie within close distance to the projected tunnel alignment, and conflicts may occur during construction of the new railway tunnels. The sections of the tunnel alignment that must be carefully excavated due to close proximity to existing structures is presented in Appendix A. 2. In the following sections, three nearby structures that need consideration will be discussed; the Alna River tunnel, Ekeberg Oil storage and Ekeberg road tunnels.

2.2.1 Alna river tunnel

Alna river tunnel was constructed in the early 1920’s to divert Alna river from its original outlet in Bjørvika, where Oslo central station and several prestigious building projects, including the Opera house and Barcode office establishment lies today. Alignment of the existing Alna river tunnel is presented in figure 2.3 along with nearby road tunnels and the projected tunnels in the Follo line contract.

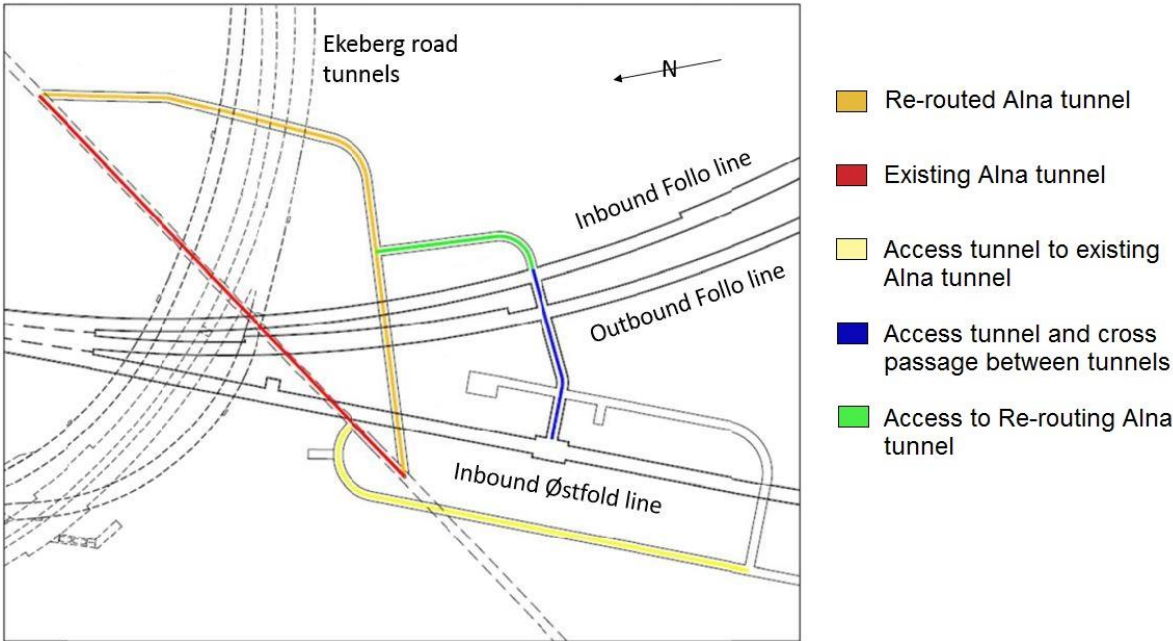


Figure 2.3 - Alna river tunnel. Modified after (NNRA, 2014b)

As shown in figure 2.3, the Alna River will be diverted into a new tunnel. This is necessary because of insufficient rock cover in the cross section between the existing Alna tunnel, Ekeberg road tunnels and the planned Follo line tunnels. This re-routed tunnel will pass over the twin tube tunnels and inbound Østfold line further south into the Ekeberg hill. Despite a new alignment, the new crossings will still have a minimal rock cover because of restrictions in possible gradients for both the railway tunnels and the re-routed Alna river tunnel. It is therefore necessary to construct concrete culverts to prevent leakage and increase stability in these crossings.

Another challenge with minimal rock cover due to the restrictive gradient arises when the re-routed tunnel passes beneath the Ekeberg road tunnels. As opposed to the twin tube tunnels and inbound Østfold line, these road tunnels are already constructed, which in turn dictates the need for careful mechanical excavation of the re-routed Alna tunnel in this crossing. This section of the re-routed tunnel will therefore be excavated using “Drill and Split”.

The existing Alna tunnel shown in red in figure 2.3 will be decommissioned. At the crossing point between this tunnel, Ekeberg road tunnel and outbound Follo line, the decommissioned Alna river tunnel must be filled with concrete to sustain carrying capacity and maintain sufficient rock cover between road and railway tunnels. This crossing is illustrated later in figure 2.5.

2.2.2 Ekeberg Oil Storage

Ekeberg Oil storage is a series of rock caverns filled with different petroleum products. It was built in the late 1960's and 70's due to requirements for safe fuel storage nearby Oslo, and the Ekeberg hill was an obvious choice because of good rock conditions and close proximity to the existing oil terminal at Sjursøya (Føsker, 2007). Even after more than 40 years in service, the storage facilities are still operative with few reported problems.

The facilities are used for temporary storage of petroleum products. Estimates from 1995 witness that approximately 50% of Norway's annual fuel demand passed through the facility (Føsker, 2007). In addition to this, it is solely responsible for serving Oslo airport Gardermoen with over one million litres of jet fuel daily. This implies that there would be massive economic and social cost of interrupting the facility's daily operations.

The cisterns were excavated using conventional drill and blast. Because of volatile petroleum products, the caverns are unlined and situated below the groundwater table. This suggests that the Follo line tunnels and inbound Østfold line should be excavated carefully nearby these

structures. Appendix A. 2 illustrates the sections of in- and outbound Follo line, as well as the inbound Østfold line, where alternative excavation methods to drill and blast must be used due to vibration restrictions. Detailed layout, storage capacity and product information of the facility is not available to the public for strategic reasons. Note that no reports of troubles during excavation work, together with few problems during the facility’s lifespan, witness of good bedrock quality in the area.

2.2.3 Ekeberg road tunnels and Grønli tunnel

The Ekeberg road tunnels were constructed in the early 1990’s to expand the capacity of road networks in Oslo, as well as diverting the traffic underground. These road tunnel tubes will cross the Follo lines and the inbound Østfold line near their northern tunnel entrance. Figure 2.4 shows in yellow the different road tunnels that need consideration.

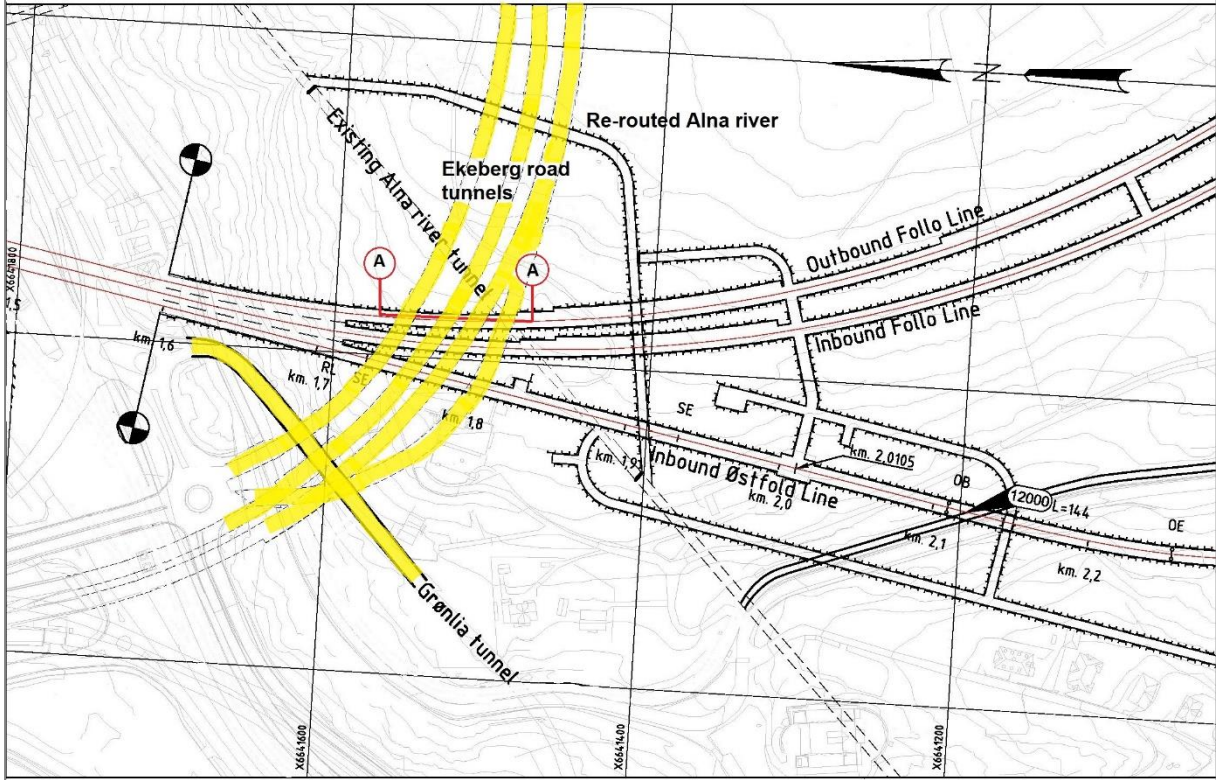


Figure 2.4 - Follo line crossing Ekeberg road tunnels and Grønli tunnel - road tunnels in yellow (modified after (NNRA, 2014c))

Potential stability issues due to limited rock cover and interruption of traffic in the road tunnels are major concerns that need to be assessed during construction. The minimum rock cover between the tunnels is estimated to be around 3.5 meters. However, it may be as low as 1 meter in certain locations – depending on the depth of ditches (NNRA, 2012). Profile A-A presented in figure 2.5 illustrates the in depth situation at the crossing.

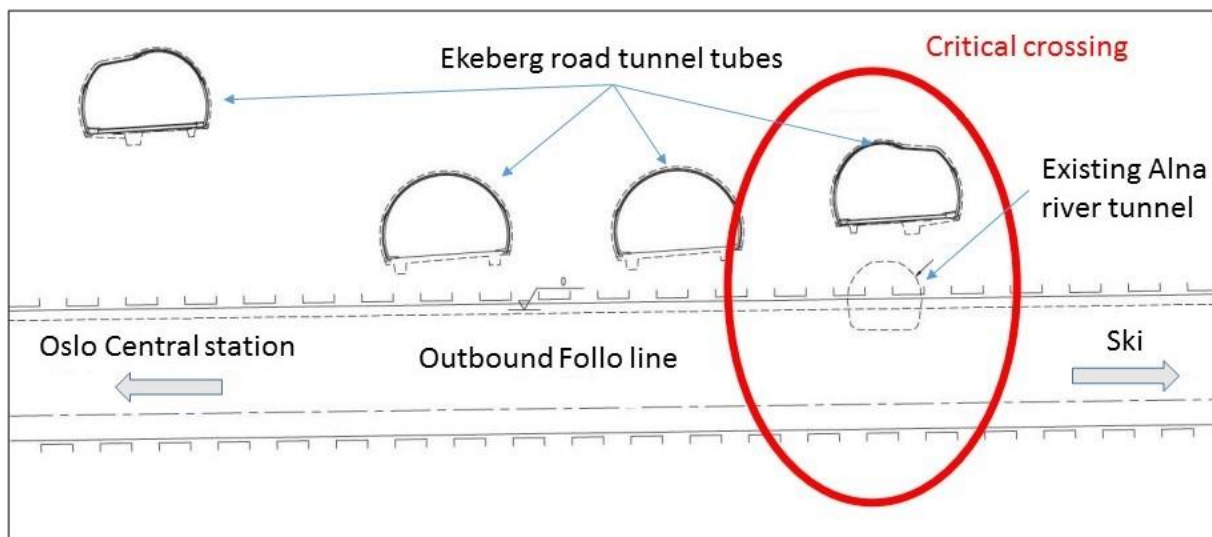


Figure 2.5 - Profile (A-A) along outbound Follo line (modified after (NNRA, 2012))

As shown in figure 2.5, the most critical crossing is where the existing Alna river tunnel passes both outbound Follo line and one of the Ekeberg tunnel tubes. This profile illustrates both the need for careful excavation and heavy rock support in the crossing, as rock cover is minimal. Given this special situation, numerical analysis has been conducted on this profile for estimations about the stability and stress situation after excavating the Follo lines (NNRA, 2012). This report concludes that the rock cover should be sufficient, if supported with cast-in-place concrete lining (NNRA, 2012).

In addition to the Ekeberg tunnel tubes, a separate road tunnel (Grønlia road tunnel) passes the planned Follo tunnel entrance with limited rock cover (figure 2.4). This road tunnel was completed in 2008, which means that it is considered a new tunnel with modern requirements to documentation and safety requirements. Reports from this tunnel witness that few challenges were encountered and good work progress was obtained (Norwegian Public Road Administration, 2009).

The planned three-track tunnel will pass the Grønlia tunnel with close proximity near the northern tunnel entrance. To investigate potential stability issues due to stress redistribution in the Grønlia tunnel after excavating the large span three-track tunnel, numerical analysis were undergone. The study concluded that the pillar between the two tunnels should maintain a satisfying carrying capacity, but at the same time emphasized the need for careful excavation near this pillar (NNRA, 2013c).

3 Geological conditions

As several other constructions are located inside the Ekeberg hill, the local geology is well understood due to several investigation stages. However, the high project cost and massive consequences of conflicting nearby constructions enhances the need for accurate geological mapping to reduce uncertainty to a minimum. Therefore, extensive pre-investigations have been conducted. Interpretations made in the following sections are based on previous reports and several ground investigations ordered by the NNRA. In later sections, these results will be compared against the authors’ own interpretations of the geology.

3.1 Bedrock

Regional geology around Oslo can be seen in figure 3.1 below. This area is strongly affected by several geological activities; most notably the Cambric-Silurian sedimentary deposits underlying Oslo central city and Permian intrusions originated from the creation of regional graben structures in north-south direction (Ramberg, Bryhni, & Nøttvedt, 2006).

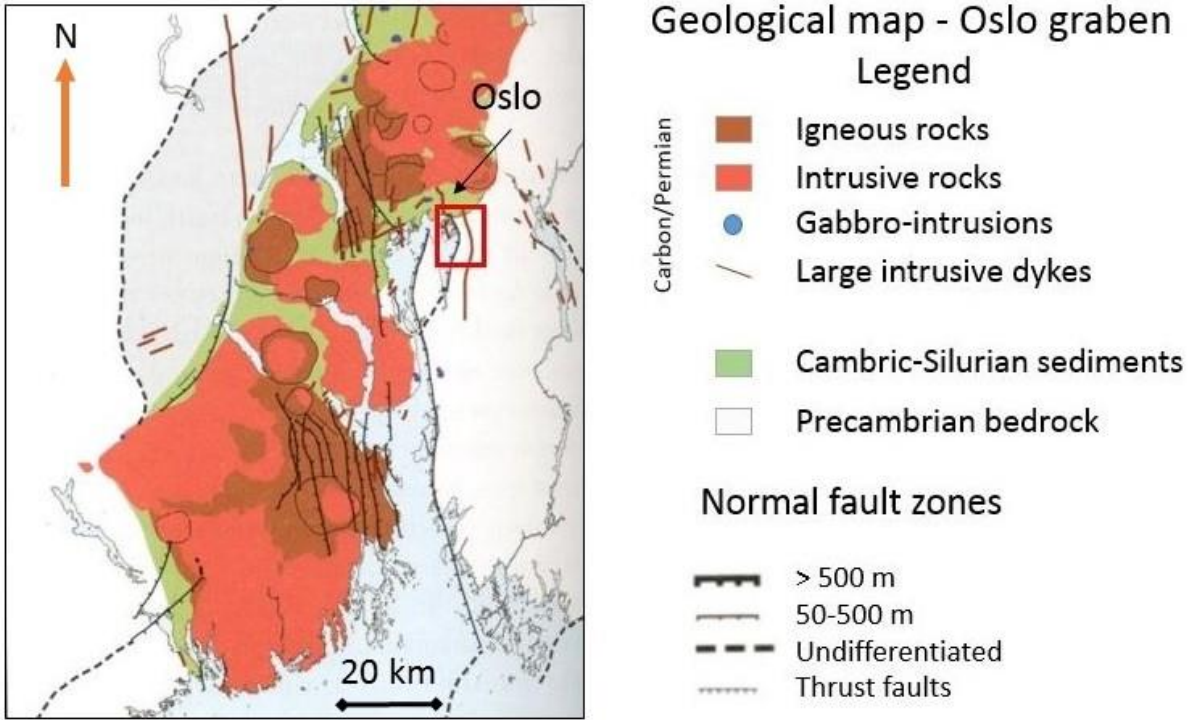


Figure 3.1 - Geological map over Oslo graben (modified from (Ramberg, Bryhni, & Nøttvedt, 2006))

As shown in figure 3.1, several faults oriented mainly in N-S direction is present throughout the area. The framed area illustrates the relevant area for the Drill and Blast contract on the Follo line project. Figure 3.1 suggests that the subjected area lies on the border between Precambrian bedrock and younger Cambric-Silurian sedimentary rocks, separated by a distinct

fault zone. An enlarged and rotated geological map of the framed area is presented in figure 3.2 below. Note that the colour legend differs between the two figures.

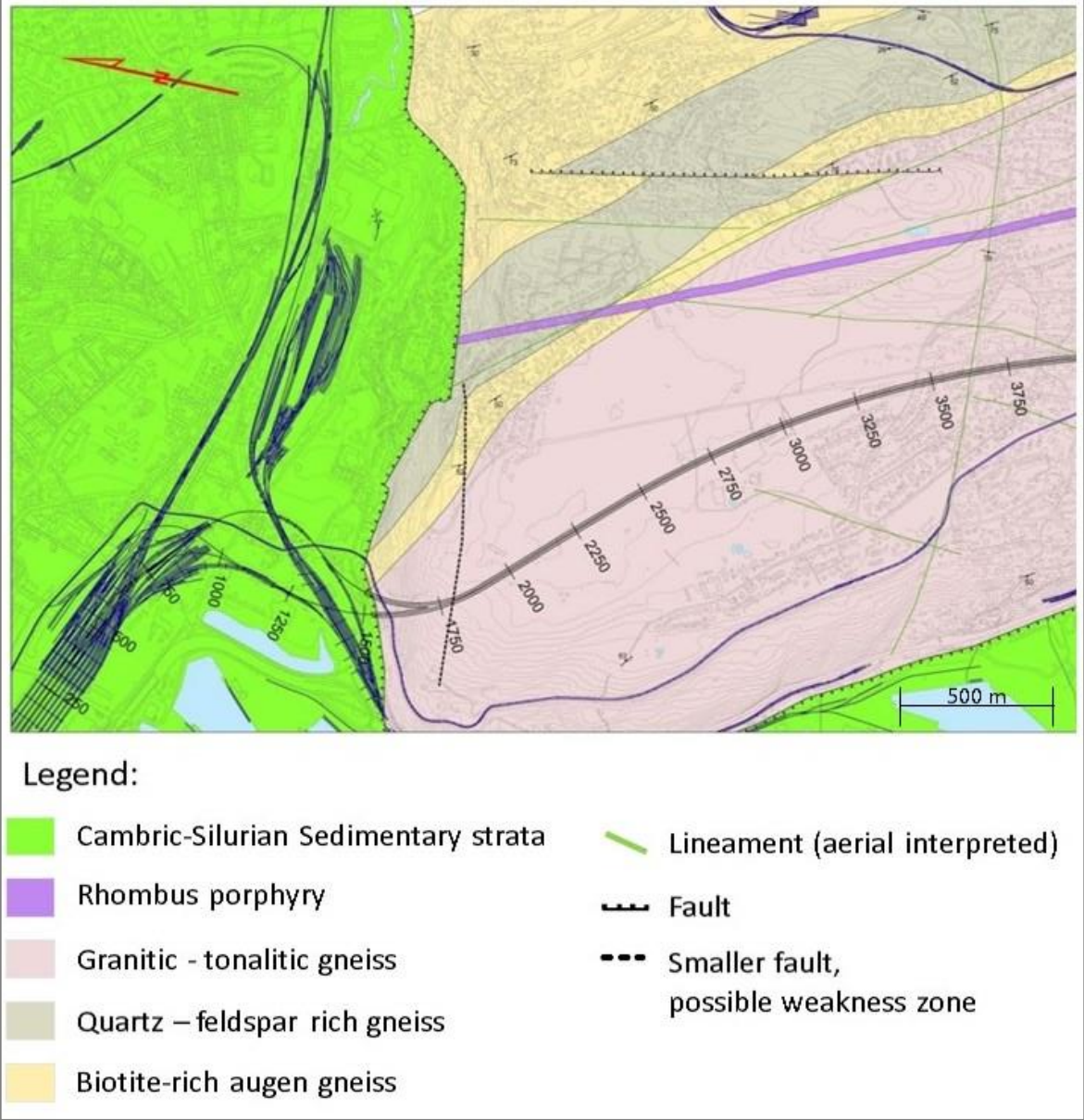


Figure 3.2 - Geological map for the D&B contract (NNRA, 2014a)

Figure 3.2 presents the local geology relevant for the Drill & Blast enterprise of the Follo line project. As indicated by the regional geology map in figure 3.1, the main fault zone oriented in the N-S direction as well as a transverse fault oriented in E-W direction is the most notable geological features within this area. The faults marks a distinct boundary between Precambrian bedrock and Cambric-Silurian sedimentary rocks. The bedrock area southeast of these faults also marks a pronounced feature in the topography around Oslo, in which it rises steeply from the fjord and surrounding lowland. In addition to the obvious fault-mechanism, this also suggests that the sedimentary rock could be weaker and thus more prone to weathering than the

Precambrian bedrock (Graversen, 1984). An engineering geological map by NNRA focusing more upon weakness zones and jointing is presented in Appendix B. 1 for comparison to this bedrock map.

The bedrock surrounding the Follo line tunnels consists of gneiss with a granitic to tonalitic composition. Further east from the tunnels, the bedrock is interpreted as biotite-rich augen gneiss with a section of quartz-enriched gneiss. Additionally, a 20-metre wide dyke of rhombus porphyry runs approximately parallel to the tunnel alignment. This dyke is not expected to interfere with the tunnels, but it remains evidence that intrusions randomly occur within the Precambrian bedrock. Intrusions may present challenging or be beneficial towards excavation work, as they exhibit different mineralogical composition and possibly other mechanical behaviour. Due to their random occurrence, it is not realistic to map all these, and they need to be handled properly when encountered.

3.1.1 Mineralogy

As a part of the study of the evolution of Precambrian rocks around the Oslo fjord conducted in 1984, Ole Graversen at the Geological Survey of Norway (NGU) investigated the mineralogical difference between the gneiss types located within the Ekeberg hill. A simplified summary of the mineralogy for the different gneiss types are presented in table 3.1 below.

Table 3.1 - Mineralogy of the different gneiss types (Graversen, 1984)

	<i>Quartz</i> (%)	<i>Feldspar</i> (%)	<i>Biotite</i> (%)	<i>Other minerals</i> (%)
<i>Granitic gneiss</i>	30	65	<5	<5
<i>Tonalitic gneiss</i>	30	40	20	10
<i>Biotite-rich augen gneiss</i>	25	60	10	5
<i>Quartz-feldspar rich gneiss</i>	40	50	<5	>5

As suggested by table 3.1, the mineralogical difference between the gneiss types remains limited. The augen gneiss is distinctive due to its occasional garnets and large feldspar lenses, which bears resemblance to eyes in a cross section. The tonalitic gneiss is likely to express a slightly darker appearance than both the granitic and the quartz-feldspar gneiss due to its higher content of dark mica (Graversen, 1984). In general, rocks with a higher mica content usually expresses more anisotropic strength behaviour due to the sheet structure of mica minerals (Nilsen & Broch, 2011). However, the differences in mica content remains small for these rocks, and the different gneiss types are assumed to exhibit similar mechanical behaviour. The gneiss types will also be difficult to separate visually without aid from laboratory analysis.

Combined, these reasons suggest that it is convenient to denote the gneiss types with a similar preface. From now, the author chooses to denote the bedrock as gneiss.

3.1.2 Intact rock strength

Several investigations has been carried out to assess the rock quality and to obtain intact rock properties for relevant rock masses. Table 3.2 below presents assessed parameters from locations relevant for the D&B contract. Note that the properties found from borehole ET6 is excluded in calculation of average values in the last column due to it being an intrusive rock that randomly occurs in dykes.

Table 3.2 - Intact rock properties (NNRA, 2013b)

<i>Borehole</i>	<i>ET3</i>	<i>ET6</i>	<i>Pillar</i>	<i>Pump station</i>	<i>BH841</i>	<i>Average¹</i>
<i>Rock type</i>	Gneiss	Diabase	Gneiss	Gneiss	Tonalitic gneiss	Gneiss
<i>E-modulus (Gpa)</i>	50.1	70.8	62.6	43.9	47	50.9
<i>Poissons ratio, ν</i>	0.14	0.25	0.15	0.12	0.15	0.14
<i>UCS (Mpa)</i>	127.2	211.9	119.1	76.9	95.4	104.7
<i>Tensile strength σ_t (Mpa)</i>	15.9	18.5			6.2/11.8 ²	-
<i>DRI</i>	29	43			37	-

With the exception of boreholes 841 and pump house are all the parameters in table 3.2 derived from core samples located nearby the planned crossing between Follo lines and Ekeberg road tunnel. Borehole 841 was bored from the entrance of Grønli tunnel and 80 meters through the Ekeberg fault and into undisturbed bedrock. The gneiss tested from this core drilling is from near the bottom of the borehole. It is assumed that the sample is relatively undisturbed from tectonic fault movement (NNRA, 2013b).

Pillar and pump station boreholes were bored horizontal and vertical, respectively. These boreholes were bored with the main intention of measuring in-situ stress conditions. Because of this, the amount of available testing material is limited, which in turn limits the number of test that is possible. This is the reason that the tensile strength and drill rate index (DRI) were not tested for these samples.

¹ Averaged values for gneiss only

² Values are parallel and perpendicular to the foliation, respectively

Based on the data summarized in table 3.2, some general features can be assigned to the gneiss:

- UCS is classified as high to very high (ISRM, 1977)
- High E-modulus and low Poisson's ratio suggests a rigid rock that expands little when subjected to loading
- Tensile strength varies significantly with foliation orientation in relation to testing direction – suggesting an anisotropic behaviour
- Low drillability (low DRI) is consistent with a moderate quartz content

In addition to these features, clear distinctions are seen between gneiss and diabase properties. Even though it is a limited statistical basis with only one diabase sample, its compressive strength is notably higher in comparison to the gneiss. It also has a higher drillability in comparison to the gneiss, which most likely originates from a lower quartz content.

3.2 Discontinuities

Discontinuities refers to geological or structural features that alters the rock mass from being a continuous medium. In general terms, discontinuities refers to any form of mechanical discontinuity within the rock mass that has zero or close to zero tensile strength (Nilsen & Palmstrøm, 2000). This includes any scale and covers everything from large weakness zones to detail joints and bedding. It is common to divide discontinuities into sub-groups depending on its size (figure 3.3).

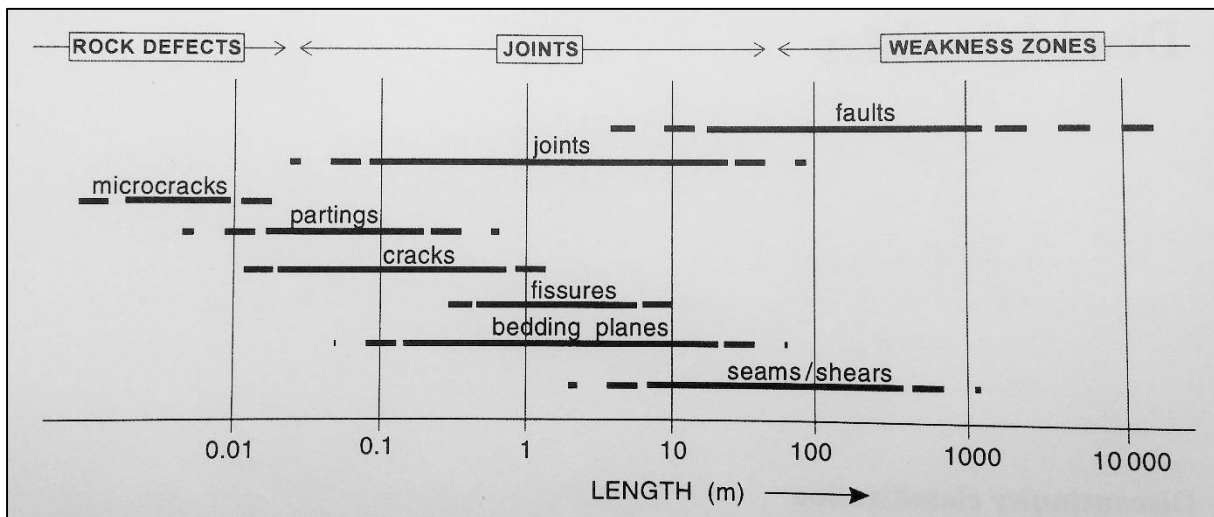


Figure 3.3 - Types of discontinuities defined after size (Nilsen & Palmstrøm, 2000)

Figure 3.3 lists a number of terms used to describe geological discontinuities. Note that this definition is based upon size rather than origin. This leads to overlap between joints of different origin and composition, but similar size. It is emphasized that joints of different origin might

present very different characteristics and behaviour despite similar size (Nilsen & Palmstrøm, 2000).

Three main groups of discontinuities is defined in figure 3.3 based upon their length:

- Rock defects
- Joints
- Weakness zones

This section will not focus on rock defects, as this represents microscopic joints of limited interest for an engineering geological description. The following sections will focus on joints and weakness zones mapped during site investigations.

3.2.1 Joints

As suggested from the definition given in figure 3.3, joint refers to discontinuities with lengths ranging from a few centimetres up to approximately one hundred meter. Joints are usually mapped in terms of their spatial orientation (strike/dip), along with a note of their characteristics (infill, roughness, likely origin etc.) (Nilsen & Palmstrøm, 2000). It is commonly seen within the rock mass that joints tend to have similar strike and dip directions and so constitutes distinct joint sets. This can be observed as the most dominant cluster of strike directions when several individual joints are plotted in a joint rosette.

NNRA has performed detailed joint mapping to identify the main joint set orientations within the rock mass on site at the Follo line project. A joint rosette with sufficient statistical basis of measurements is given in figure 3.4 below.

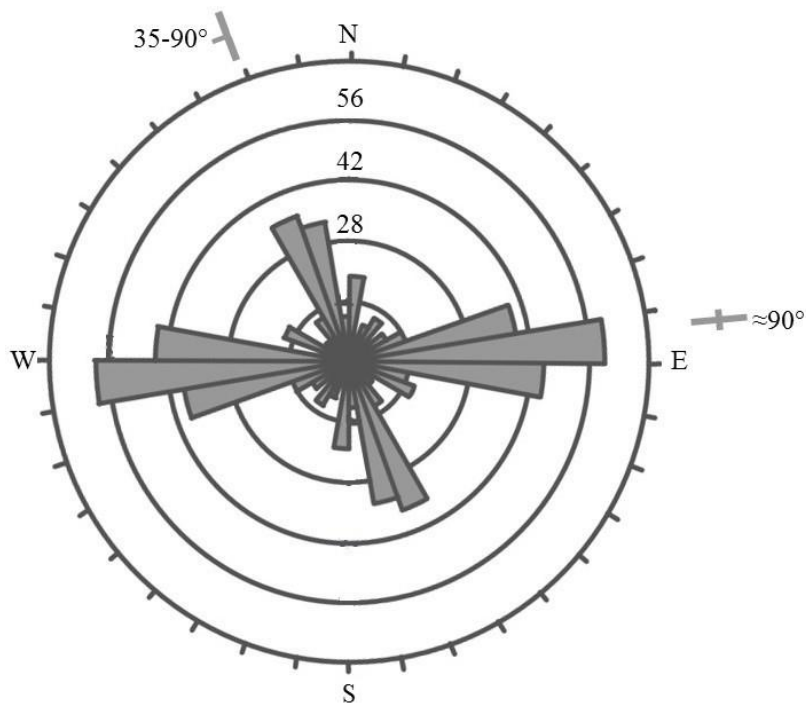


Figure 3.4 - Joint rosette modified from engineering geological map (Appendix B. 1)

Two main joint sets are detected according to the joint rosette:

- Joint set 1: Strike: N70-100°E, Dip: Steeply dipping
- Joint set 2: Strike: N150-170°E, Dip: 35-90°W

In addition to the two dominant sets, a number of random joints are also included. These are assumed to occur due to the presence of nearby fault zones. Joint set 2 represents the foliation of the bedrock, which are dipping westwards with varying inclination. Joint set 1 is steeply dipping with an east-west strike direction.

3.2.2 Weakness zones

Weakness zones refers to discontinuities with lengths from tens to several hundred meters, and comprises fault zones, shear zones, weak material zones and other planar zones within the rock mass that has significantly lower mechanical properties than adjacent rock mass (Nilsen & Palmstrøm, 2000). As they often are of considerable extent, weakness zones are usually interpreted from digital topography models of surface lineaments. However, the unique situation with several nearby structures at the Follo line project gives an edge to reduce the uncertainty of misinterpreting lineaments and helps detecting zones that are not so apparent on the surface. Both inspections of the unlined Alna river tunnel (NNRA, 2013a), as well the end report from construction of the Ekeberg tunnels (Norwegian Public Roads Administration, 1994) gives valuable information of actual thickness and location of different weakness zones.

The most prominent weakness zones within this area are the pronounced faults aligned in the N-S and E-W direction. The N-S fault will not encounter the tunnels due to similar alignment and sufficient spacing, but the tunnels need to cross through the Ekeberg fault (E-W fault). This zone has been investigated for several purposes, and a borehole profile along the Follo line tunnel alignment showing the variations in strata can be seen in figure 3.5.

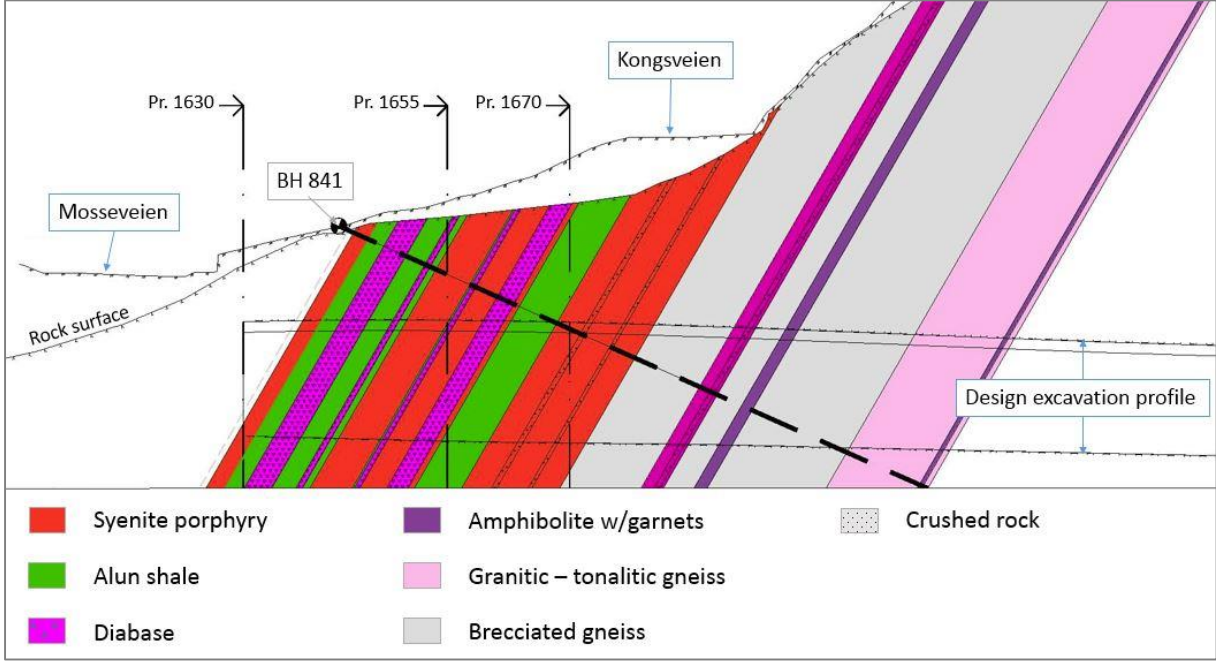


Figure 3.5 - Profile through the Ekeberg fault (modified after drawing UOS-30-V-30107 from NNRA)

The rock layers interpreted from this borehole suggests a great variation between intrusive, sedimentary and brecciated rocks through the fault zone. This zone is heavily influenced by the tectonic movement, which has caused the north block to descend with a vertical offset of approximately 900 meters (Ramberg, Bryhni, & Nøttvedt, 2006). On both sides, this movement has caused a brecciated influence zone varying from 30 up to 100 meter (NNRA, 2013a). This brecciated zone has later been partly cemented together with quartz intrusions so it appears as a massive rock mass. Further reports suggests that there is a gradual transition zone between brecciated rock masses and granitic gneiss (Løset & Lien, 1980).

In general, the rock mass within this zone is strongly affected by the tectonic movement and transitions between intact and crushed rock is often irregular. According to investigations, the sedimentary Alun shale generally presents itself as the lowest quality rock mass within the zone, but the reports underline the need for extensive support throughout the entire zone (NNRA, 2013a).

Minor weakness zones are drawn into the engineering geological map given in Appendix B. 1. Their character remains uncertain, ranging from heavily jointed fracture zones to crushed zones with potential mineral alterations. The zones are divided into three categories on the engineering geological map according to their width:

- 1-5 meter
- 5-10 meter
- More than 10 meters

It is important to recognize that these widths does not necessarily reflect the actual width encountered in the tunnels while excavating, as they may cross the tunnel profile with a non-perpendicular angle. Furthermore, the inclination angle of these zones remain to some extent uncertain, making it harder to predict the exact intersection along the tunnel alignment.

3.3 In-situ stress

Rock masses everywhere experiences a three-dimensional loading state that is commonly referred to as the in-situ stress field. Rock stresses has a magnitude and direction, and are the result of previous geological activities on site. Convention in rock mechanics defines compressive stresses as positive and tensile stresses negative (Nilsen & Palmstrøm, 2000).

We are usually interested in the principal stresses that constitutes the stress field in rock mechanics. The principal stresses within the rock mass are defined as the three perpendicular stresses acting normal on surfaces with zero shear stress (Myrvang, 2001). These stresses are denoted σ_1 , σ_2 and σ_3 , where the subscript refers to highest, intermediary and lowest magnitude respectively (Nilsen & Palmstrøm, 2000).

For any underground structure, the in-situ stress field plays a major role in governing both orientation and geometry of the structure. By measuring the in-situ stress distribution, it is possible to avoid potentially unstable situation caused by undesirable stress concentrations in vulnerable places. Certain situations may even benefit from a particular stress distribution, as favourable stress distribution and magnitude in relation to underground structure helps maintain stability.

There are two principal ways of estimating the stress situation (Myrvang, 2001):

- Calculated from measured strain or deformation using accurate measuring devices.
- Estimated from overburden, unit weight and an assumed K -factor³. Much less accurate than the method mentioned above, but significantly cheaper

Due to the close proximity to nearby structures and size of project, budget allows for extensive pre-investigations. Therefore, two separate strain measurements has been conducted by SINTEF to accurately describe the stress field in two different locations (NNRA, 2014a):

- 2D Doorstopper stress measurements in the Ekeberg road tunnel
- 3D cell stress measurements inside the Ekeberg halls (petroleum storage)

Their approximate location are given in figure 3.6. Note that the measurements are taken inside existing underground structures.



Figure 3.6 - Stress measurement locations (figure from Google Earth)

³ K -factor is defined as the ratio between vertical and horizontal stresses ($K = \sigma_h / \sigma_v$)

The measurements inside Ekeberg road tunnels were performed using doorstopper method, which estimates stresses in the plane perpendicular to the borehole axis. Consequently, it is necessary to perform this operation in two perpendicular directions to be able to model a three dimensional stress field (Myrvang, 2001). Therefore, the boreholes were drilled vertically (roof measurement) and horizontally (pillar measurement). A basic assumption for this configuration is that one of the principal stresses act vertically.

3D-measurements uses an advanced cell that is able to model strain in three different directions inside a single borehole. This measurement was done inside the Ekeberg halls. Results from both measurements are summarized in table 3.3.

Table 3.3 - Stress measurements (NNRA, 2014a)

	3D-measurement			2D - Pillar		2D - Roof	
<i>Stress</i>	σ_1	σ_2	σ_3	σ_v	σ_h	σ_H	σ_h
<i>Value (MPa)</i>	9.9 ± 1.9	7.5 ± 1.9	1.9 ± 2.8	10.5	3.3	6.9	-2.1
<i>Direction</i>	N248°	N145°	N14°			N240°	N150°
<i>Dip</i>	24°SW	27°SE	61°NE				

The stress field estimated from 2D-measurements inside Ekeberg road tunnel presents different values than 3D-measurements from the Ekeberg halls. It is believed that close proximity to the E-W Ekeberg fault may have altered the stress field in nearby locations. This is especially of importance while evaluating the horizontal stresses gained from 2D-measurements (roof), as they were conducted closer to the fault zone. While questionable as general values for the entire area, the resulting horizontal stresses indicates favourable directions and magnitudes that are likely to provide good stability for the three-track tunnel (NNRA, 2014a).

Measurements from the horizontal borehole can also be questioned, as it was bored into a rock pillar that is likely to have experienced stress redistribution after excavation. The relative high vertical stress measured within this pillar remains evidence of this, as it most likely expresses an accumulated value caused by stress re-distribution. Given this, it is reasonable to question the validity of this measurement as representative for other areas. Accounting for these considerations, the author deem the 3D measurements to be most valid for an overall stress field assessment because they were taken deep within the rock mass outside the fault influence zone. These measurements are therefore used as basis for the forthcoming analysis.

3.4 Rock mass quality

When speaking of *rock mass quality* in engineering geology, it refers to the bedrock including discontinuities and other properties. Consequently, to give an assessment of the overall rock mass quality, all the aspects mentioned in previous sections are taken into consideration. Several classification systems is developed for the purpose of assigning numerical values to the rock mass, which in turn gives reliable and quantitative measures of the rock mass quality. Among the most common rock mass classification schemes are the rock mass rating (*RMR*) and the Q-system. Although both these has weaknesses and strengths over the other, the Q-system is most commonly used in Norwegian projects.

Due to numerous investigation stages for different underground projects located nearby, the statistical basis of assessed Q-values remains large in the area. Summaries of Q-value assessments around some of the nearby structures are given below:

- End report from construction of the Ekeberg road tunnels estimates Q-values ranging from 2.5-65 in the crossing zone given in figure 2.4 (Norwegian Public Roads Administration, 1994)
- Rock quality documentation during construction of Grønli road tunnel suggests variable Q-values from 0.01 to 75. The large deviation in values originates from variable rock mass qualities through the fault zone (NNRA, 2014a)
- Investigation of the existing Alna river tunnel suggests Q-values between 23-48 (NNRA, 2014a)
- Investigation in the Ryen tunnel near the Oil storage facilities reveals Q-values between 20-34 (NNRA, 2014a)

Based on these results and other reports, estimated Q-value along the tunnel alignments are presented in table 3.4.

Table 3.4 - Rock mass quality (NNRA, 2013a)

	Km	Km	Length (m)	Rock class⁴	Description
In- and outbound Follo line	1.655	1.700	45	G	Exceptionally poor
	1.700	1.770	70	F	Extremely poor
	1.770	2.850	1080	C	Fair
Inbound Østfold line	1.655	1.775	120	G	Exceptionally poor
	1.775	1.805	30	F	Extremely poor
	1.805	1.905	100	D	Poor
	1.905	2.971	1066	C	Fair

It is expected lower rock mass quality in areas near the fault zones than within the massive gneiss region. This is recognized in the rock class assessment of the tunnel alignments where the first 100 meters or so (through the Ekeberg fault) presents much lower quality than the rest (Table 3.4). It is also important to recognize that more local variations in rock class may occur, and that table 3.4 only illustrates a general estimate for the respective distance.

Overall impression of rock mass quality in the subjected area suggests that there are some challenging zones through the Ekeberg fault with low quality rock mass, but otherwise decent quality can be expected. Due to the nature of the rock mass as a discontinuous, inhomogeneous and anisotropic medium, local variations in quality will occur. Through extensive pre-investigations, the geological uncertainty for this project is minimized considerably. Consequently, unexpected geological challenges is not expected to occur frequently.

⁴ Rock class is based upon classification by the Q-system given in Appendix D. 2

4 Drill and Split

Drill and Split is a mechanical excavation method specifically developed for situations where the features mentioned below are encountered. This shortlist is based upon the project assignment report conducted by the author in the fall of 2014 (Volden, 2014):

- Vibration limits restrict the excavation work
- The total distance is relatively short
- The excavation design require some amount of flexibility
- The geology is comprised of hard rocks

As cities grow, the profit from relocating an increasingly larger traffic volume underground becomes gradually more apparent. Additionally, structures for other purposes such as storage facilities and sewer systems occupies underground space, which in sum means that the underground becomes very exploit with increasingly shorter spacing between structures. To avoid conflicting nearby structures, vibration limits are often set to ensure minimal influence during excavation. In turn, this excludes use of explosives as a large portion of the energy released during blasting propagates through the rock mass and creates a damage zone around the profile (Hoek E. , 2007). In exposed areas, the energy released in explosions would exceed the set vibration limits, which in turn prohibits blasting. In such situations, mechanical breaking becomes the most viable alternative.

Alternative methods that satisfies requirements towards careful excavation includes TBM and Roadheader. While both these methods are well established and has potentially high productivity rates, none of the options proves cost-efficient given the nature of this project and the geology on site (Volden, 2014). TBM does not satisfy the required degree of flexibility and is not cost-efficient on the relative short distances where vibration limits are set. Roadheader is excluded for its limited productivity and high cutter consumption in hard rock masses, such as it is expected to encounter beneath the Ekeberg hill. Other possible excavation methods such as expansive mortars and diamond wire sawing are not applicable to larger scale tunnel excavation due to time-consuming nature, complicated setup and altogether low cost-efficiency (Volden, 2014).

4.1 Principle

The need for breaking rocks into smaller fragments has always been a great challenge for mankind. At some point, it was discovered that the forces of nature could be applied to exert an internal expansive force, which breaks the rocks with ease. This discovery was exploited by inserting wooden wedges into open cracks, which then were saturated causing them to swell and exert an internal force. Alternatively, the principle was exploited by filling water into open joints, let it freeze and thus causing an expansion (Darda, 1999). Naturally, these techniques do not satisfy modern requirements toward efficiency and economic productivity so the principle is modernized using hydraulic wedges inserted into boreholes.

The reason for easier breaking when subjected to an internal pressure descends from anisotropic strength properties within the rock material. Rocks exhibit very anisotropic strength properties characterized by a considerably lower tensile strength compared to their compressive strength. As a first approach, the ratio of tensile strength to compressive strength can be assumed to be in the order of 1/10 (Cai, 2010). Note that this ratio has considerable variation, and for hard rocks it is not uncommon to encounter ratios in the order of 1/20 (Nilsen & Broch, 2011). Results presented in table 3.2 illustrate similar behaviour. This mechanical behaviour is typical for rocks, as they are able to handle large compressive loads, while they easily fail in tension.

4.2 Method

Modern techniques are based upon inserting hydraulic wedges into accurately drilled holes. Once inserted, the wedge initiates a mechanical expansion that induces tension yielding in the surrounding rock. Two principal wedge designs are presented in the following sections. The designs incorporate both handheld and machine-operated variants, which usually are scaled versions of each other with size, splitting force and area of applicability as the main differences.

It is possible to exert directional pressure using specialized equipment, which in turn renders it possible to decide breaking direction. This is achieved by orienting the equipment in the borehole such that the elements are expanding perpendicular to the desired splitting direction. For the situation illustrated in figure 4.1, the splitting direction would be in and out of the paper plane.

4.2.1 Wedge splitter

The most commonly way to utilize this principle is by using a hydraulic wedge with counter wedges. This is the most common types of equipment, and a product brochure of the most likely used equipment at the Follo line is presented for reference in Appendix C. 1. Principal sketch of the splitting process utilized by this equipment is given in figure 4.1.

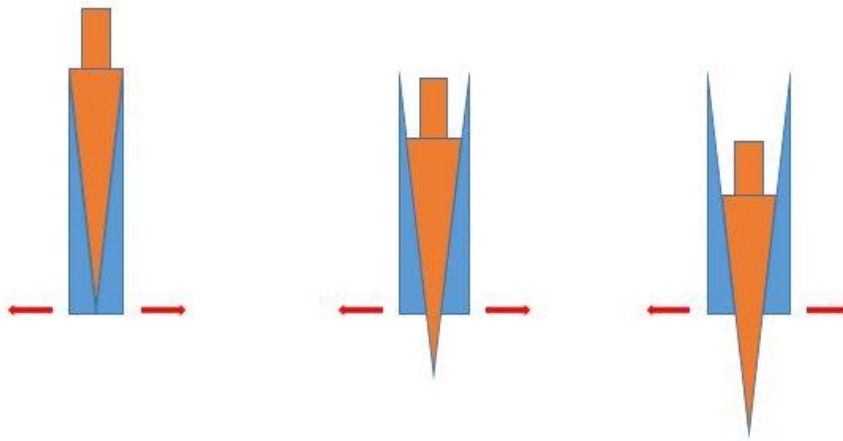


Figure 4.1 - Wedge principle

In the configuration illustrated in figure 4.1 the basic principle is that a centre wedge forces its way in between angled counter wedges. This induces a perpendicular expansion, which causes the surrounding rock to break in tension. Assuming the wedge elements are of sufficient stiffness, the efficiency of this configuration relies on two components; the pushing force acted on the centre wedge and friction between wedges. To maintain a low friction between the wedges, it is necessary to frequently remove dirt and lubricate with appropriate grease. Suppliers recommend manually greasing every 5-10 borehole (Ståhlbåge, 2014).

While using the configuration above, a three-step splitting process is necessary for optimal breaking. The principle is shown in figure 4.2 below:

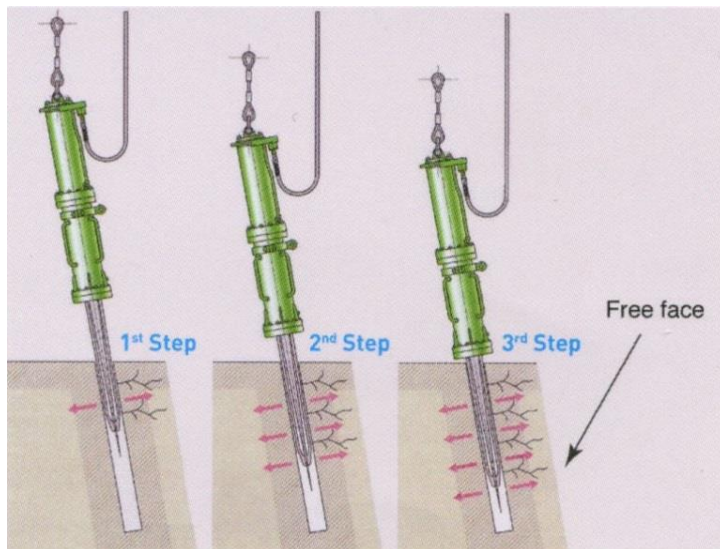


Figure 4.2 - Three-step splitting process (Yamamoto Rock Machine CO.,LTD., 2014)

The reason behind a three-step process is that it increases efficiency and reduces the risk of incomplete rock fracturing (Yamamoto Rock Machine CO.,LTD., 2014). The steps are marked with small humps on the wedge at distances $\frac{1}{2}$ and $\frac{3}{4}$ of the total wedge length (Ståhlbåge, 2014). Larger scale splitting wedges are normally adopted to excavators, where they make use of the hydraulic system already incorporated. Usually 12 tonnes class excavators operate them.

The main advantages and disadvantages for using this kind of equipment are summarized below (Ståhlbåge, 2014) and (Volden, 2014):

- + Can be mounted to excavators that are common among contractors
- + Relatively cheap investment (assuming the contractor owns suitable excavators)
- + Intuitive system to use, needs little time to learn how to operate efficiently
- + Can be operated from a safe distance inside excavator

Disadvantages:

- ÷ Maintenance, greasing every 5-10 hole
- ÷ Tip may break off if borehole is insufficiently deep
- ÷ Counter wedges may break if borehole is not straight
- ÷ Only one splitter pr. Excavator limits productivity (this can be overcome if cross section is large enough for two excavators side by side)

4.2.2 Piston splitter

An alternative design for exerting internal expansion in a borehole can be seen in figure 4.3 below. These rods are operated by hand, usually in collaboration with a number of similar rods working in cooperation to fracture the rock.

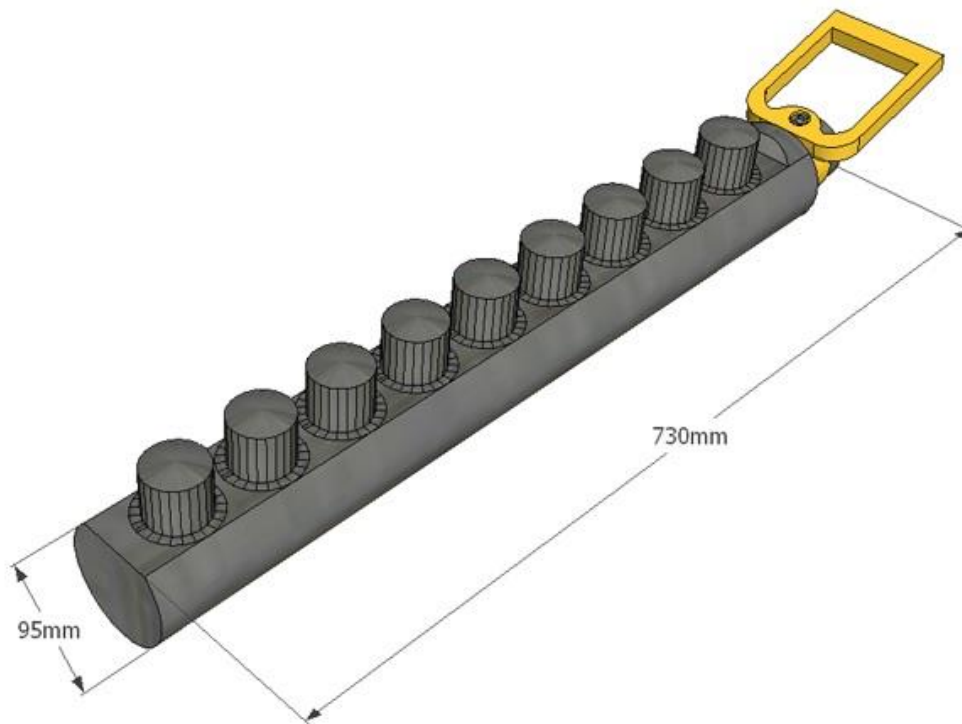


Figure 4.3 - HRD Rock Splitter (Hwacheon Engineering Co.,Ltd., 2014)

These rods has a number of pistons that expands radially in the chosen direction towards the borehole wall. Although the design differs from the wedge presented earlier, their function is very similar. In a similar manner as the wedge configuration, the splitting direction is decided by orienting the rod such that the pistons expand perpendicular to the desired splitting direction. This configuration offers some clear advantages to the wedge configuration (Volden, 2014):

- Individual pistons gives less rigid system, with less chance of damaging equipment
- Less downtime due to less maintenance (greasing)
- Possible to exert splitting force closer to the bottom of the borehole

However, this configuration is little established and less intuitive to use than the wedge systems. Additionally, their handheld nature may present challenges in creating a safe working environment while operated on vertical faces. This could result in an unsafe working environment if necessary precautions are not taken. They are also a reasonably new type of equipment, which suggests that contractors are not likely to be experienced with their use (Hwacheon Engineering Co.,Ltd., 2014).

4.3 Borehole configuration

Because the entire method of splitting relies on exerting internal pressure within the rock mass, it is necessary to drill boreholes in the profile. The recommended spacing between boreholes in a quadratic grid for splitting purposes is in the range of 500 to 800 mm (Yamamoto Rock Machine CO.,LTD., 2014). Given this close spacing, it is obvious that an efficient borehole configuration is crucial to maximize productivity. It is also important to ensure that boreholes are accurately bored before splitting, as deviating boreholes increases the probability for damage to the splitting equipment that may causes further delays (Ståhlbåge, 2014).

4.3.1 Borehole drilling

The force transmission between the splitting wedge and rock mass is dependent on contact between the two. Accurate drilling with respect to borehole diameter and depth is therefore crucial for effective splitting. Diameter and depth of boreholes depends upon features of the splitting wedge. To the author's knowledge, the wedge diameter is largely adapted to standardized borehole diameters, so no additional investment need to be assigned for this.

There are two frequently encountered problems regarding borehole drilling that need to be addressed (Ståhlbåge, 2014):

- Boreholes are bored insufficiently deep
- Boreholes are deviating from a straight alignment

It rarely happens that boreholes are deliberately bored too short, so the problem related to insufficiently deep boreholes can be traced back to other causes. One major reason is that the wedge splitter removes only around 70% of the borehole depth, which means that a short borehole remains after each splitting cycle (Yamamoto Rock Machine CO.,LTD., 2014). It is important to colour code old and new boreholes for each cycle to avoid attempts of splitting in old boreholes, as they probably are insufficiently deep. For vertical boreholes, it is also recommended to cover boreholes with a cloth after drilling to ensure that rock fragments and other objects does not fall in and reducing the effective depth.

If the boreholes are deviating, the risk of bending or breaking the wedge increases significantly. As these boreholes are relatively short, (approximately 1.5 meters deep, depending on equipment (Yamamoto Rock Machine CO.,LTD., 2014)) the chance for critical borehole deviation is small. However, three main reasons for borehole deviation are recognized and presented (Volden, 2014):

- Re-usage of old boreholes. It is nearly impossible to achieve the exact same direction
- Bore too close to existing boreholes. This could cause the new borehole to merge into the path of the other borehole
- Foliation or other planar geological feature may cause boreholes to deviate if the angle between them and the drill axis is small

Necessary precautions should be taken to avoid this from happening. The first cause for deviation can easily be avoided by establishing a good drilling practice with colour coding of boreholes. Hard rock conditions may present situations where it is necessary to decrease the spacing between boreholes for a good splitting result (Yamamoto Rock Machine CO.,LTD., 2014). However, suppliers recommends this spacing not to be less than 400 mm, as this is regarded the minimal safe spacing to avoid borehole merging (Ståhlbåge, 2014). Borehole deviation caused by geological structures may be harder to identify up front, especially for operators with limited geological understanding. This problem could occur at the Follo line project, as the foliation direction is sub-parallel to the alignment of the tunnels.

4.3.2 Free face

Free face refer to an excavated spatial void at the tunnel face that rock mass can move towards during splitting. If splitting occurs without a free face to split against, stresses from surrounding rock mass would actively oppose the induced tension fracturing resulting in only minor scaling at the surface. Creating a free face gives a way for the rock to move during splitting, which in turn makes it possible to induce longer tension cracks. This is crucial for splitting efficiency and therefore for the overall productivity of the excavation method.

There are several ways to create a free face at the tunnel face (Ståhlbåge, 2014):

- Diagonal splitting in inclined boreholes until a pit is created, similar to a v-cut used for drill and blast (Bruland, 2013)
- Drill several holes close together and break out rock using both splitter and hammer
- Drill large diameter holes into the face
- Drill overlapping holes in a continuous line (slot drilling)

In general, the choice of which free face design is the most viable comes down to practical and geological considerations. For instance would it be difficult to establish a v-cut in a tunnel face where the cross section area is too small for splitter or drilling apparatus to achieve a sufficiently small angle between the tunnel face and borehole axis.

Close drilling and hammering out the rock mass is another option, but whether this is a viable solution strongly dependent on drillability and characteristics of the rock mass on site. Large diameter boreholes is also strongly dependent of local geology, but has the advantage of being able to construct free face deeper into the tunnel face that in turn can be used in several splitting cycles.

Slot drilling depends on specialized equipment that can handle continuous drilling of overlapping holes without deviating into neighbour hole. This kind of equipment is designed to fit onto a general purpose drill jumbo. A step-by-step illustration of how it works is presented in figure 4.4.

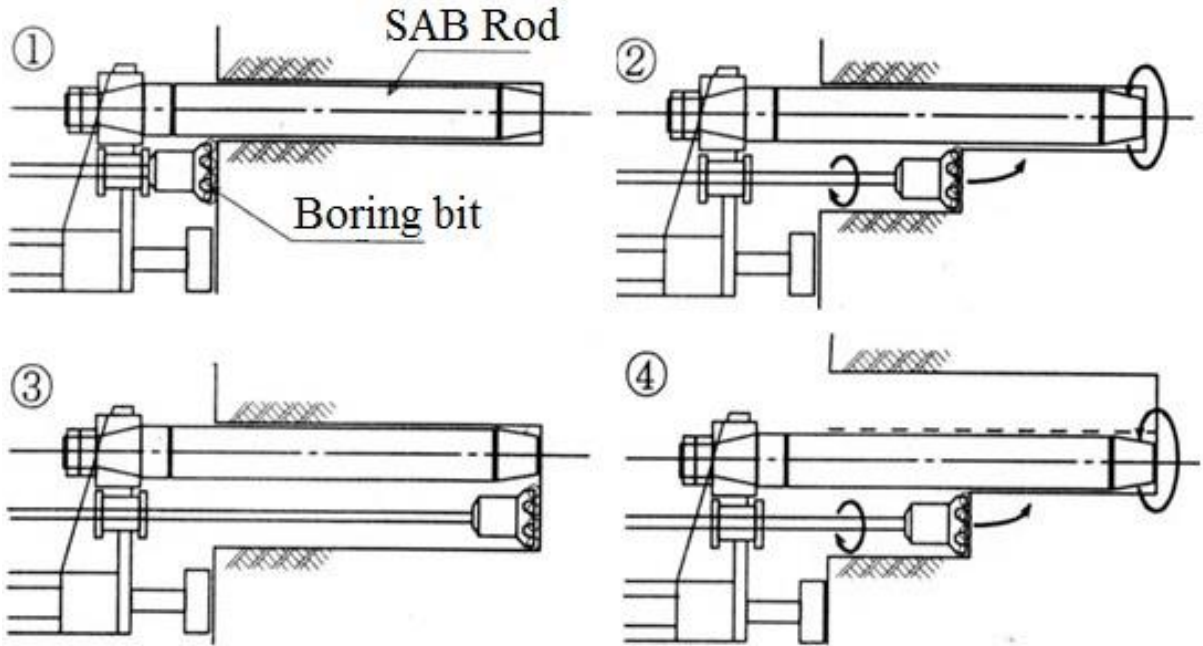


Figure 4.4 - Continuous hole drilling using SAB rod (Noma, Tsuchiya, Hada, & Nakayama, 1991)

As shown in figure 4.4, the SAB (“Spinning Anti Bend”) rod rotates in the opposite direction of the drill bit. This enables both the drill bit to keep in place and still perform efficiently (Noma & Tsuchiya, 2003). A major advantage is that it enables the operators to divide the cross section into smaller sections, as shown in figure 4.7. This creates several free faces in different angles that can be split towards.

4.4 Experience with this method

Drill and split is an excavation method with obvious limitations regarding productivity and cost-efficiency in comparison with established excavation methods such as drill and blast or full profile tunnel boring machines. It is just recently that the excavation method arose due to vibration sensitive situations, which in turn limits the existing experience and available literature regarding the method. Two studies undergone in Japan where the focus was to look upon the efficiency of continuous borehole drilling using the SAB rod are presented in the following sections.

4.4.1 Evacuation tunnel for existing highway tunnel

New fire regulation with stricter requirements towards evacuation in the event of tunnel fire requires construction of new cross cut tunnels between tubes in Japanese highway tunnels. Given their nature as cross cuts, these tunnel sections are both relatively short and constructed in immediate vicinity to existing structures. Additionally, the bedrock on site is comprised of hard rocks with an estimated UCS in the order of 200 Mpa (Noma, Tsuchiya, & Mitsugochi, 2009). These features suggests that drill and split is the most viable option for the situation.

The cross section area for the evacuation tunnels are 20 and 10 m². Because of this, it was only room for one excavator to perform splitting. Borehole configuration and free face forming was done according to figure 4.5.

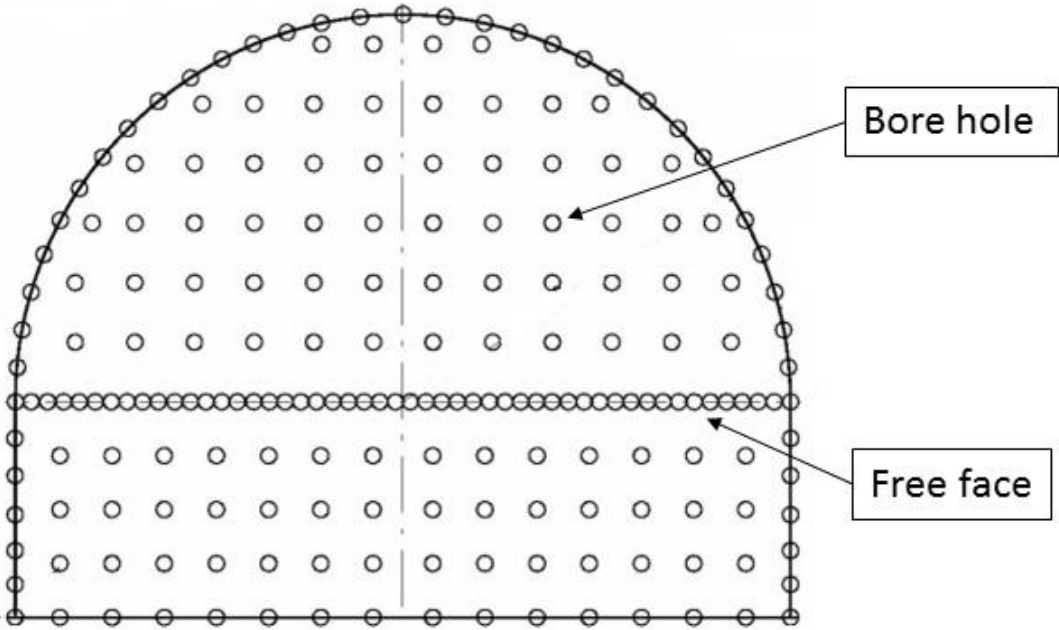


Figure 4.5 - Conceptual borehole configuration for evacuation tunnels, modified after (Noma, Tsuchiya, & Mitsugochi, 2009)

Due to the small cross section area, it was only possible to do continuous borehole drilling in one direction and thus split the tunnel face into two sections. This reduced the time for forming a free face significantly, but at the sacrifice of small distances between split holes because of higher confinement. This was a lesser problem in the 10-m² tunnel than the 20-m² tunnel, causing the tunnels to have a 500×500 and 400×400 mm borehole grid, respectively. Additionally, it was necessary with closer borehole drilling along the contour of the tunnel face for the bigger tunnel (20 m²). This further increased the borehole density in comparison to the smaller cross section tunnel (10 m²).

Time consumption given for this configuration with the different cross section areas are given in figure 4.6.

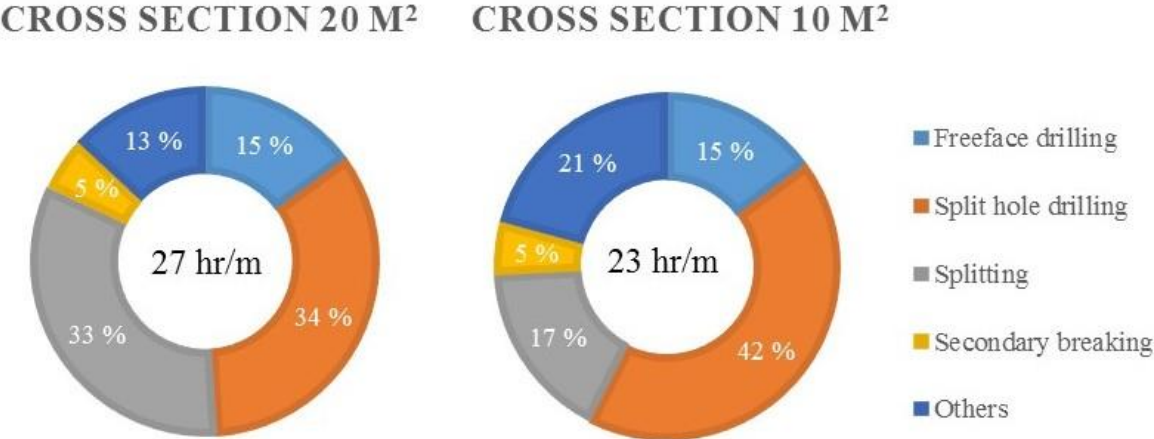


Figure 4.6 - Time consumption for small section tunnels, modified after (Noma, Tsuchiya, & Mitsugochi, 2009)

Figure 4.6 suggests that despite a lower borehole density, the time consumption spent on drilling these holes are higher than for a larger cross section. Two reasons are suggested for this (Noma, Tsuchiya, & Mitsugochi, 2009):

- Split hole drilling was done with a one-boom rig for the 10-m² tunnel, in comparison with a two-boom rig for the 20-m² tunnel
- The capacity of the drifter used for the bigger tunnel has approximately 50% higher capacity than the one used for the smaller

This study identifies drilling rather than splitting as the main time constraint for excavation by drill and split. Based on this study, it is reasonable to believe that for larger cross section areas where a three-boom rig and larger capacity drifter can be used, the percentage associated with split hole drilling would be lower.

4.4.2 Kaminiko tunnel

The Kaminiko tunnel is a 550-meter long two-lane road tunnel located in Hiroshima, Japan. It is located in close proximity to housing areas and in addition, there was many loose boulders located close to the construction site. To avoid rock fall towards housing areas, vibration limits were set. Additionally, the rock mass on site was granite with compressive strength ranging from 100 to 250 MPa.

Because it is a two-lane road tunnel, the cross section area is significantly larger than the previous presented evacuation tunnels with an estimated cross section area of 68 m². Due to the large cross section area, the tunnel face had to be divided into more than two sections for splitting. Therefore, the free face configuration differs from the previous concept:

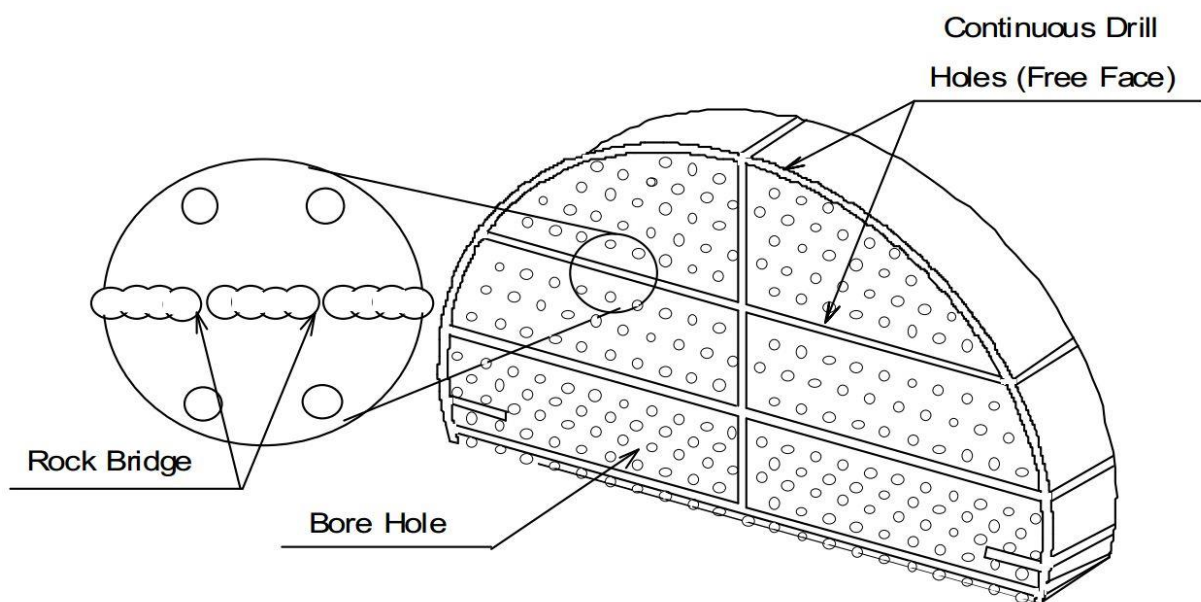


Figure 4.7 - General concept of free face configuration for large cross sections using slot drilling (Noma, Tsuchiya, & Mitsugochi, 2009)

Figure 4.7 show a free face configuration applied for large cross sections. Because of very high rock strength in certain locations, it was necessary to create quite a comprehensive free face. Note that the configuration assumes use of continuous slot drilling. Using horizontal slot drilling in two levels, as well as a vertical line it is possible to create six sections within the tunnel face. The conceptual configuration also assumes continuous drilling along the entire contour and some additional drilling to lessen the confinement in the bottom corners.

According to available information for this configuration, the time consumption solely for free face forming is estimated at 6 hours with an assumed borehole depth of approximately 1 meter

(Noma & Tsuchiya, 2003). This free face configuration is far more comprehensive than previously discussed solutions, and it is highly likely that it would encompass more than 15% of the total time consumption as suggested by figure 4.6. For comparison, the time used for creating free face for the two evacuation tunnels is around 4 hours each.

4.5 Preliminary conclusion from project work

The conclusion from the project work done by the author was based upon theoretical studies of the excavation method, and its assumed applicability for the Follo line project. Key points from this study includes:

- Unlike drill and blast, this method will not create a damage zone around the tunnel profile, which in turn maintains more of the rock mass' self-carrying capacity.
- Accurate drilling is crucial for both a good result and to avoid damaging the equipment
- Establishing a free face is critical for efficiency.
- Optimal borehole configuration is based on a minimum of split holes and maximum utilization of free faces
- Little literature on the method increases uncertainty, but it is likely that operators quickly build up competence during construction

The key points mentioned above is largely based upon background information gained from several key personal and assumptions made by the author. To further investigate the applicability of the method for use at the Follo line tunnels, numerical modelling of the splitting process will be attempted to identify potential rock mass properties that acts as restraint for productivity.

5 Field mapping

Supplementary field mapping was done to assess the rock mass quality and some detailed joint mapping in the area. In addition, relevant rock samples for laboratory testing of elastic parameters were obtained. The mapping was done in and around the Sjursøya tunnel near Sydhavna, Oslo the 11 and 12 of February 2015 by the author in collaboration with representative from NNRA. Site locations for rock quality assessments are shown in figure 5.1 below.

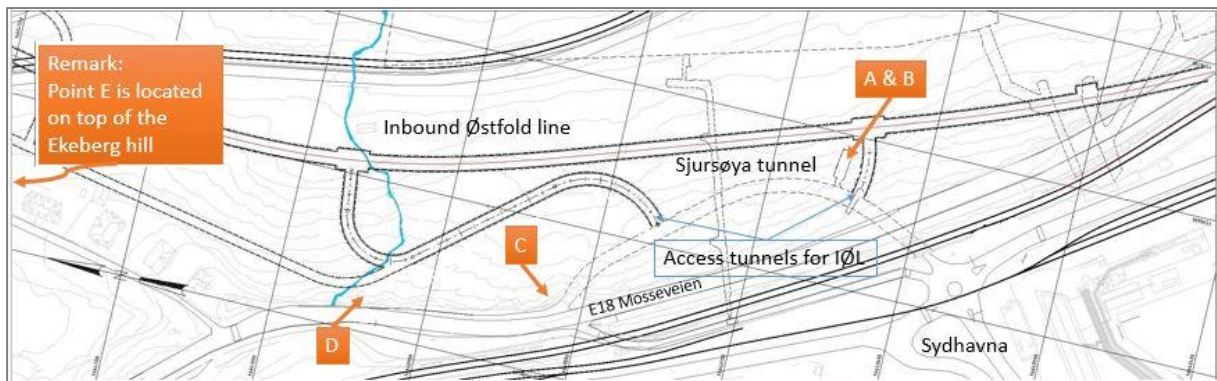


Figure 5.1 - Location for rock quality assessments (modified from internal drawing UOS-30-D-30301 by the NNRA)

As suggested by figure 5.1, the Sjursøya tunnel lies in close proximity to the inbound Østfold tunnel, where a major part of the Drill & Split work will be done. Due to the close proximity between rock assessment site and the planned tunnel alignment, the rock mass classifications are assumed to reflect the actual conditions within this tunnel accurately. According to existing geological maps and interpretations, the rock mass is believed to be similar throughout the project area, with the possible exception of the three-track tunnel that passes through the Ekeberg fault. This suggests that the classifications undergone can be assumed valid even for the other parts of this project that are planned excavated using Drill and Split method.

Field mapping is necessary to assess the general quality of the rock mass, since the rock mass is observed to scale in its in-situ state. Because discontinuities act on a larger scale than what is practically possible to test in the laboratory, the effect of these remain unaccounted for after laboratory testing. As the general stability and mechanical behaviour of the rock mass is largely dictated by extent and character of discontinuities (Nilsen & Broch, 2011), field mapping is essential for a thorough and accurate rock mass classification.

5.1 Classification systems

Rock mass classifications are used to assess numbers to the geology for establishing comparable quality assessments between rock masses in different locations across time. Different systems weights different aspects of the rock mass, which means that some systems may be more suitable for certain situations than other systems and should therefore be chosen accordingly. The rock mass is assessed according to two different classification systems:

- The Q-method
- Geological Strength Index (GSI)

In addition to these, the author recognize the RMR (Rock Mass Rating) system as an alternative to the Q-method. It is standard practice to assess rock mass quality according to the Q-system in Norway, and therefore the statistical basis of Q-values is superior to that of RMR. This causes the Q-system to be a relatable value for workers and personnel experienced in tunnelling in Norway, while the corresponding RMR-value is harder to relate to if one is not used to this system. GSI classification is done due to its simplicity and because it is needed as input parameter to numerical analysis.

5.1.1 Q-method

Barton, Lien and Lunde from NGI first introduced the Q-system in 1974. The initial system was based upon empirical studies of approximately 200 rock tunnels and underground caverns (Nilsen & Broch, 2011). The method has since been revised a number of times to incorporate a larger empirical database and to accommodate modern rock support options (NGI, 2013). Because it originated in Norway, the method is very well suited for Norwegian rock conditions. Consequently, it is widely used in Norwegian tunneling for comparison and rock support decisions.

The parameters included in the classification are as follows (NGI, 2013):

- Rock quality designation (*RQD*)
- Joint set number (J_n)
- Joint roughness number (J_r)
- Joint alteration number (J_a)
- Joint water reduction factor (J_w)
- Stress reduction factor (*SRF*)

The parameters are assigned numbers according to their visual appearance during field mapping. For numerical values and further insight into the different parameters, the author

refers to tables given in Appendix D. 1. Using the assessed numerical values for each parameter, the corresponding Q-value is calculated according to the following equation:

Equation 5-1 - Q-method (NGI, 2013)

$$Q = \frac{RQD}{J_n} \times \frac{J_r}{J_a} \times \frac{J_w}{SRF}$$

The value obtained is called the Q-value for the rock assessed. Based on this value, the rock mass can be classified into categories ranging from exceptionally poor (Q-value less than 0.004) to exceptionally good (Q-value over 400) (NGI, 2013).

A major drawback with this method is that it poorly estimates the quality of weak rock masses (NGI, 2013). In addition, the non-linear scale may lead to confusion, as the value itself is rather meaningless without references or experience with the method. Other drawbacks include a rather conservative rock support scheme, which gives little innovation towards development of new types of support, and that the system poorly accounts for spatial orientation between structures and joints (Nilsen & Broch, 2011).

5.1.2 GSI – Geological strength index

Both the Q-system and RMR was developed with respect to estimations of underground excavation and support, and therefore they include parameters that are not required for estimating rock properties (Hoek, Marinos, & Marinos, 2005). Parameters accounting for groundwater, stress field and orientation of structures should not be incorporated in this rock property classification as they are explicitly accounted for in effective stress numerical analysis. Because of this, a new classification system called GSI arose with the main purpose of characterizing rock mass properties based on simple observations of lithology, structure and discontinuity surface conditions (Hoek, Marinos, & Marinos, 2005). Using a generalized chart (Appendix D. 3), this system offers a quick and preliminary quality assessment of the rock mass in the field. The GSI value is given on a scale from 1-100 where higher value means better quality.

The main value of a GSI assessment comes apparent when a numerical analysis is preformed, because it enables quantification of rock aspects that need to be accounted for in numerical models. Along with parameters obtained in laboratory tests of intact rock core samples, the assessed GSI-value comprises the input parameters needed for performing a numerical analysis based on the Hoek-Brown failure criterion.

The main limitations using this criterion are listed under (Hoek, Marinos, & Marinos, 2005):

- Due to its sole purpose of estimating rock mass strength, it is not applicable for estimating rock support directly
- GSI is not applicable to situations where the mechanical behavior of the rock mass is controlled by anisotropic rock mass properties. E.g. undisturbed slate
- Inappropriate to use in hard rock surfaces where the distance of discontinuity spacing is in the same order as the subjected tunnel cross section
- Inaccurate at great depths where the rock mass structure is subjected to massive stresses and therefore appears intact. Stress induced stability problems can be expected in such situations.

Because of its limitations as a classification system, it is advised to use it as a supplement to other established systems rather than a standalone classification. Assessed values for the locations given in figure 5.1 are given alongside corresponding Q-values in the following section.

5.2 Results

Nearly the entire Sjursøya tunnel is supported with shotcrete lining and concrete segments, which make rock mapping impossible. There was however, a side room inside the tunnel with exposed rock where a couple of rock quality assessment and some detailed joint mapping was possible. The remaining mapping and assessments were taken from a road cut outside the northern tunnel entrance and further north along E18 Mosseveien.

Results of rock quality assessments are summarized in table 5.1.

Table 5.1 - *Q*-value and GSI for a number of locations

<i>Location</i>	<i>A</i>	<i>B</i>	<i>C</i>	<i>D</i>	<i>E</i>
<i>Description</i>	Side room inside Sjursøya tunnel (northern)	Side room inside Sjursøya tunnel (Southern)	Road cut outside northern entrance to Sjursøya tunnel	Road cut along E18 Mosseveien	Road cut beneath school Ekeberg Hill
<i>Q</i> -value	40	28	13	18	16
<i>Classification</i> ⁵	Very good	Good	Good	Good	Good
<i>GSI</i>	80	75	85	75	75

The resulting values given in table 5.1 suggests that the rock quality is of generally good quality. Individual parameters for the *Q*-value assessments are presented in Appendix D. 4.

Detailed joint mapping was performed in the same areas as the rock quality assessments that are given in figure 5.1. Joints were registered in terms of their spatial orientation (strike/dip direction), and a note of other characteristics. Actual measured dip and dip directions are presented in Appendix D. 5. The resulting joint rosette is presented in figure 5.2 below:

⁵ Based on intervals from classification scheme given in Appendix D. 2

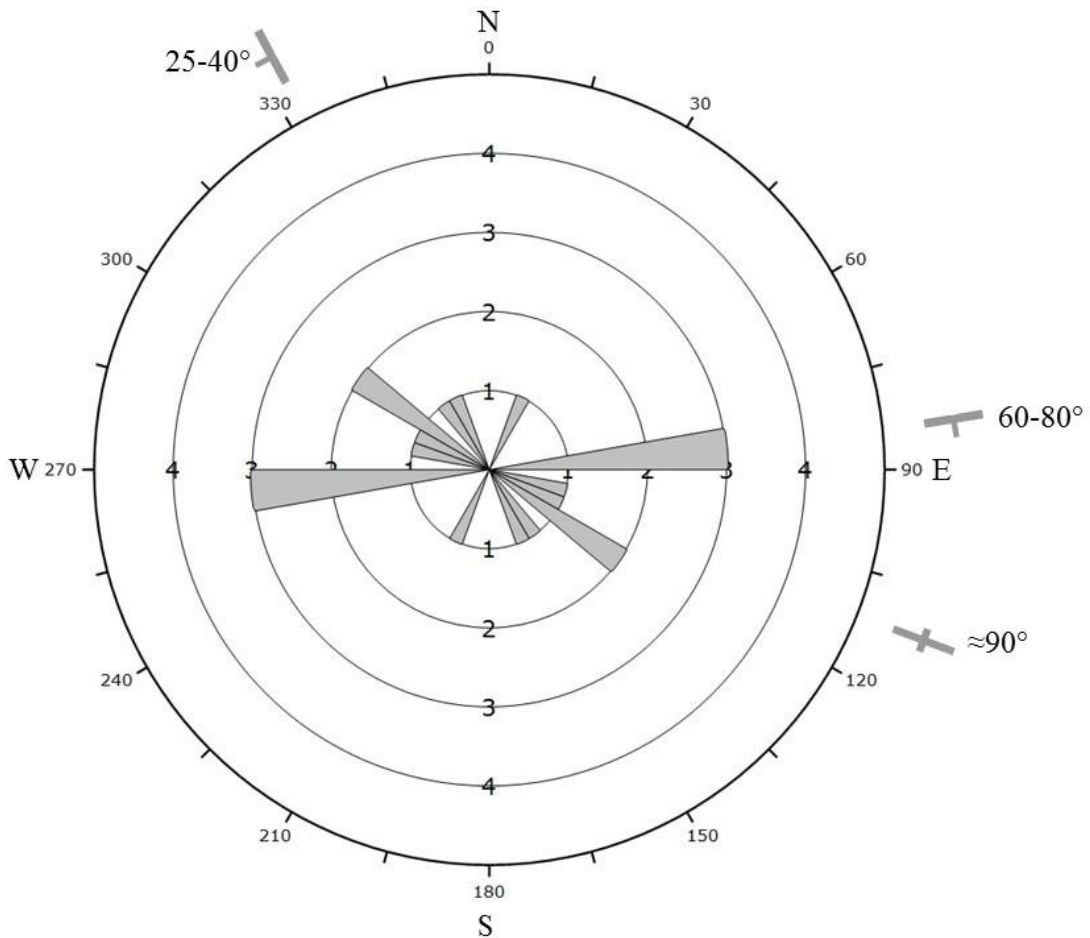


Figure 5.2 - Joint rosette from field mapping

For the joint rosette in figure 5.2, each circle increment represent one strike/dip measurement. It is not registered any joint infill material in any of the joints. Although the total number of registrations are limited, three joint sets can be identified from figure 5.2:

1. East-west strike (N80-90°) and dipping towards south (60-80°)
2. East-southeast strike (N110-120°) and steeply dipping either north or south (>75°)
3. South-southeast strike (N145-155°) and dipping westwards (25-40°)

Note that several of these joint measurements are taken near the fault zone, and could be more affected by tectonic movement than the area in general.

5.3 Evaluation of results from field mapping

The results obtained from this mapping is consistent with previous investigations carried out in the area, and therefore enhances the impression of generally good quality rock mass. It should be noted that it is registered higher Q-values inside the tunnel than at the road cuts outside. This relates to the stress reduction factor, where a confined stress situation within the rock mass is deemed more favourable than near surface. This is because surface near locations lacks overburden that induces stresses, which in turn results in an anisotropic stress field. The GSI system does not account for in-situ stress situation; therefore, this trend is not reflected in the GSI classification.

The joint sets corresponds well with the sets found from previous mapping of the entire project area. Strike and dip of the east-west going joint set 1 can be seen distinctively in the joint rosette plot in figure 3.4, and joint set 3 corresponds reasonably with the previously registered foliation direction (joint set 2 in figure 3.4). Joint set two from this field mapping is not registered as a distinguished joint set in previous mapping. Possible causes for this may be:

- They may represent random joints, as the statistical basis is limited
- Natural local variations. Close proximity to fault zone makes this reasoning plausible

Overall impression from joint property comparisons reveals reasonably well consistency in the orientation measurements, but it is emphasized that the statistical basis is limited. It was not registered any infill material in any of the assessed joints. This is probably related to their surface near nature, which have caused their previous infill – if any at all - to be washed out.

Comparing with assumed Q-values along alignment of the tunnels (table 3.4), the assessed rock mass quality corresponds reasonably well. The location of the assessed rock masses lies close to the later section of the inbound Østfold line tunnel, and assumed rock qualities along its alignment in the nearby area suggests that the previous estimation is somewhat more conservative. Previous estimations consider the rock mass to be “fair”, while the authors’ assessment is slightly more optimistic with generally “good” quality.

6 Laboratory testing

Laboratory testing of core samples remain an important assessment for any underground project. There are several motives for deriving rock parameters in laboratory, including:

- General assessment of rock quality and characteristics
- Assess the difference in properties between different rock masses
- Quantify parameters for use in numerical analysis

Due to the massive size of the Follo line project, several laboratory investigations has already been conducted (see section 3 for details). The main purpose for this round of investigations is to assess parameters for use in the later numerical analysis. Additionally, the results from this laboratory analysis will be compared against previous results for assessment of local geological variation in the area.

Uniaxial compressive test has been undergone for determination of the peak compressive strength, as well as elastic parameters E and ν . The peak compressive strength (*UCS*) denotes the amount of compressive loading the specific rock can take before failing, and is such a strength parameter for the rock. The latter two parameters are essential to describe elastic behaviour of isotropic rock masses under loading, and are therefore necessary input for numerical analyses.

In addition to uniaxial compression test, the density of the rock is decided. This is done according to standard using an accurate weight and exact measurements of core dimensions (ISRM, 1979b). The density is then found from the fraction between weight and volume (g/cm^3).

6.1 Rock sample

The author was responsible for collecting representative rock material suitable for UCS testing in laboratory. The material was collected in accordance with representative from NNRA on the 11th of February 2015 at the location given in figure 6.1. Based on geological maps and current understanding of the local geology, the samples from the location given in figure 6.1 are assumed to reflect rock conditions further inside the Ekeberg hill where the Follo lines and inbound Østfold line are planned.



Figure 6.1 - Rock sample location (figure from google earth)

Two rock samples, roughly 30 kg each, were gathered from a stone pile left behind after road cut excavation work for E18 Mosseveien. The road cut was excavated using drill and blast, which implies that the samples could suffer from blasting damage. In general, rocks suffering from blasting damage contains additional blasting induced fractures, which in turn could give problems with core drilling or affect the test results. However, the preliminary visual inspections revealed few blasting induced joints, and the blocks appeared intact. Because the samples were collected from a pile of stones, their in-situ spatial orientation remains unknown. A picture showing one of the block samples prior to core drilling can be seen in figure 6.2 below.



Figure 6.2 - Block 1 prior to core extraction

Visually, the rock samples appear massive without recognizable foliation planes. Further inspection of the samples revealed some larger lenses of quartz and several quartz-filled narrow joints. A few of the joints has some greenish mineral infill, while other joints were strongly weathered and thus appeared open. Depending on the infilled material strength and relative orientation to testing apparatus, such joints may act as failure planes during uniaxial compressive test.

No thin section analysis of the rock mass has been performed, so exact mineralogy remains uncertain. General appearance and close proximity to previous mapped rock masses suggests that the rock is likely to be a coarse-grained gneiss with a granitic to tonalitic composition similar to those presented in table 3.1. However, the close proximity between sample location and the N-S fault zone (figure 3.1) suggests that the nearby rock mass could be jointed and partly crushed by tectonic movement along this fault. Given that the quartz intrusions found in the block samples were of minor character and that the rock does not present a brecciated texture, it is likely to assume that the samples is to a lesser extent affected by this movement and that it should be denoted as granitic gneiss.

6.2 Sample preparation

The blocks were transported to Rock mechanics laboratory at NTNU in Trondheim, where testing was undergone. Natural water content is unknown, as it is unknown how long the samples lied in the stone pile before collecting, and where the block was situated in relation to groundwater table prior to excavation. However, the water content is assumed to be of limited interest in this case, given the nature of the rock as a low permeable gneiss with predominant joint permeability (Nilsen & Broch, 2011). Accompanied and supervised by PhD-candidate Chhatra Bahadur Basnet, the author prepared the core samples for uniaxial testing on the 3rd of March 2015.

Five core samples is the recommended number of core samples for uniaxial compression test as this is considered to give a sufficient statistical basis and account for natural variations within the rock (ISRM, 1979a). In practice, amount and condition of material –as well as practical considerations such as cost and time consumption- dictates the possible and affordable number of core samples for testing.

The geometry and conditions of the block samples as well as available core drill diameters dictates the possible core sample dimensions. Standard core diameter for uniaxial testing is 54 mm (ISRM, 1979a), while different diameters can be used as long as it is specified. It is emphasized that results obtained from testing on different core diameters should not be directly compared against each other, as the statistical probability of more irregularities in the sample increases as the volume of the sample increases (Hoek E. , 2007). In practice, this tendency would reflect in generally higher compressive strengths for smaller samples (Hoek E. , 2007).

To negate the effect of friction between the rock sample and the apparatus, the core sample should have a length/diameter ratio between 2.5 to 3 (ISRM, 1979a). As the suggested core diameter for uniaxial testing is 54 mm, this gives core lengths between 135 and 162 mm. Irregular shape of the blocks presented challenges as to how many core samples with sufficient length it was possible to drill without selecting a smaller core diameter. In addition to this, a tight time schedule at the laboratory restricted the total rounds of core drillings to five. Three of the cores were extracted from block 1 (Appendix E. 1), while the remaining two were taken from block 2 (Appendix E. 2).

One of the core samples from block 2 proved to have a major discontinuity plane that formed a 45° angle to the core length axis (figure 6.3). This is an unfortunate angle in relation to testing direction in the apparatus, as it may act as a failure plane depending on joint characteristics.



Figure 6.3 - Core #5 with discontinuity plane

From a preliminary visual investigation, the major joint appears planar with a rough surface. The joint also looks weathered with no apparent infill. These joint characteristics implies that the shear strength of this joint is likely to be far less than the compressive strength of the surrounding rock matrix. In combination with an unfortunate angle in relation to testing direction, it is very likely that failure would be initiated along this discontinuity, and not within the rock material. This sample is therefore discarded from further testing.

The remaining four samples were -as far as possible- prepared according to testing standards defined by the International Society for Rock Mechanics (ISRM, 1979a). These core samples can be seen in figure 6.4.



Figure 6.4 - Core samples 1-4 after sample preparation

As shown in figure 6.4, core sample number four is slightly shorter than the other three. This is due to smaller discontinuity planes close to the ends of the sample, which caused rock fragments to break off during preparation. Some larger quartz lenses is also present within this sample. This sample was collected from block 2, from which the already discarded sample 5 also originates. This suggests that there exists failure planes within this block that were not detected during preliminary inspections. The presence of discontinuities and a lower length/diameter ratio than recommended by standards suggests that the results may differ from the other samples. The remaining three core samples are expected to express similar behaviour.

As a summary, dimensions and weight are presented in table 6.1 below.

Table 6.1 - Density of the core samples

Sample no.	1	2	3	4
Height (cm)	13.90	13.93	13.89	11.99
Radius (cm)	2.715	2.712	2.712	2.712
Foliation ⁶ (°)	90°	No apparent	90°	52°
Weight (g)	878.53	883.24	881.86	753.5
Volume (cm ³)	321.84	321.91	320.94	276.95
Density (g/cm ³)	2.73	2.74	2.75	2.72

⁶ Angle between foliation direction and length axis of the core sample

The density is calculated as the ratio between weight and volume of the core samples. As shown in table 6.1, the density is ranging from 2.72 to 2.75, which gives an average of 2.73 g/cm³. This is considered a typical density value for gneiss (Myrvang, 2001).

Closer inspection of the core samples revealed foliation direction within the samples. Generally, the testing is done either parallel or perpendicular to the foliation direction for rock strength assessment. If testing in a non-perpendicular angle, the risk of fracturing along foliation increases significantly. This situation would assess the foliation shear strength rather than the intact rock strength that we are interested in. Table 6.1 suggests that this may be the case for core sample 4, and the influence of this will be evaluated after testing when the failure surface is examinable.

6.3 Test procedure

Uniaxial compressive testing was done at the rock mechanics laboratory at NTNU on the 23rd of March 2015. Testing was performed by laboratory responsible Gunnar Vistnes without the author present. The test procedure involves continuous axial loading of the core samples until failure occurs, while continuously measuring the axial and radial strain of the sample. The measured radial and axial strain is then plotted against the stress. From this curve, the peak compressive strength and elastic parameters Poisson's ratio (ν) and E-modulus (E) are estimated.

6.3.1 Poisson's ratio

To describe the elastic behaviour of isotropic rock during loading, the radial strain of the rock in relation to the axial strain under axial loading must be known. This property is called Poisson's ratio and is defined by the following equation (Myrvang, 2001):

Equation 6-1 - Poisson's Ratio

$$\nu = -\frac{\Delta\varepsilon_r}{\Delta\varepsilon_a}$$

ε_a and ε_r represent the axial and radial strain, respectively. It is important to note that it is not the absolute strain, but rather the differential strain in a defined stress interval. The ratio is estimated from strains measured in the uniaxial compression test. The negative pre-sign is there to express the Poisson's ratio as a positive value, as the radial strain is usually extensional (negative pre-sign), while axial strain is compressive (positive pre-sign) (Myrvang, 2001). Given that this property is strain divided by strain, it is dimensionless.

6.3.2 E-modulus

The E-modulus (also called Young's modulus), is estimated as the ratio between a certain axial stress increment, and the axial strain it induces. As the modulus expresses the proportionality between axial stress and axial strain, it can be regarded as the rigidity of that material. This parameter is given in unit of stress and because rocks generally are very rigid, it is convenient to denote it as GPa within rock mechanics.

As rocks rarely behaves perfectly elastic, the corresponding stress-strain curves are usually not perfectly linear. The reasons for this non-linear behaviour can roughly be summarized into three points (Myrvang, 2001):

- Initial stress loading causes microcraks to close, which causes initial non-linear behaviour
- After initial closing of microcraks, the curve expresses an approximately linear behaviour until it approaches yielding
- Fracture development as the sample is close to yielding gives non-linear behaviour

This non-linear behaviour means that the stress interval of which the E-modulus is determined from must be chosen carefully, as it should be representative for the elastic portion of the rock deformation. Different modules can be calculated depending on the stress interval the gradient is estimated from, but the author choses to estimate the E-modulus from the linear portion of the curve as this is likely to best represent the elastic properties of the rock.

6.3.3 Other parameters and features

In addition to the elastic parameters, the uniaxial compressive strength (UCS) is measured as the peak strength before failure. This value gives a rough strength classification of the rock, and is also an input parameter in numerical analysis.

The post testing failure surface is interesting to investigate because the dominating failure mode can be interpreted. Figure 6.5 shows the different theoretical failure modes (Jaeger, Cook, & Zimmerman, 1969).

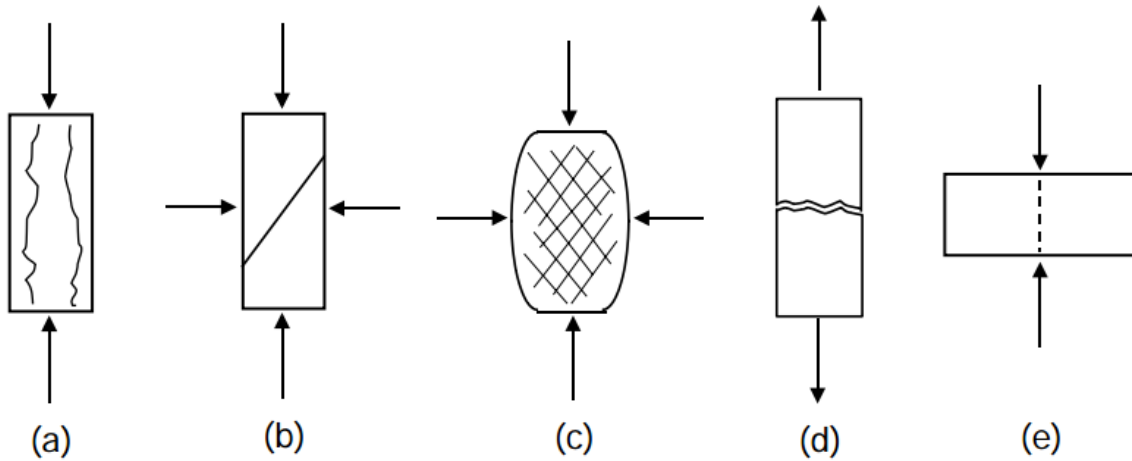


Figure 6.5 - Failure modes. A) longitudinal splitting, b) simple shear, c) complex shear, d) direct extension fracturing, e) induces extension fracturing (Jaeger, Cook, & Zimmerman, 1969)

The failure modes presented depends on loading direction, as represented with arrows in figure 6.5. Given that it is a uniaxial compression test, failure mode 1 is most likely to occur. This mode is called longitudinal splitting and occurs in the loading direction.

6.4 Results

The resulting curves for the four samples can be seen in Appendix E. 3. All curves are cut off shortly after yielding to remove the post peak behaviour. A summary of the calculated and interpreted parameters from these curves are presented in table 6.2 below:

Table 6.2 - Results of UCS test

Sample:	1	2	3	4	Average	Standard deviation
UCS (Mpa)	146.8	163.4	158.8	103.4	143.1	27.4
E-modulus (Gpa)	51.8	48.5	54.5	47.0	50.5	3.4
Poisson's ratio, ν	0.23	0.21	0.28	0.32	0.26	0.05

According to classification by ISRM, rocks with UCS ranging from 100 to 250 Mpa is characterized as very strong rocks (ISRM, 1977). The standard deviation of each parameter is calculated in MS excel from the available selection for use in sensitivity analyses.

6.5 Evaluation of results from laboratory testing

Comparing the results obtained from this analysis (table 6.2) with previous investigations (table 3.2), generally higher compressive strengths are estimated. This parameter can vary a lot depending on sample location and condition of testing material, which is apparent from the difference between sample 4 and the others. This most likely represents natural variation caused by the rock mass' inhomogeneous, discontinuous and anisotropic nature. Because of large variability, a high standard deviation is calculated for UCS. This may have a significant influence on the sensitivity analysis, since the standard deviation of UCS is large in comparison to the other parameters.

The calculated Poisson's ratio is higher than typical values from gneiss/granitic gneiss (0.1 – 0.2 according to (Myrvang, 2001)). It is also slightly higher than previously tested material from nearby locations. Despite a higher than usual value, the difference is assumed to represent natural variation rather than it being error from wrongful measuring or calculation.

Post failure photos of the core samples are presented in Appendix E. 4. Visual investigation of the failure surface indicates that failure occur as splitting or shear fracturing through the material matrix and not along foliation or other existing joints. This validates that it is the intact rock material strength and not joint shear strength that is assessed. The fracture mode for sample 1 and 3 is interpreted as longitudinal splitting, and simple shear fracturing for sample 4. Sample 2 is regarded as a combination between shearing and longitudinal splitting.

7 Numerical analysis

Numerical analysis are preformed to investigate stress distribution and yielding during rock splitting at the tunnel face. The scope of this study is to investigate the sensitivity of different rock mass parameters towards the splitting process, and to do an overall assessment of the applicability of “Drill & Split” at the Follo line project. This will in turn improve the current understanding of splitting in different ground conditions. Figure 7.1 illustrates the step-by-step principle behind numerical modelling.

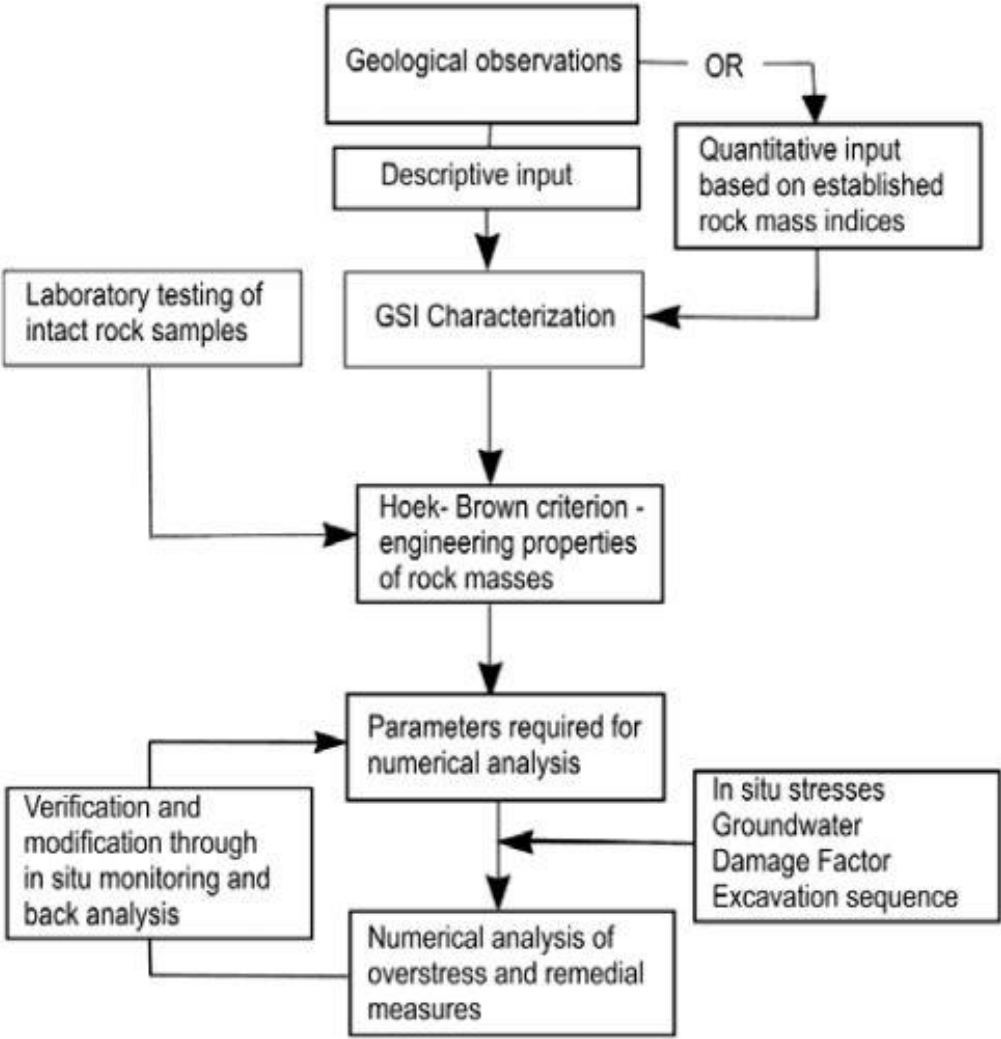


Figure 7.1 - Flow chart of numerical analysis (Hoek, Carter, & Diederichs, 2013)

Numerical modelling involves several steps in order to give a satisfying result. In order to perform a meaningful analysis, it is critical to replicate the site geology as accurately as possible. This acknowledgement gives root to the popular phrase “crap in – crap out”, which underlines the importance of valid input data for a meaningful analysis.

7.1 General

Numerical modelling is an analytical approach for estimating stress distribution and calculate deformations around underground excavations. Situations encountered in rock mechanics generally involves a range of rock parameters and a complex geometry, which in sum makes it impossible to perform an mathematical assessment manually. Consequently, computer software that can model custom geometry within an interpreted geological situation is developed for personal computers. The basic principle behind numerical modelling is to discretize the rock mass into numerous small elements, to which individual properties are calculated. Although a wide range of different codes exists, the discretization process is approached using one of two principal models (Nilsen & Palmstrøm, 2000):

- Continuous models
- Discontinuous models

In continuous modelling, the rock mass is essentially treated as a continuous medium with only a limited number of discontinuities influencing (Nilsen & Broch, 2011). This is the most common way of modelling. Continuous models are further divided into two sub-groups:

- Differential models such as Finite Element Method (*FEM*) or Finite Difference Method (*FDM*)
- Integral methods such as Boundary Element Method (*BEM*)

Main difference between these applies to which part of the model that is discretized. For differential models the entire rock mass is discretized, while only the boundaries are discretized for integral models.

Discontinuous models treats the rock mass as a discontinuous medium by dividing the rock mass into individual blocks. Consequently, this method is assumed to better represent the rock nature (Nilsen & Palmstrøm, 2000). The Distinct element model (*DEM*) is the most prominent method in this category.

7.1.1 *Phase*² code

*Phase*² is a program that is created for solving a wide range of geotechnical and civil engineering problems related to stress distribution and displacements around underground openings. The program uses finite element method for calculation, and it operates in two dimensions. Other features include (Rocscience, 2014):

- Elastic or plastic materials
- Probabilistic analysis
- Incorporates both Hoek-Brown and Mohr-Coulomb failure criteria (among others)
- Multi-stage excavations
- Support analysis (bolt pattern, concrete/shotcrete lining etc.)

There are three basic program modules in *Phase*²; model, compute and interpret. The model modulus is where the user defines and edits any input data going into the model. This includes material parameters, in-situ stresses, geometrical boundaries and more depending on the situation. Next, the model is processed in the compute module before the resulting model is presented for interpretation in the interpreted module (Rocscience, 2014).

7.1.2 Failure criterion

The numerical modelling that will be attempted in *Phase*² consists of deliberately inducing directional tension failure within the rock mass. *Phase*² offers several options as to which failure criterion it should evaluate the situation up against, with the Mohr-Coulomb and Hoek-Brown as the two most prominent choices. A simple sketch illustrating the difference in these criteria are summarized in figure 7.2 below.

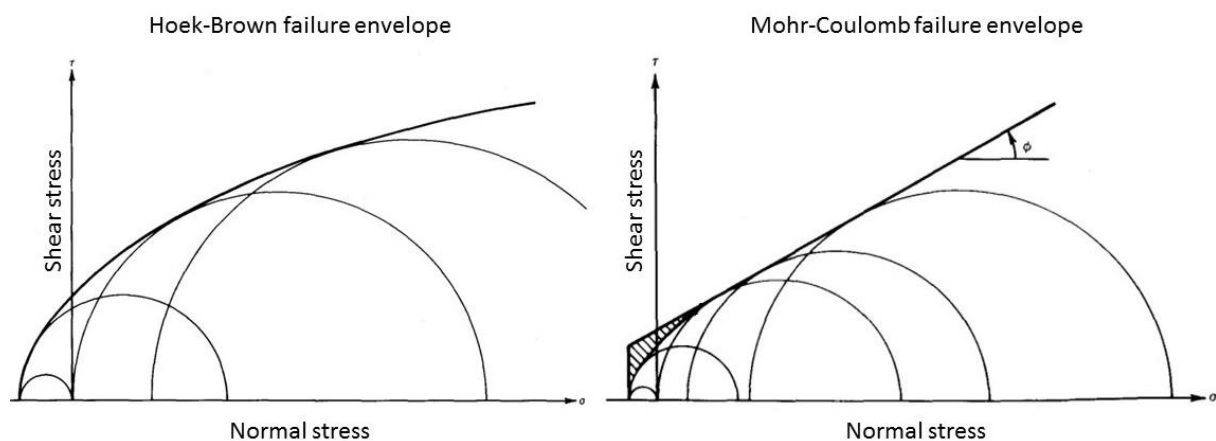


Figure 7.2 - Hoek-Brown and Mohr-Coulomb failure envelope (Jaeger, Cook, & Zimmerman, 1969)

From figure 7.5, the most apparent difference between the criteria is the non-linear (Hoek-Brown) versus linear (Mohr-Coulomb) curvature. This is especially noticeable in the tensile region (negative normal stress); where the Mohr-Coulomb curve need to be cut off in order to present realistic results. Additionally, the parameters needed for creating the Mohr-Coulomb curve (friction angle, ϕ and cohesion, C) is hard to obtain in laboratory, while the basis for determining Hoek-Brown parameters are easily estimated from laboratory testing (Hoek E. , 2007). Although conversion formulas between Hoek-Brown and Mohr-Coulomb parameters exist, these are not 100% accurate for all situations and thus adds extra uncertainty to the analysis. Because of the reasons mentioned above, the author recognizes the Hoek-Brown criterion as the most suitable for use in the following analysis.

The generalized Hoek-Brown failure criterion follows from the following equation:

Equation 7-1 - Generalized Hoek-Brown failure criterion (Hoek, Carranza-Torres, & Corkum, 2002)

$$\sigma_1' = \sigma_3' + UCS \times \left(m_b \frac{\sigma_3'}{UCS} + s \right)^a$$

Where σ_1' and σ_3' are the maximum and minimum effective stresses at failure and m_b , s and a are rock constants. These are defined by the following equations:

Equation 7-2 - Hoek-Brown m_b parameter (Hoek, Carranza-Torres, & Corkum, 2002)

$$m_b = m_i \times \exp\left(\frac{GSI - 100}{28 - 14D}\right)$$

Equation 7-3 - Hoek-Brown s parameter (Hoek, Carranza-Torres, & Corkum, 2002)

$$s = \exp\left(\frac{GSI - 100}{9 - 3D}\right)$$

Equation 7-4 - Hoek-Brown a parameter (Hoek, Carranza-Torres, & Corkum, 2002)

$$a = \frac{1}{2} + \frac{1}{6} \times \left(e^{-\frac{GSI}{15}} - e^{-\frac{20}{3}} \right)$$

The equations above suggests that the following parameters need to be assessed in order to construct failure envelopes:

- UCS – Uniaxial compressive strength
- m_i – intact rock constant based upon rock type (Hoek E. , 2007)
- GSI – Geological strength index (Hoek, Carter, & Diederichs, 2013)
- D – Disturbance factor due to blast damage and stress relaxation (Hoek E. , 2007)

7.2 Analysis assumptions

In order to present a meaningful analysis, the input need to replicate actual conditions as accurately as possible. As some of the parameters and choices are hard (or even impossible) to quantify, some assumptions must be made. This section is subdivided into assumptions regarding rock properties and assumptions toward modelling of the splitting process.

7.2.1 Rock properties

The gneiss in the Ekeberg hill is assumed to be of homogeneous nature and express isotropic mechanical behaviour. Average rock properties estimated from laboratory testing are summarized in table 7.1. To account for geological uncertainty, standard deviation for the given values are also calculated for use in probabilistic sensitivity analysis.

Table 7.1 - Parameters for input in Hoek-Brown failure criterion

	<i>UCS (Mpa)</i>	<i>E_i (Mpa)</i>	<i>ν</i>	<i>GSI</i>	<i>m_i</i>	<i>D</i>
<i>Average value</i>	143	50450	0.26	78	28	0
<i>Standard deviation</i>	27	3400	0.05	5	5	0

UCS, *E_i* and *ν* are all found from laboratory analysis, while *GSI* was assessed on site. The material constant (*m_i*) and disturbance factor (*D*) are assigned according to tabulated values (Appendix F. 1 and Appendix F. 2). It is assumed undisturbed rock mass, and that the rock type is foliated gneiss.

The underlying assumption is that the rock mass exhibit isotropic behaviour that can be expressed by the Hoek-Brown failure envelope. In order to model this behaviour, the *GSI*, *m_i* and *D* parameter (table 7.1) must be translated into the equivalent Hoek-Brown parameters *m_b*, *s* and *a*. These relationships are given through equation 7-2, equation 7-3 and equation 7-4 in section 7.1.2.

The program *RocLab* that is incorporated with *Phase2* automatically calculate Hoek-Brown parameters based on *GSI*, *m_i* and *D* using the equation mentioned above. Resulting output parameters can be seen in figure 7.3.

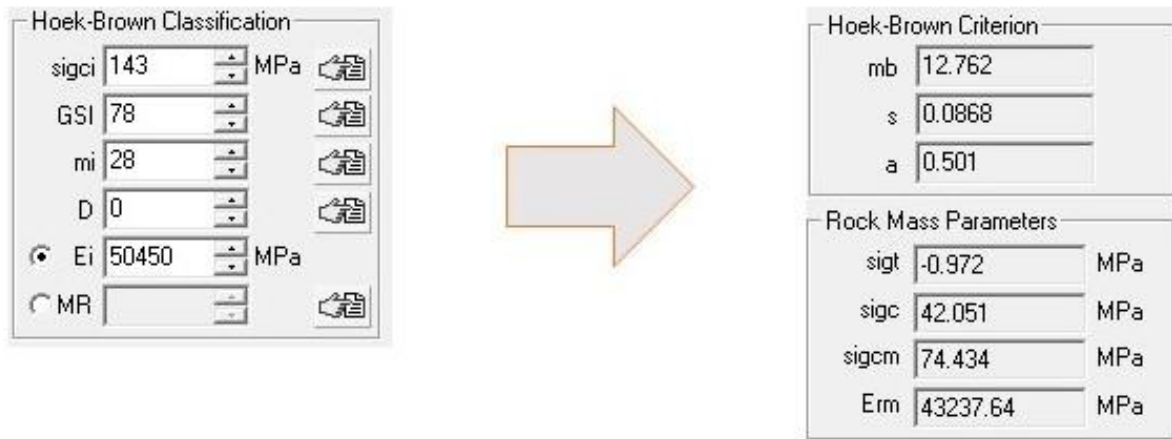


Figure 7.3 - Rock mass properties estimated in RocLab

Note that in addition to the Hoek-Brown parameters, RocLab also calculate an equivalent rigidity modulus for the rock mass (E_{rm}) in figure 7.3. This is necessary because the E-modulus from laboratory testing (E_i in table 7.1) signifies the rigidity of intact rock, which is not representable for a rock mass that is set with discontinuities.

7.2.2 Residual rock parameters

Phase² gives the option of modelling the rock material as elastic or plastic. If the rock material is modelled elastically, the rock strength parameters are used only for calculating strength factors as the rock mass cannot theoretically yield. Although the strength factor can be regarded as yielding, this situation does not account for a changed stress field and lowered rock mass strength after yielding. A plastic material type uses the strength parameters after yielding occurs and allows changes in the stress distribution stage by stage. Given that this analysis is trying to replicate a splitting process, yielding is both necessary and desirable. It is assumed that a plastic analysis in *Phase²* represents actual conditions better than an elastic analysis.

A plastic material analysis offers the possibility of assigning residual Hoek-Brown parameters that applies after yielding occur. To determine these parameters, extensive testing beyond the scope of this thesis is required. Consequently, assumptions regarding residual parameters are necessary. After careful consideration and discussions with supervisor, it is found reasonable to assume that only a minor strength reduction occurs after splitting. This is because the splitting process only involves tension fracturing of one joint with no disturbance to surrounding rock mass. It is assumed that the additional tension fracture caused by splitting has a minimal effect upon the overall rock mass strength, and consequently the residual parameters are assumed just slightly lower than intact properties.

It is possible to assign residual parameters for GSI , D and m_i , or directly modifying the Hoek-Brown parameters m_b , s and a . The author chooses to assign residual values for GSI , m_i and D , which can be seen in figure 7.4.



Figure 7.4 - Residual parameters estimated in RocLab

Note that both the disturbance factor and m_i remains constant, while a lower residual GSI of 65 is assumed. Compared with intact parameters in figure 7.3, this gives slightly lower Hoek-Brown parameters. The corresponding Hoek-Brown failure curves for intact and residual rock mass are presented in figure 7.5 below.

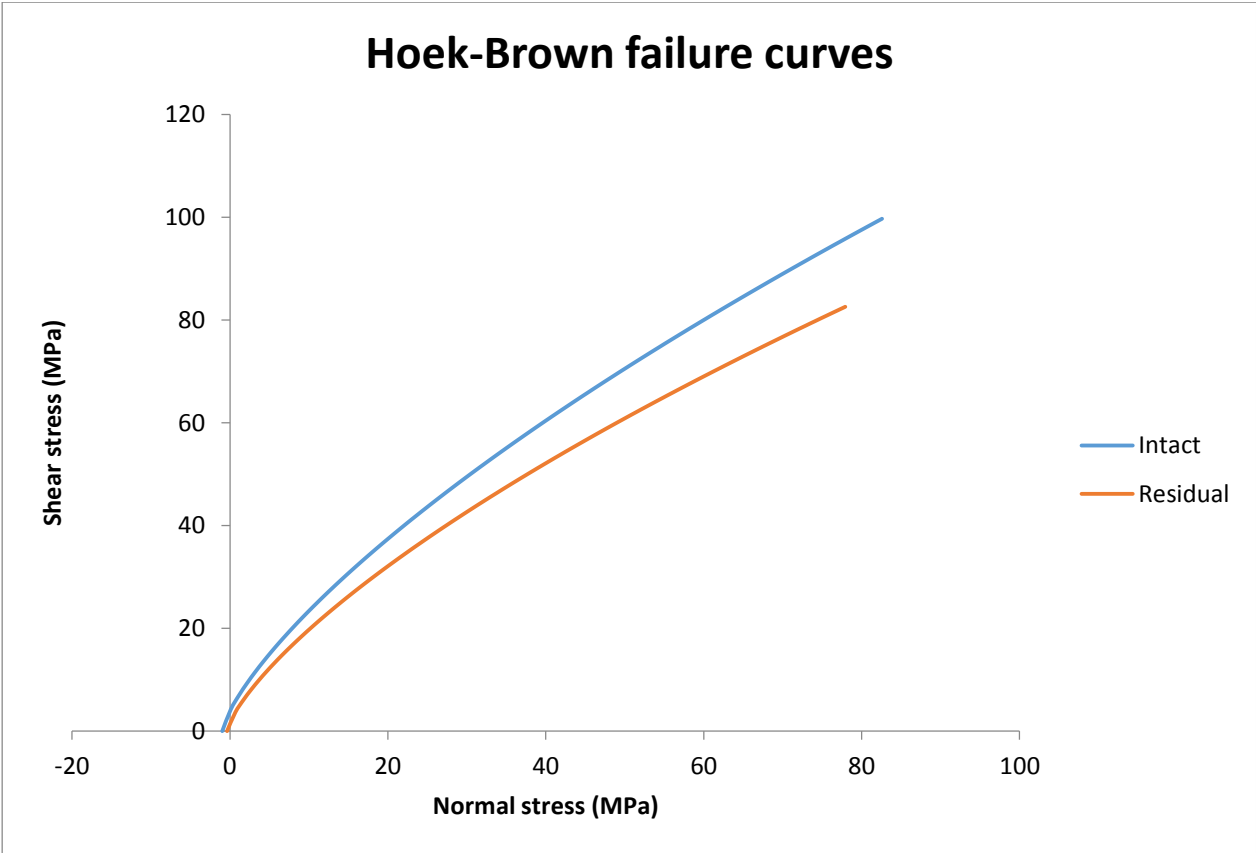


Figure 7.5 - Hoek-Brown failure envelopes for intact and residual rock mass

7.2.3 Splitting process

Because *Phase²* is a program that works in two dimensions it assumes infinite depth inwards. This is not a realistic scenario, as both the boreholes as well as the cut is of limited depth. In reality, this situation gives less fracturing near the bottom of the borehole due to a more confined situation. The model is therefore only realistic at the uppermost part of the borehole.

Some other assumptions regarding the splitting process are listed under:

- Splitting force given in product brochure exceeds the rock strength by far. It is therefore assumed that only the initial splitting in the borehole can be modelled by staged loading with small stress increments
- The working area of the splitter wedge is approximated to be half the borehole surface area (one quarter on each side). This situation is illustrated in figure 7.6
- The splitting force is assumed to work in opposite directions on each side, and to be of equal magnitude
- For all analysis, it is assumed that the splitting equipment is similar to the one presented in Appendix C. 1. This involves splitting boreholes with a diameter of 76 mm.
- Initial splitting occurs in the borehole closest to the cut.

Figure 7.6 illustrates the load applied in the borehole:

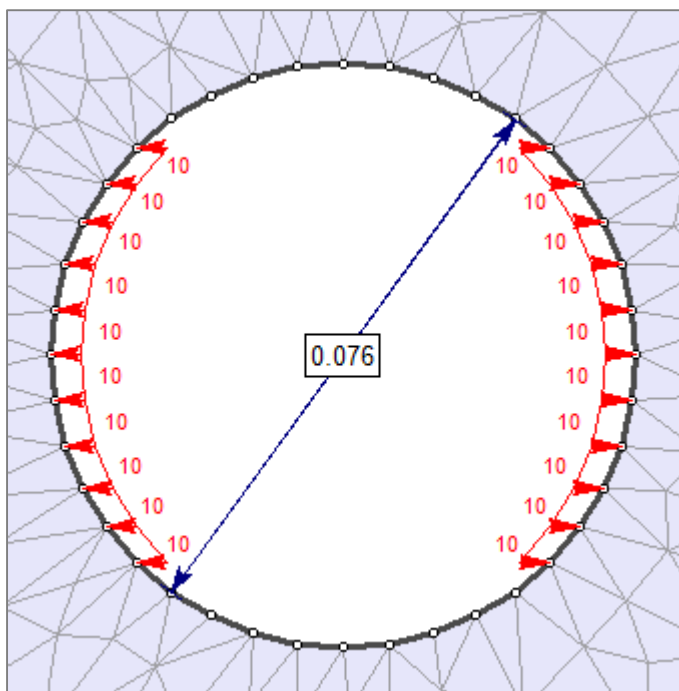


Figure 7.6 - Load applied inside the borehole. This is the initial loading of 10 Mpa

The situation simulated in figure 7.6 assumes that expansion and crack propagation is restricted only by the strength of surrounding rock mass and stress field. In reality, the splitting process is limited by a maximum expansion of the wedge rather than a lack of thrust. This situation is not possible to model in *Phase*². A model with staged loading is assumed to represent the initial splitting and crack propagation fairly in the early stages, but may give unrealistic scenarios as the load increases. The reason for this is that it is not possible to model a maximum expansion induced by the load, and therefore *Phase*² would assume total failure of the rock mass when maximum splitting force is applied.

Due to the uncertainties mentioned above and limited data on actual performance of the splitting process, it is necessary to downscale the situation from looking at the entire face to looking at the situation in immediate proximity to the free face. Especially the limitation of not being able to model a maximum expansion is regarded as a restraint from being able to model the actual situation properly. The analysis will therefore focus on splitting in a limited number of boreholes close to the free face, rather than excavating the entire cross section.

7.3 Free face design

Free face forming is crucial for efficiency of Drill & Split. There are several ways of obtaining free faces in the tunnel face, for insight see section 4.3.2. Depending on the method of choosing, the final design of the cut varies. For this analysis, the fracture propagation for the following three different free face configurations are investigated:

- Quadratic box (2×2 m)
- Circular cut with 1.5 meter diameter
- Continuous line drilling with a spacing similar to the borehole diameter (76mm), and a length of 4 meter.

These different configurations can be seen in figure 7.7 and are assumed to cover the variety of free face forming designs mentioned in section 4.3.2. The splitting holes are aligned in a straight vertical line 0.5 meter away from the free face, with a vertical spacing of 0.5 meter as well.

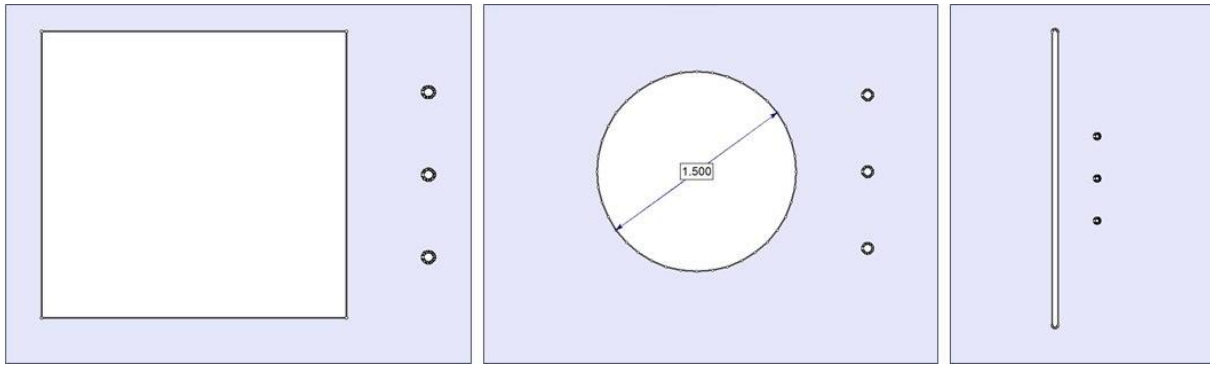


Figure 7.7 - The three different cut configurations. A) Box, B) circular and C) line

For all the different configurations, the load is applied horizontally in the middle borehole. This is assumed to induce tension fractures between boreholes before bending towards the free face.

The entire analysis is staged into eight separate stages as follows:

Table 7.2 - Stage configuration

Stage 1	Stage 2	Stage 3	Stage 4	Stage 5	Stage 6	Stage 7	Stage 8
In situ prior to excavation	Excavate free face	Excavate the three boreholes	10 MPa load each side	20 MPa load each side	30 MPa load each side	40 MPa load each side	50 MPa load each side

This is assumed to represent the actual situation realistically. The load increment of 10 MPa for each cycle is found by a try-and-fail approach under idealised conditions. This means that the actual experienced splitting force in a real life situation may differ from these values.

For this initial analysis, a hydrostatic stress field of magnitude 5 MPa is assumed for all configurations. This is done to neglect the influence of the external stress field and thereby isolate the splitting load as the single variable unit. The results are interpreted in terms of yielded zones. The yielded zones represents zones within the rock mass that fail in tension during incremental loading inside the borehole.

7.3.1 Results from cut configuration

Table 7.3 on the following page summarizes the fracture propagation from load stage 1 to 5 for the three different free face configurations. Figure 7.8 gives the yield contour colours.

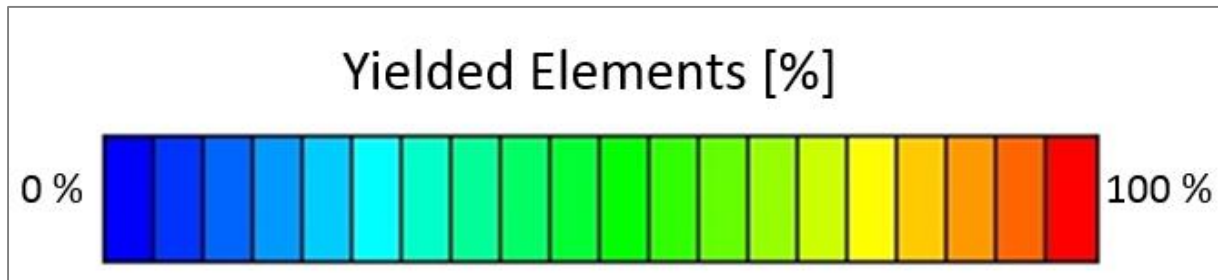


Figure 7.8 - Contour colouring for yield figures

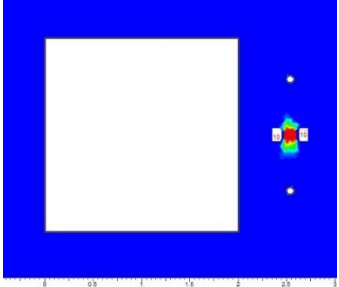
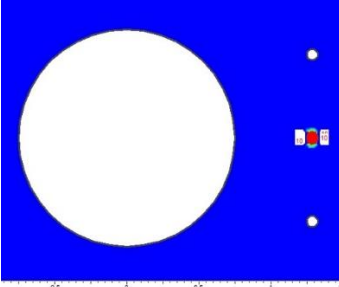
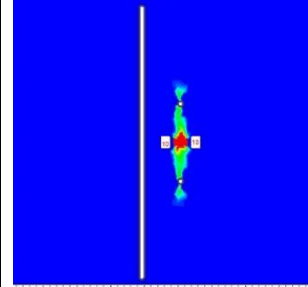
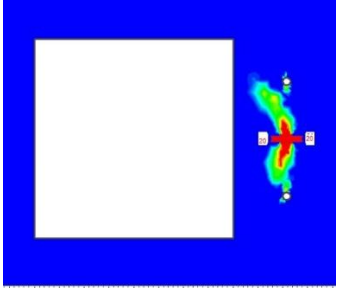
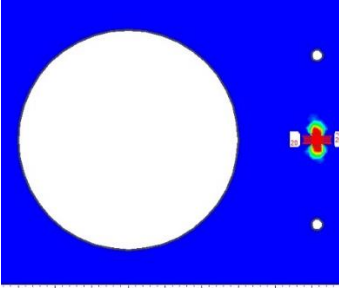
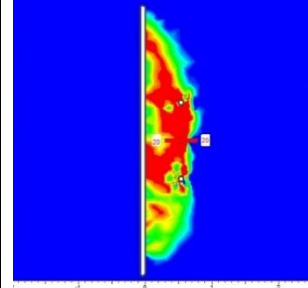
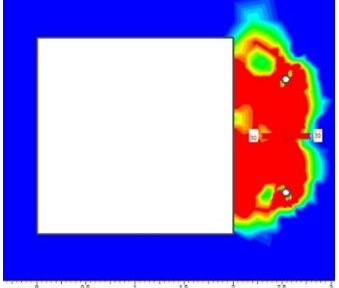
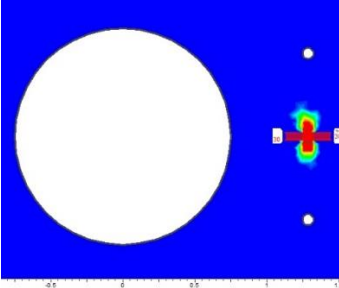
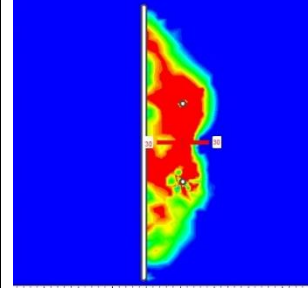
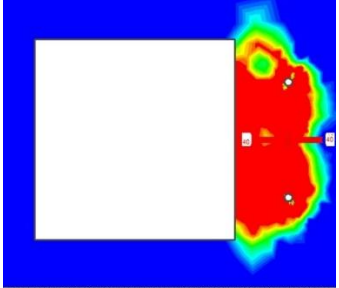
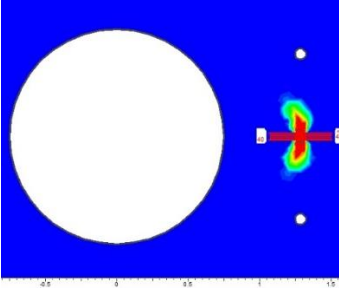
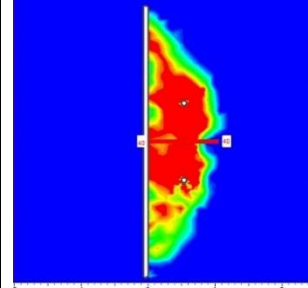
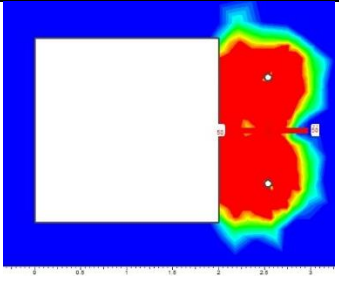
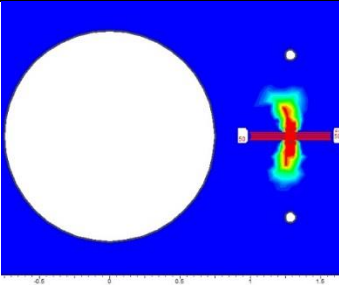
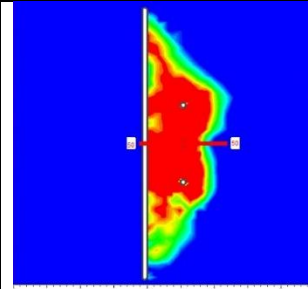
Fracture propagation for the configurations before total failure suggests that tensile fracturing occur between boreholes perpendicular to the loading direction. This is an important accomplishment, as it verifies the underlying assumption that the initial splitting process actually can be reasonably modelled with a finite element program such as *Phase*².

Further investigation of the fracture propagations in table 7.3 reveal large differences between when total yielding through to the free face occur for the different free face designs:

- Quadratic design fails between 20-30 MPa loading
- Circular design does not fail. Heavier loading than 50 MPa, or different borehole configuration needed
- Line design yields between 10-20 MPa, and even at 10 MPa a distinct tensile joint between splitting boreholes occur.

The preliminary conclusion from this testing suggests that a line configuration is beneficial toward splitting, and may therefore be preferable in a real life situation. Poor breaking for a circular free face suggests that a different design should be considered. An analysis of alternative borehole configurations around the circular free face is presented in the following section to further investigate this situation.

Table 7.3 - Fracture propagation for different free face design

Load	Quadratic design	Circle design	Line design
10 MPa			
20 MPa			
30 MPa			
40 MPa			
50 MPa			

7.3.2 Alternative circular cut

Results from previous analysis (table 7.3) suggests that a circular design gives poor breaking in comparison to other designs under equal conditions. Consequently, a redesigned borehole configuration based on the same free face design is developed. In this situation, the boreholes are aligned in a curve around the circular opening, not in a straight line. This configuration gives a constant distance between boreholes and the free face, and is assumed to represent a real life borehole configuration more realistically. In addition, the absolute distance between the boreholes and the free face is varied. Three different borehole configurations are investigated:

- a) Boreholes in arc with 0.5 meter spacing
- b) Boreholes in arc with 0.4 meter spacing
- c) Boreholes in arc with 0.3 meter spacing

The different configurations are visualized in figure 7.9 below:

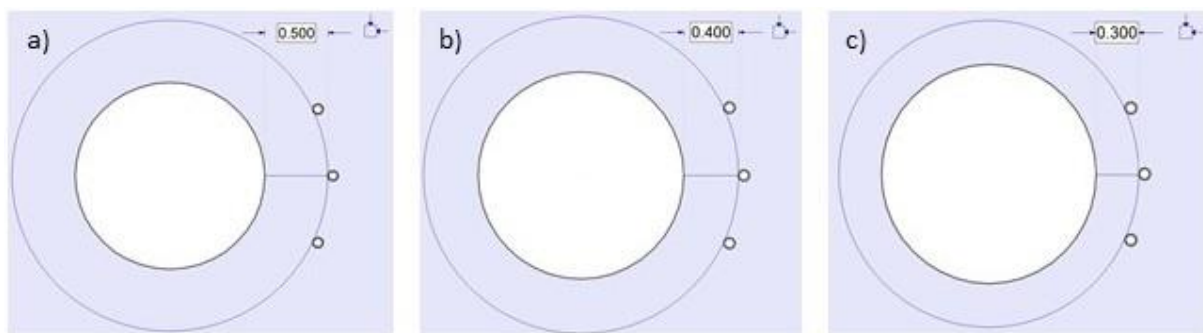


Figure 7.9 - Alternative borehole configurations for circular free face

For all these configurations, rock parameters, stress field and loading remains as for previous analysis. For details regarding input parameters, it is referred to previous sections and tables. For comparison between the configurations, table 7.4 summarizes the fracture propagation for each load increase. The total number of yielded elements at the final loading stage is also included in the bottom row of table 7.4 for quantifiable comparison. The results can be seen on the following page.

Table 7.4 - Results from alternative borehole configurations around circular free face

Load	Configuration a (0.5m)	Configuration b (0.4m)	Configuration c (0.3m)
10 Mpa			
20 Mpa			
30 Mpa			
40 Mpa			
50 Mpa			
Yielded elements	187	194	347

Comparing the situation of a straight (table 7.3 – circle) versus a curved (table 7.4 – configuration a) borehole alignment, it is apparent that just aligning the boreholes in an arc with constant distance towards the free face has limited effect. Consequently, it was necessary to reduce the spacing between boreholes and free face.

As suggested in the final load stage in table 7.4, decreasing the spacing between boreholes and free face has a positive effect on splitting efficiency. However, the differences between configuration (a) (0.5 m) and (b) (0.4 m) remains very small – as evident by the numbers of yielded elements. Even for configuration (b), the effect of altering the borehole alignment and spacing does not result in sufficient splitting between boreholes and towards free face. The situation at the final loading stage in configuration (b) (50 MPa load) is close to create tensile failure between boreholes, and it is likely that a further increase would have provided failure between splitting boreholes.

Further decrease in spacing to a distance of 0.3 meter (configuration c) provides even more fracturing, and the situation in the final load stage seem to be on the verge of total failure. A decrease from 0.5 to 0.3 meter spacing equals 40% reduction, which in turn would require drilling of significantly more boreholes. Additionally, a spacing of 0.3 meter is below the minimum recommended borehole spacing, as it increases the risk of borehole deviation (Ståhlbåge, 2014).

The differences between a circular free face and line or quadratic design remains significant even after reducing the spacing and aligning the splitting boreholes in an arc around the free face. Following analysis of parameter sensitivity will therefore assume a borehole configuration that utilizes continuous borehole drilling in a line (figure 7.7 C).

7.4 Rock parameter sensitivity analysis

Sensitivity analysis is performed to assess influence of various rock parameters. All analysis in this section assumes a line free face configuration as in figure 7.7 C. The parameters are first varied individually, before an accumulated analysis is performed. The assessed parameters are presented in table 7.5:

Table 7.5 - Parameters for sensitivity analysis

Parameter	Average value	Standard deviation (σ)	Standard deviation % of average value
<i>UCS (Mpa)</i>	143	27	19
<i>E_{rm} (Gpa)</i>	43	3	7
<i>GSI</i>	78	5	6
<i>v</i>	0.26	0.05	19
<i>mi</i>	28	5	18

All the respective standard deviations except from the rock mass rigidity constant, E_{rm} are calculated from the data sample gained from laboratory testing and field observations. E_{rm} is assumed to have a variation distribution similar to the intact rock rigidity (E_i), which result in a standard deviation of approximately 3 Gpa.

Given the relative small sample pool, the standard deviation may be strongly affected by individual values. The last column illustrates the percentage the standard deviation constitutes out of the average value. A larger value here increases the variability of that sample and consequently increases the likelihood for that parameter to dominate the results relative to other parameters with a lower percentage.

7.4.1 Individual sensitivity analysis

Individual sensitivity refers to only applying a standard deviation of one of the parameters listed in table 7.5, while all other parameters and the geometry is kept constant. This makes it possible to assess the influence of each parameter separately and compare the results against the other parameters. The results are interpreted in terms of no. of yielded elements. Figures of fracture propagation for all parameters are given in Appendix F. 3 – Appendix F. 7. Their corresponding yield curves illustrating the number of yielded elements per stage are presented on the following pages.

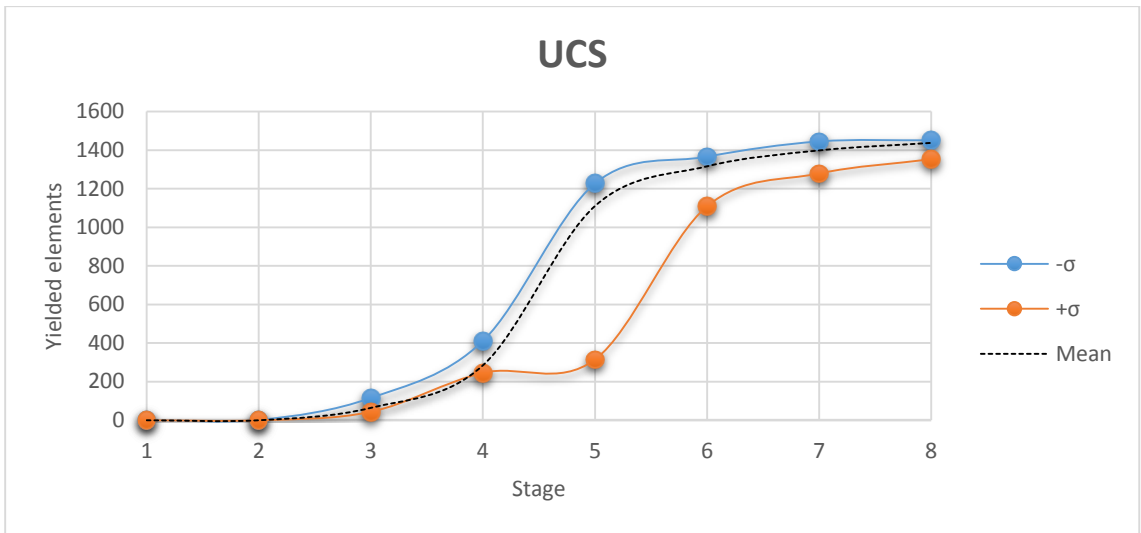


Figure 7.10 - Influence of UCS

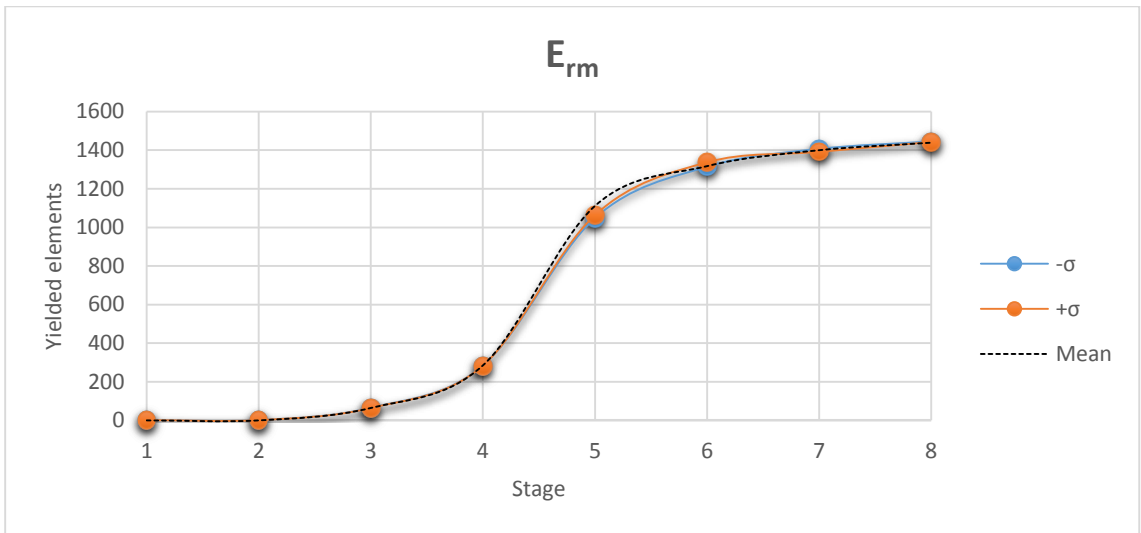


Figure 7.11 - Influence of E_{rm}

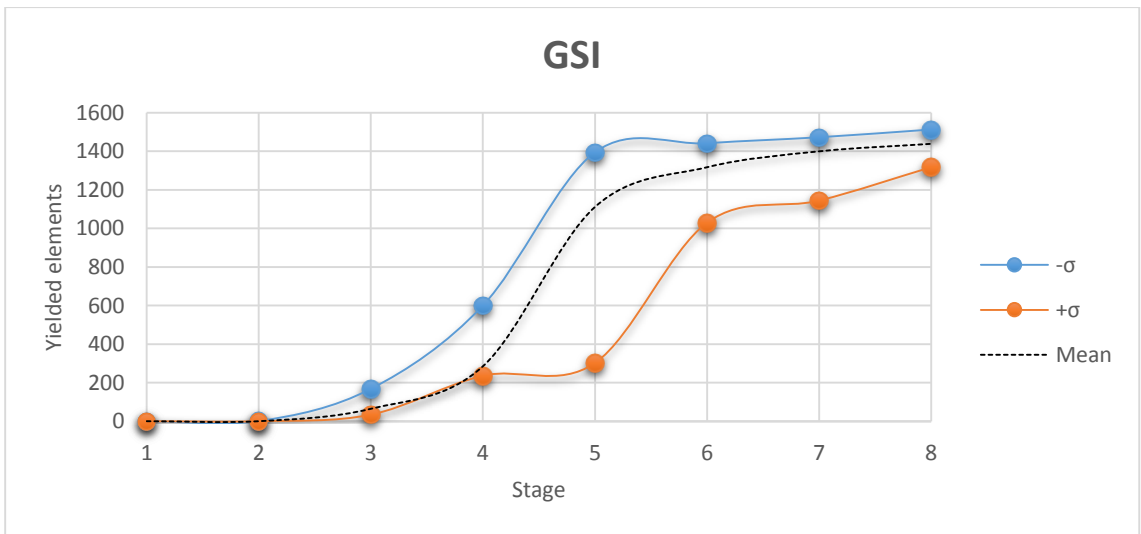


Figure 7.12 - Influence of GSI

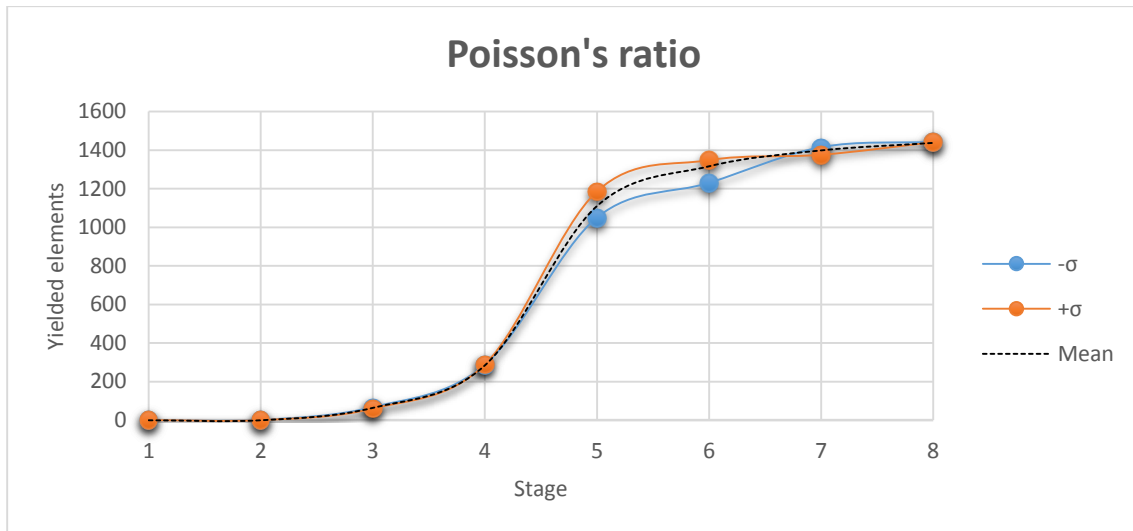


Figure 7.13 - Influence of ν

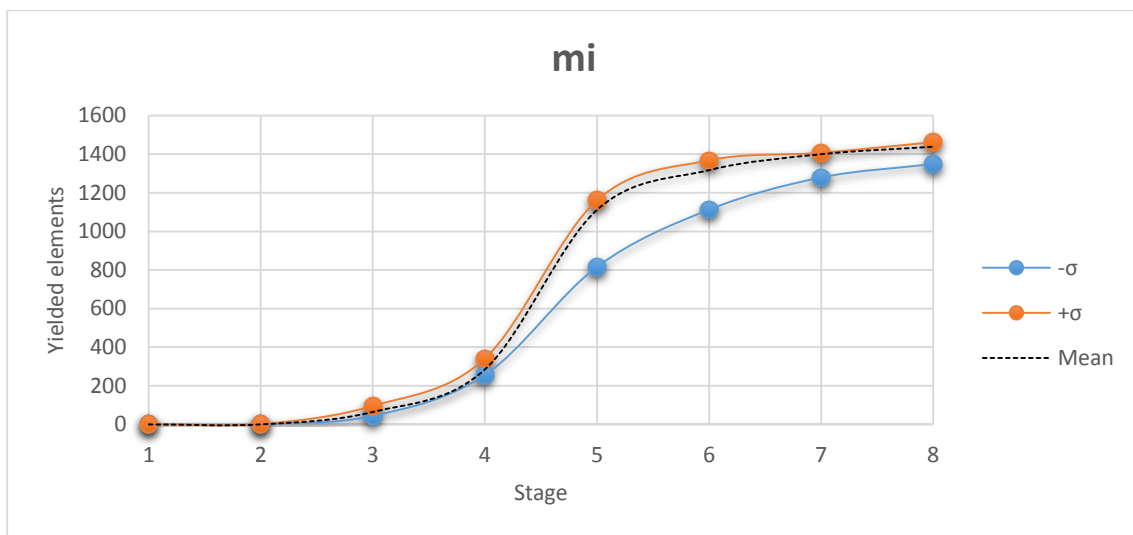


Figure 7.14 - Influence of m_i

Each of the graphs above represents the yielded element curve from stage 1 through stage 8. The average yield curve (dashed line) is plotted in all diagrams along with the plus/minus standard deviation curves for each parameter. The splitting process is more sensitive to the parameter if its standard deviation curves plots far away from the dashed line. The following observations are made:

- UCS and GSI seem to influence the splitting process the most. An increase in these parameters decreases number of yielded elements
- m_i has some influence. A decrease in m_i appear to decrease yielding. An increase seem not to influence much.
- E_{rm} and ν appears to have very little influence.

7.4.2 Accumulated sensitivity analysis

Accumulated sensitivity analysis refers to the accumulated effect of simultaneously varying all the parameters within their respective standard deviations. This represents the worst and best combination of parameters, and the scope is to identify whether superpositioning of the yielding curves occur. During this analysis, all possible combinations of the parameters given in table 7.5 were assessed. The best and worst parameter combination is presented in terms of yield curves in figure 7.15. Fracture propagation is given in figure 7.16.

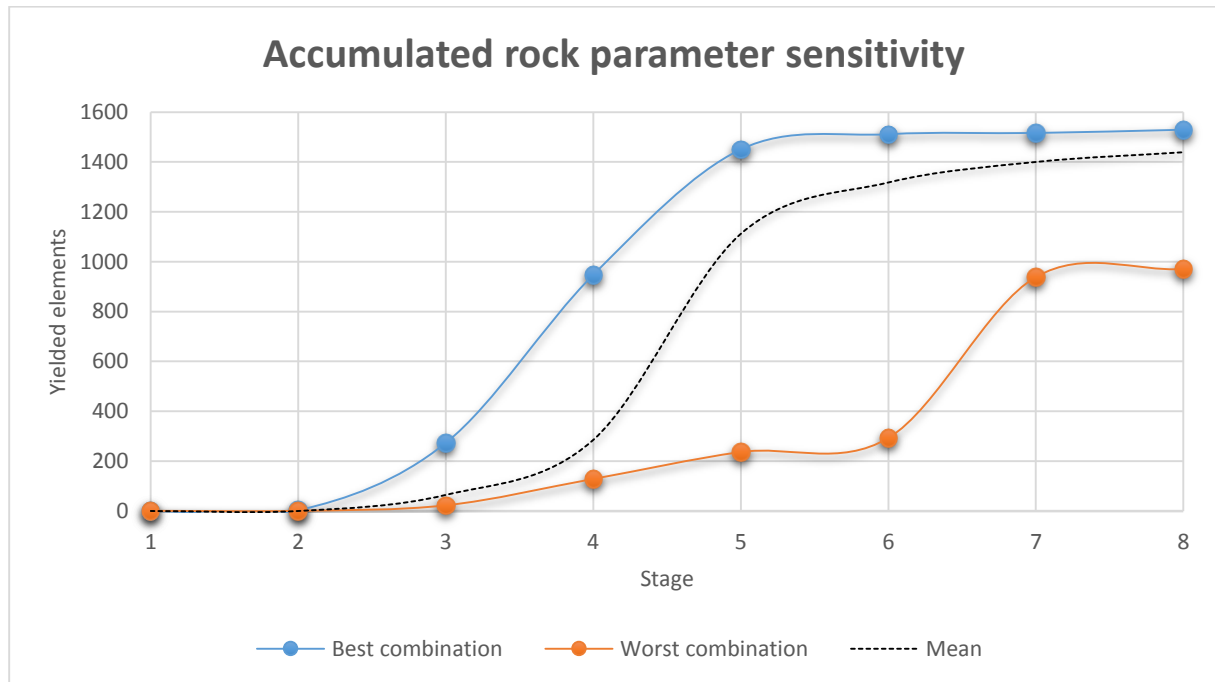


Figure 7.15 - Best and worst accumulated rock parameter combination

Because the analysis is modelling the splitting process, the more yielding the better. Therefore, the parameter combination that renders most yielding is considered the best situation for splitting. It is important to recognize that the combination referred to as best in this analysis does not represent the best parameter combination with respect to overall stability and rock mass quality. Table 7.6 shows the parameter combinations:

Table 7.6 - Best and worst parameter combination

	E (GPa)	ν	UCS (MPa)	GSI	m_i
Best Combination	40	0.31	116	73	33
Worst Combination	40	0.21	170	83	23
Mean	43	0.26	143	78	28

Table 7.6 shows the parameter combinations:

Table 7.6 also includes the dashed line in the diagram, which represents the mean values. The values reveal that the best combination has lower UCS and GSI values and a higher m_i and ν

than the worst combination. Note that the E-modulus remains lower than average for both cases. These results are consistent with results from individual sensitivity analysis. Fracture propagation for the two different parameter combinations is given in figure 7.16.

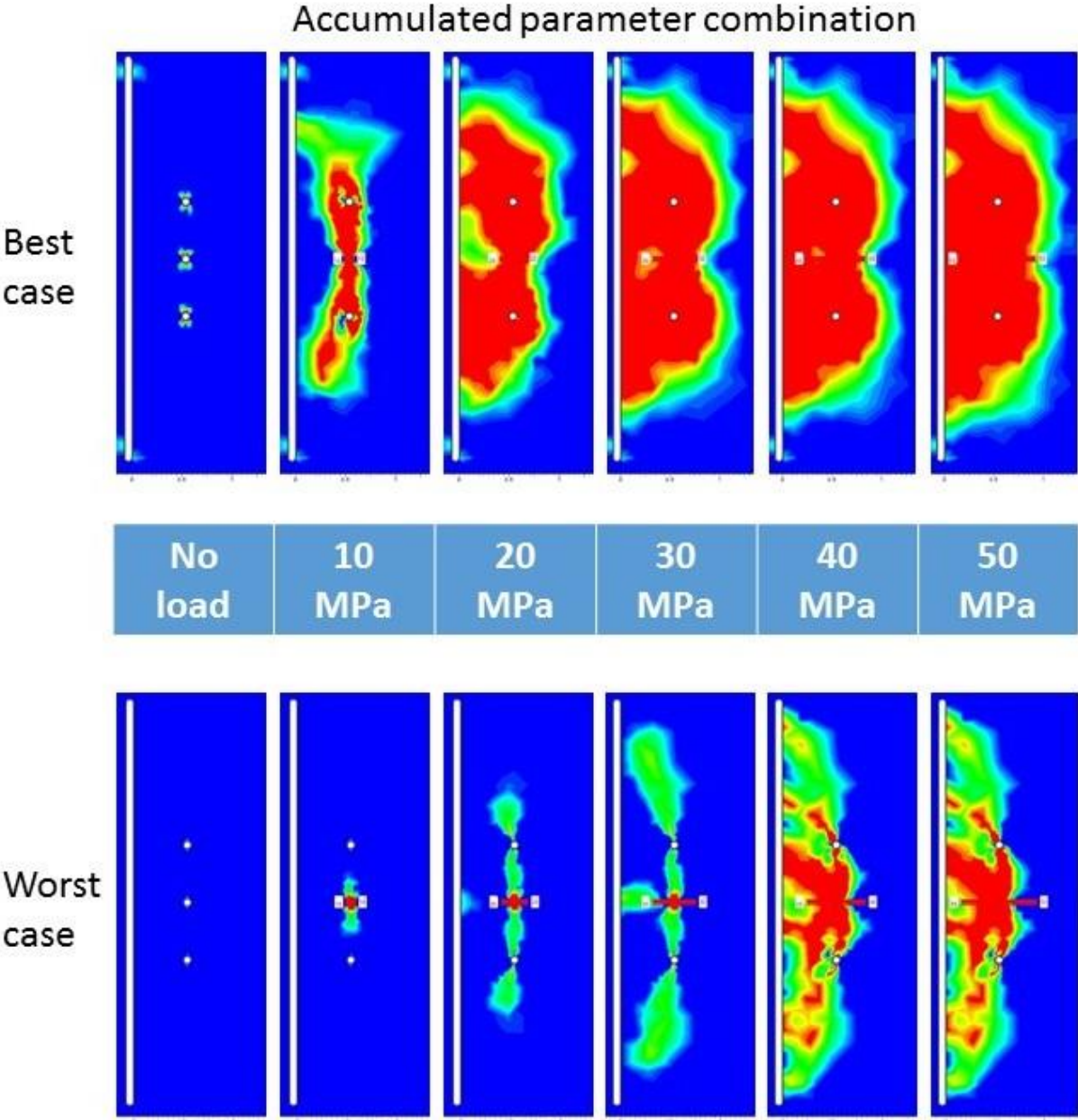


Figure 7.16 - Fracture propagation for best and worst parameter combinations

The relative big differences interpreted from the yield curves is visualized in figure 7.16. The figure suggests a substantial difference in the extent of the yield zone between the two parameter combinations.

7.5 Stress analysis

So far, the stress situation has been assumed hydrostatic with a magnitude of 5 MPa. This section investigates the effect of altering the in-situ stress field in terms of both magnitude and anisotropy. Because the scope is to investigate the splitting efficiency under different in-situ stress conditions, it is important to minimize shape effects caused by unfortunate borehole and free face design. Therefore, all stress field calculations are tested on a circular free face, as it is principally independent towards stress orientation and ideal for stress redistribution.

The basic configuration assumed for all stress analysis follows from configuration a) given in figure 7.9. This configuration assume a circular free face with 1.5-meter diameter, with three boreholes located in an arc 0.5 meter away. Rock mass parameters and analysis stages remain constant for all following analysis. For their respective values, see section 7.2.

7.5.1 Hydrostatic stress state

Previous analysis assume a hydrostatic stress state of 5 Mpa. To investigate the effect of an increase in absolute magnitude of the stress field, a hydrostatic stress field of magnitude 10 Mpa is applied. This is then compared to the initial 5 Mpa stress field and evaluated in terms of yielded elements. The resulting yield curves from stage 1 to 8 is presented in figure 7.17.

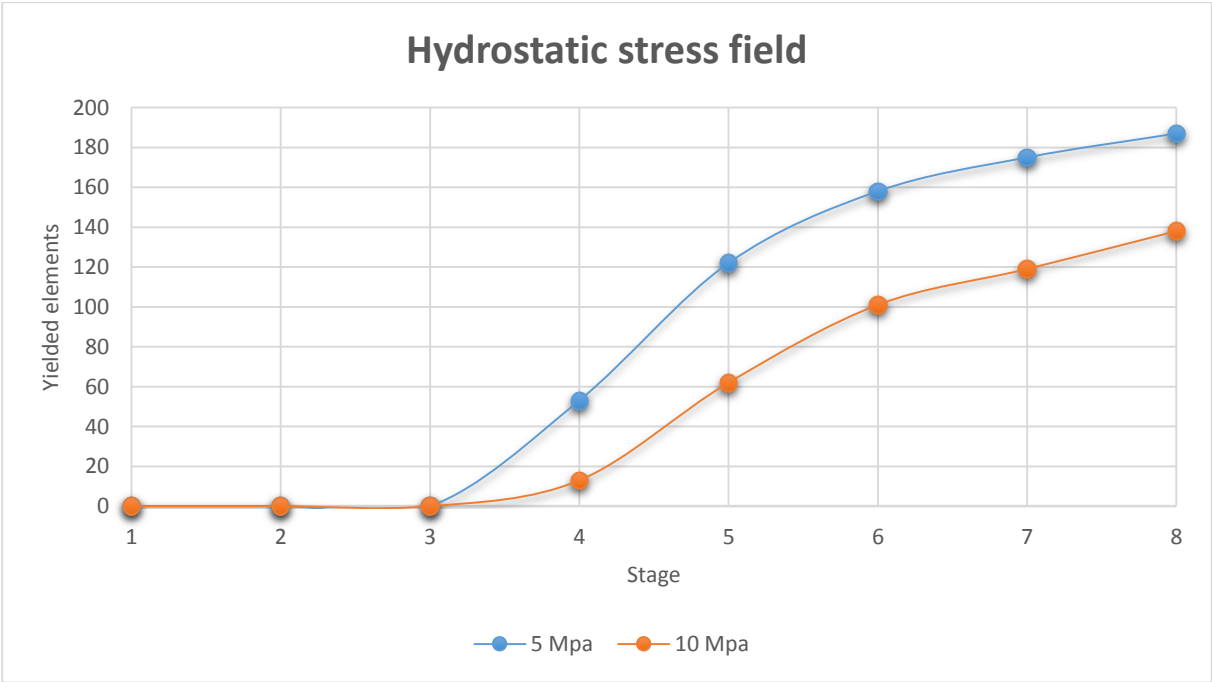


Figure 7.17 – Hydrostatic stress field, effect of changing magnitude

Figure 7.17 suggests that a lower confining stress gives easier yielding. This is consistent with the intuitive assumption that it is easier to open tensile fractures if the confining pressure is lower.

7.5.2 In-situ stress conditions at Follo

Different stress field analysis has been performed for the Follo line project, close to the tunnel alignment. For location, description and results of the stress measurements, it is referred to section 3.3 and table 3.3. As discussed in section 3.3, the author consider the 3D-measurements inside the Ekeberg halls to represent on-site conditions most accurately and therefore choses to use them as basis for further analysis.

Because the minor principal stress σ_3 from 3D-measurement (table 3.3) is acting nearly vertical and need to be perpendicular to the major principal stress (σ_1), it was recalculated based on 120-meter overburden (NNRA, 2014c). Using the unit weight determined in laboratory (section 6.2), an in-plan σ_3 of 3.2 MPa is calculated. The initial variation from measurements (2.8 MPa) is very high in relation to the mean value and is likely to affect the results unrealistically much. A standard deviation of 1 MPa is therefore assumed for the in-plane σ_3 .

The resulting stresses along with their variability are given in table 7.7:

Table 7.7 – In-situ stresses used in analysis

	<i>Stress field</i>		
<i>Stress</i>	σ_1	σ_2	σ_3
<i>Value</i>	9.9 ± 1.9	7.5 ± 1.9	3.2 ± 1
<i>Dip</i>	24°SW	27°SE	61°NE

This stress field is assumed to represent actual conditions inside the Ekeberg hill reasonably well. In order to apply this 3-dimensional stress field into a 2-dimensional software such as *Phase*², it is necessary to address the corresponding stresses acting on the tunnel face. As the tunnel alignment curves throughout the area subjected for Drill and Split, different stress situations will occur along the alignment.

Additionally, fault activities and topographic effect may have altered the stress field for tunnel sections nearby the fault zones. As it happens, much of the drill and split operations is assigned for tunnel sections near the Ekeberg hill slopes, which in turn means that the estimated stress field in table 7.7 may not be applicable for these sections. This stress field is therefore most accurate for the southernmost sections of in- and outbound Follo lines, as indicated by red circle in figure 7.18. A stress cross indicating the approximate stress orientations and its applicable area (red circle) is presented in figure 7.18.

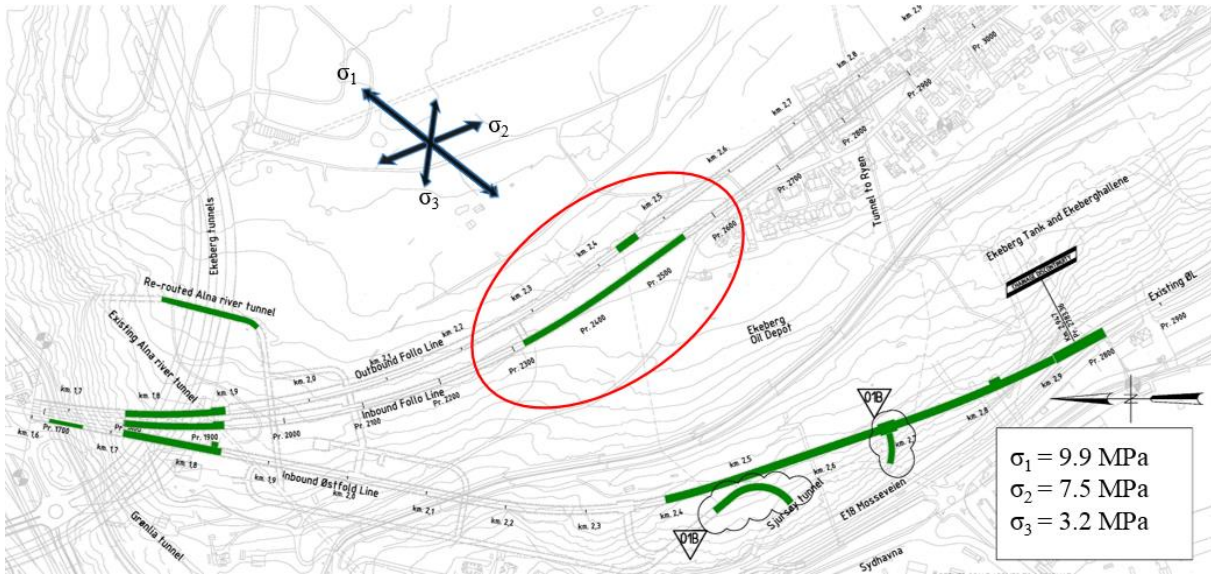


Figure 7.18 – Drill & Split locations and in-situ stress cross (Modified from drawing UOS-30-B-30400 by NNRA)

As suggested by figure 7.18, the major principal stress acts approximately normal to the tunnel alignment. Consequently, it can be regarded as the major in-plane stress in *Phase*². Furthermore, σ_2 runs almost parallel to the tunnel alignment, and is therefore assumed to be the out-of-plane σ_z in *Phase*². The re-calculated minor stress is regarded as the minor in-plane σ_3 in *Phase*².

It is also necessary to account for the inclination of the respective in-plan stresses. This is resolved by addressing an inclination angle between the major principle stress and the horizontal. This angle is given in table 7.7. The resulting in-plane stress cube is presented in figure 7.19 below:

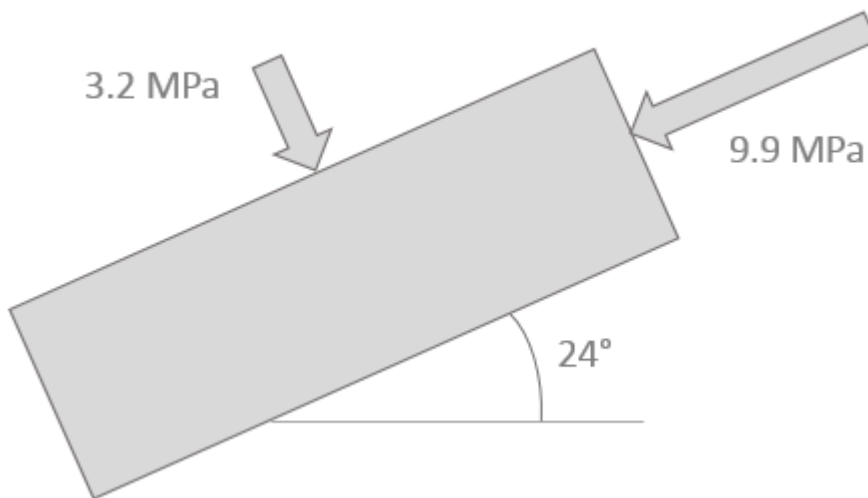


Figure 7.19 – In plane stress cube in *Phase*²

The stage-by-stage fracture propagation for the stress cube given in figure 7.19 is investigated and presented in figure 7.20 below. This stress state represents an anisotropic stress state, where the major in-plane stress is approximately three times the minor. Contour colours are as for previous tests (figure 7.8).

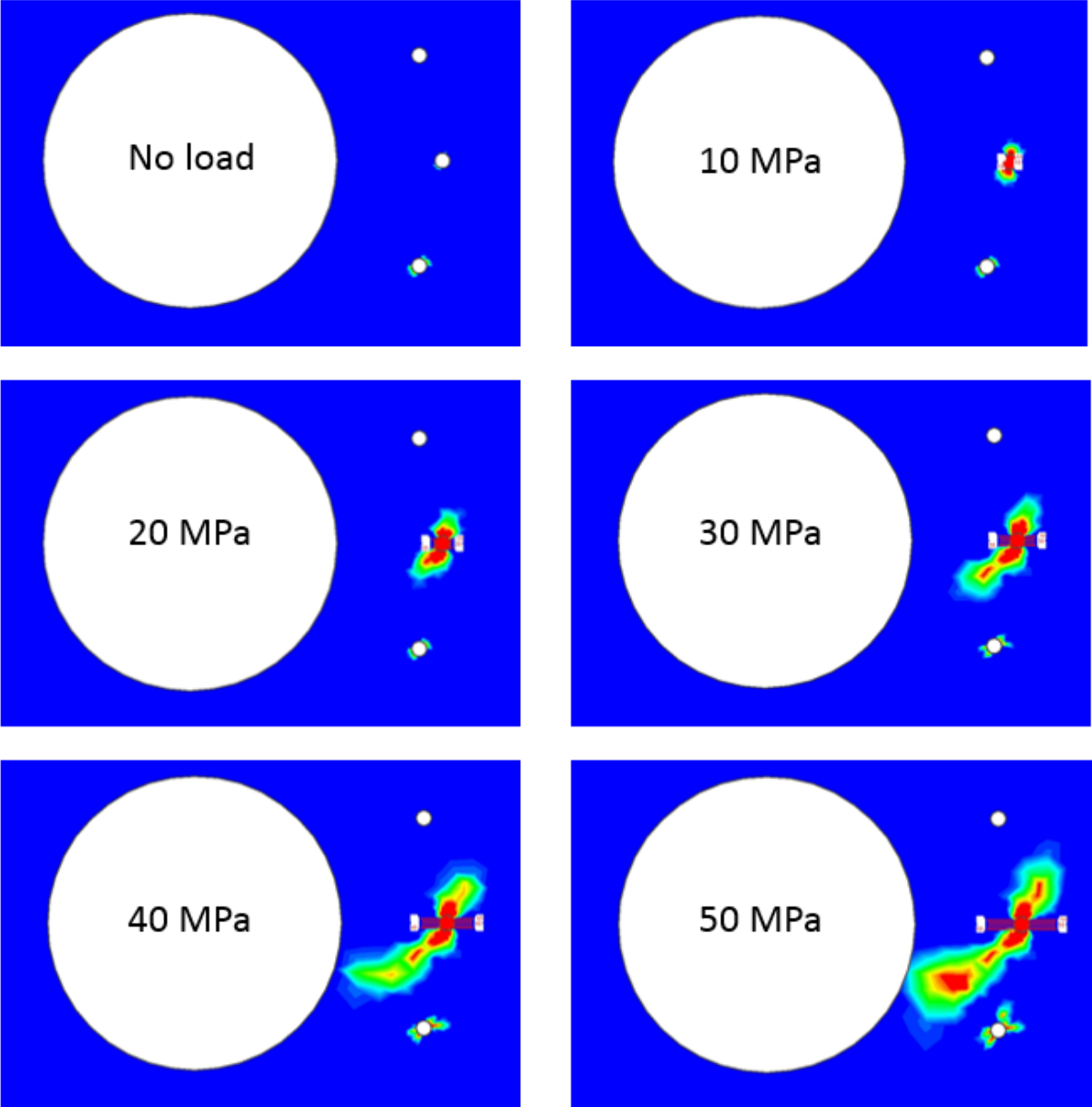


Figure 7.20 – Fracture propagation under anisotropic stress

Figure 7.20 suggests that the fracture propagation tend to aligns itself approximately parallel with the major principal stress direction. Situation at the final loading stage suggests that it is nearly tensile failure all the way through to the free face. Compared against the situation with a hydrostatic stress state, this clearly presents a more beneficial stress situation, as more fracturing in the desirable direction is achieved.

7.5.3 Individual stress sensitivity analysis

Efficiency of the splitting operation is investigated in terms of different stress states. In order to assess different stress state scenarios, a sensitivity analysis of the following stress parameters is undergone:

- In-plane Sigma 1 (σ_1)
- In-plane Sigma 3 (σ_3)
- Angle between Sigma 1 and horizontal

Their initial conditions and variability is presented in table 7.7. The initial angle between Sigma 1 and the horizontal is 24° according to measurements. A standard deviation of 5° is assumed for this parameter, effectively varying the dip angle between 19° and 29° . Resulting stage-by-stage yield curves are presented in following figures. Pictures of modelled fracture propagation is presented in figure 7.20 (mean curve) and in appendix (Appendix F. 8 to Appendix F. 13).

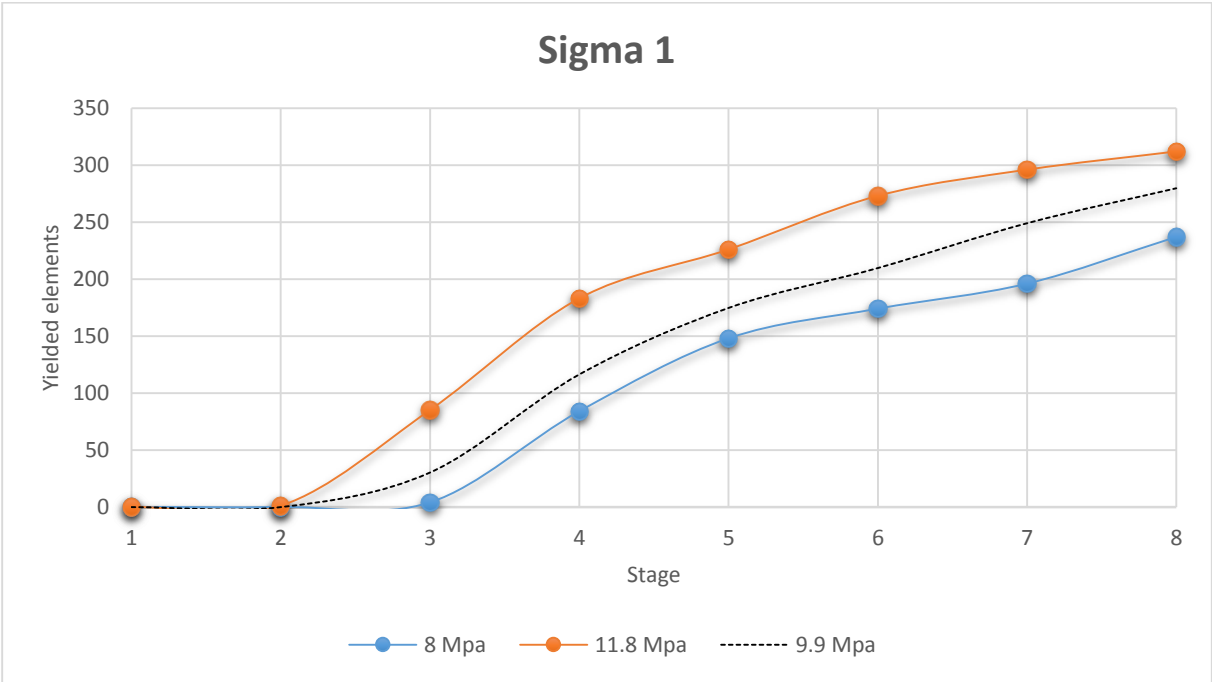


Figure 7.21 – Influence of Sigma 1

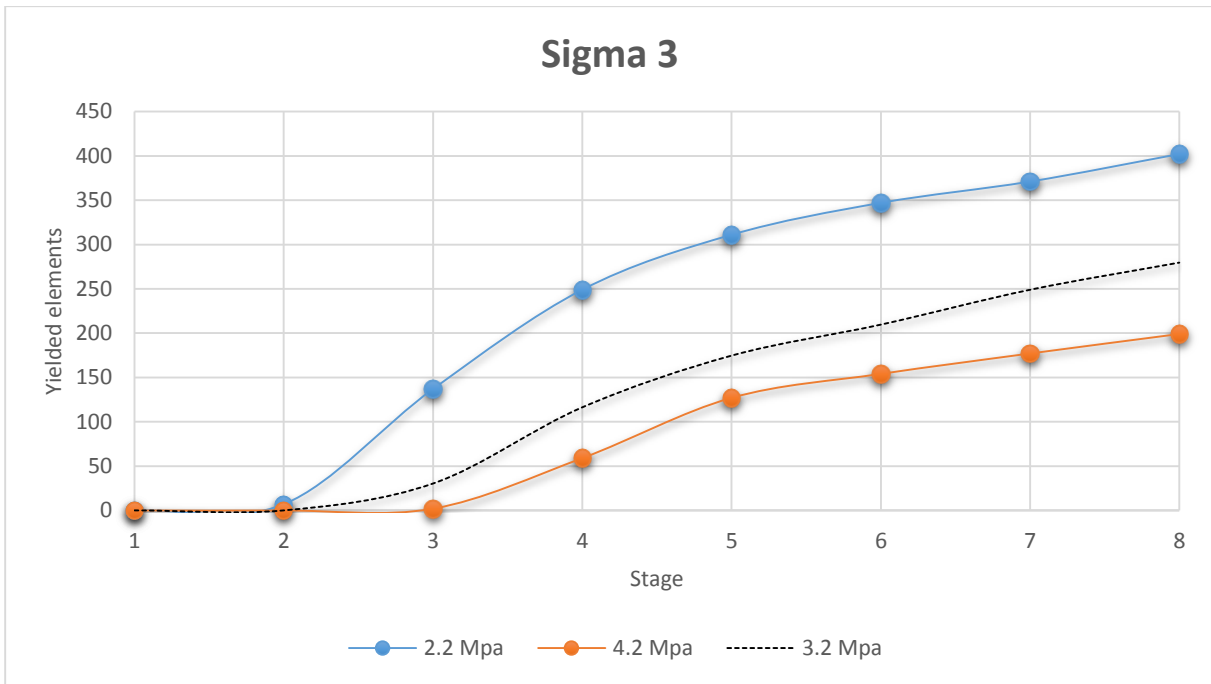


Figure 7.22 – Influence of Sigma 3

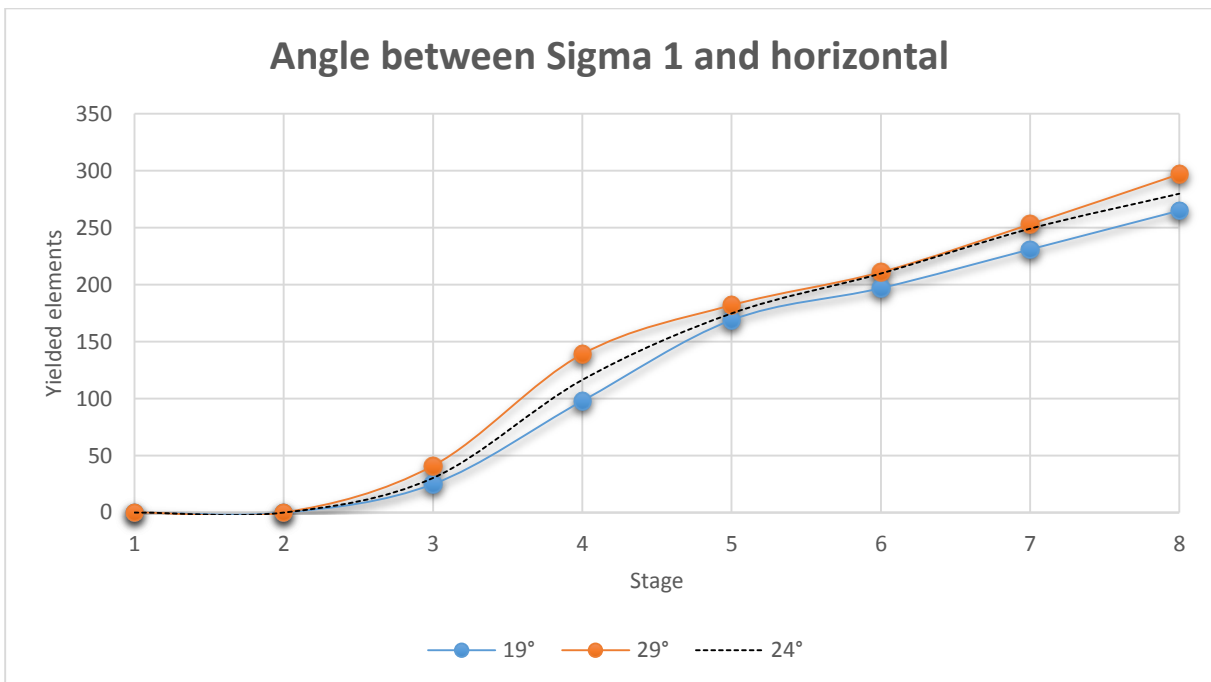


Figure 7.23 – Influence of angular stress orientation

The following observations are interpreted from the yield curves:

- Magnitude of major in-plane stress (σ_1) seem to have some influence
- Magnitude of minor in-plane stress (σ_3) seem to have most influence
- Changing the angle has little effect on yielding. Higher angle appear slightly more beneficial for splitting the lower (more yield)

7.5.4 Accumulated stress sensitivity

Similar as for rock mass parameters, analysis of the accumulated effect of best and worst stress combinations within the defined range of standard deviations are investigated. Results from individual stress analysis indicate that higher angle and major in-plane stress in combination with lower minor in-plane stress would likely present the most desirable situation in terms of easiness of yielding. This represent the most anisotropic stress state possible from the range of the given standard deviations. The yield curves from the resulting best and worst case-scenario found from the analysis is presented in figure 7.24.

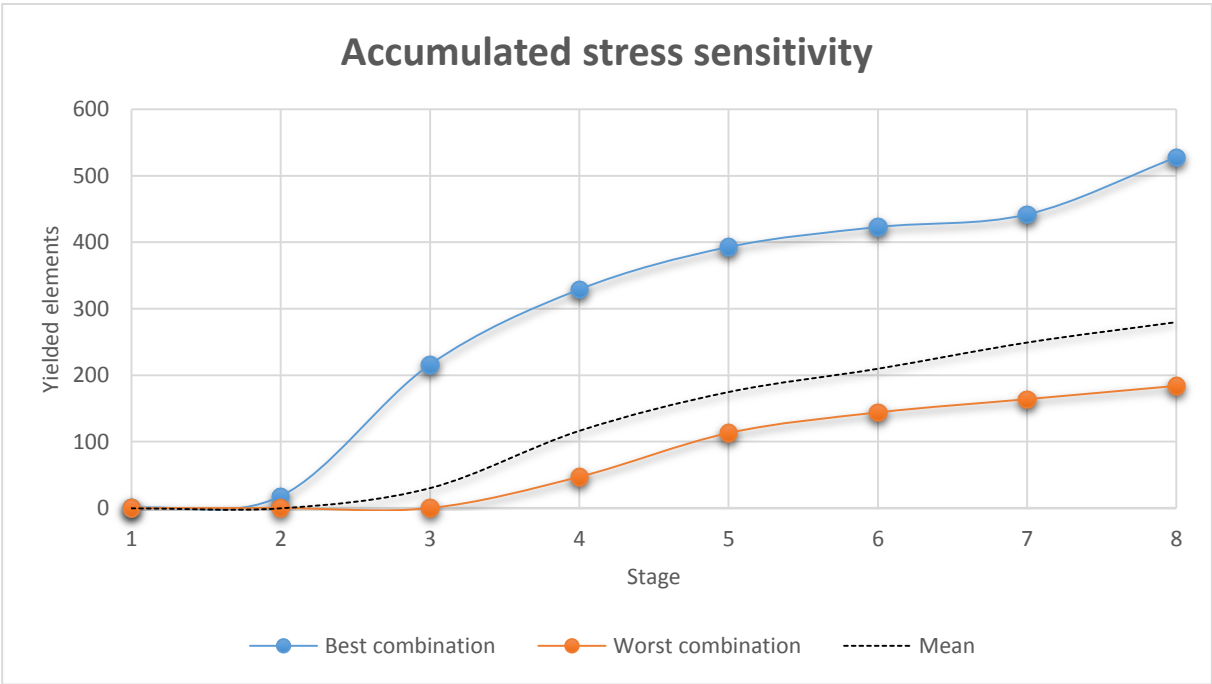


Figure 7.24 – Best and worst stress accumulated combination

The stress parameter combination yielding the two different combinations are presented in table 7.8 below:

Table 7.8 – In-plane stress field constitution

	<i>Sigma 1 (MPa)</i>	<i>Sigma 3 (MPa)</i>	<i>Angle (°)</i>
<i>Best combination</i>	11.8	2.2	19
<i>Worst combination</i>	8	4.2	19
<i>Mean</i>	9.9	3.2	24

Note that the most anisotropic stress field gives most yielding. This tendency is also seen when comparing against the hydrostatic stress field analysis (figure 7.17), which presents much less yielding even for stresses of lower magnitude (5 MPa hydrostatic) than anisotropic stress fields of higher magnitude.

8 Discussion

8.1 Geological

Rock quality and laboratory assessments undergone by the author corresponds reasonably well with previous assessments done by external personal. It is emphasized that both the rock sample site and all field mapping was undergone near the north-south going Ekeberg fault, where previous tectonic movement may have altered the rock mass' characteristics. This is not reflected in the rock mass quality assessments, as the author generally estimates higher Q-values in the area near inbound Østfold line than previous assessments. The likely cause for this is that the previous estimates were based upon far off registrations, and therefore are likely to be a conservative best guess of actual rock quality.

Inspection of the core samples extracted from the rock blocks shows slightly different features between the two rock samples, where one of the blocks included large quartz lenses and open joints while the other block appeared massive and intact. Due to discontinuity planes in the altered rock block, only one core sample was prepared for UCS testing. This block presented noticeable lower rock strength (UCS) than the other core samples from the intact rock block. It is believed that this block is more altered by tectonic movement along the fault zone, which in turn caused it to present lower strength properties. It should be noted that despite alterations, the resulting UCS value (103 MPa) for the altered block is still regarded as “very strong rock” according to ISRM (ISRM, 1977), and it is well within the region of previously registered values from nearby locations. Given that the results are representable for the rock quality in the area, it is assumed that the variations observed between core samples are a reflection of the general variability of intact rock quality in the nearby area.

Joint registrations performed by the author is fairly consistent with the previous measurements. Overall, the authors' registrations express distinct similarities to the existing joint rosette, but a relative small statistical basis limits the foundation for drawing definitive conclusions. Given that the investigated area lies close to the Ekeberg fault, it is not unlikely that the density of random oriented joint increases. The differences between the two joint rosettes are assumed to be caused by a combination of natural geological variation and registrations of random joints.

One feature regarding the joint orientation that may significantly influence the splitting ability is the registered orientation for a major joint set in relation to the tunnel axis. The tunnel axis curves from approximately N145° to N180° throughout the area, which is parallel to joint set 2. Joint set 2 is parallel to the dominating foliation direction in the rock mass, and laboratory

tests show that the rock mass exhibits very anisotropic strength behaviour parallel and perpendicular to the foliation. While this may present an unfortunate situation for the overall stability, it could lead to easier splitting, as less force is needed for fracture initiation. On the other side, the parallel foliation direction could give borehole deviation during drilling, as the borehole may deviate along the weaker layers within the rock. This could lead to the tip breaking of when the wedge is inserted.

The authors' registrations correspond well with existing assessments, which further enhances the existing belief that generally good rock mass quality can be expected, aside from the rock mass within the fault zones. It is believed that despite occasionally low overburden between underground structures, good rock quality in collaboration with suitable rock support are assumed adequate for ensuring stable situations. It is also assumed that gentle excavation by the "Drill and Split" method will have a positive effect on stability, as less support is needed than for conventional blasting where a blast damage zone occurs around the tunnel profile.

8.2 Free face design

Earlier studies of the "Drill & Split" excavation method suggests that productivity of this method largely relies on optimizing the borehole configuration at the tunnel face. Optimal borehole configuration involves minimizing the spacing between splitting holes and make most efficient use of the free face under the given geological conditions. Establishing a free face is important, as the rock need place to move during the splitting process. Without this, a force greater than the rock compressive strength would be needed in order to initiate fracturing.

Three different free face designs were investigated in *Phase*² in terms of yielding between boreholes and the respective free face under fixed staged loading. The three designs were quadratic, circular and in a line. The results from this study implies that tensile fracture propagates all the way through to the free face for both the quadratic and the line configuration, while fracture propagation for the circular free face design remained incomplete. The limited yielding obtained by this configuration suggests that this configuration is less desirable with respect to splitting under the given circumstances than the presented alternatives. Three features are identified as main causes for this:

- A circular free face presents a more confined situation because of the curvature
- Aligning the boreholes in a straight line 0.5 meter away effectively increases the distance between free face and upper and lower boreholes because of the curvature in the free face

- Hydrostatic stress distribution gives homogeneous stress distribution around the circular face, while it presents stress concentrations in corners and de-stressed areas in the centre of the sides. This is considered the greatest contributor to the big differences gained from numerical modelling.

Further investigations of altering the borehole placement and alignment around a circular free face was investigated. The results from this was that altering the borehole alignment into having a constant spacing to the free face had no effect, and that reducing the absolute spacing was necessary. Related to a real life scenario, this would cause additional borehole drilling that would add to costs and time consumption. It remains unknown whether the additional costs and time consumption of this would exceed the profit from being able to bore long, large diameter boreholes that can be re-used in several cycles.

The quadratic and line configuration expressed similar behaviour to each other, as total yielding was achieved at loads between 20-30 MPa and 10-20 MPa respectively. This suggests that a line configuration is slightly more beneficial towards splitting than a quadratic. Again, this relates to stress re-distribution caused by the design of the free face. Because the situation initially is hydrostatic, a very anisotropic design such as the line induces a correspondingly anisotropic stress field with severely de-stressed long sides that is favourable for splitting.

8.3 Rock parameter sensitivity

From the sensitivity analysis, the individual influence of parameters were investigated in terms of yielding in *Phase*². The results from this analysis suggests that *GSI* and *UCS* influences most, while E_{rm} and ν has minimal influence. m_i places in between the parameters mentioned above with some influence. When accounting for the standard deviations percentage of the mean value (last column, table 7.5), *GSI* appear to have more influence than the *UCS* because of a much smaller span in variation.

The result that the elastic parameters E_{rm} and ν has such a limited influence is interesting. This is most likely associated with them being concerned about the elastic behaviour of the rock mass and not directly influences the yielding process. Yielding in *Phase*² is determined through evaluating the calculated situation up against the chosen failure criterion, which in this case is the Hoek-Brown. Given that the Hoek-Brown failure envelope is determined using *UCS*, *GSI*, m_i and D , an alteration of these parameters effectively changes the failure envelope. This is regarded the main reason why the calculated yielding is practically indifferent of altering the parameters E_{rm} and ν , as they do not affect the underlying failure criterion.

From the accumulated parameter sensitivity analysis, the following observations are made:

- Accumulated analysis suggests that the combination of lower *UCS* and *GSI*, while a higher *mi* presents most yielding (easiest breaking). These results are consistent with results from individual analysis
- An accumulated effect is noticeable for the “worst combination”, as the yield curve is significantly lowered. The same trend is not apparent for the “best combination”, as it exhibit much less difference from the mean yield curve
- Yielding appear to converge towards a maximum yielding limit. This trend is also apparent in the individual sensitivity analysis

The trend of the yielding curves to converge towards an upper yield limit is assumed to originate from the given geometrical design of the borehole and free face. This situation invites yielding to occur between free face and boreholes, and therefore leads to a limited number of total “yieldable elements” in the rock mass. This assumption is underlined by later yield propagation seen in the later stages of the “best case combination” given in figure 7.16, where additional yielding occur in the rock mass to the right of the boreholes.

It is important to emphasise that this does not represent a realistic situation, but rather illustrates a limitation in the *Phase²* code. In a real life situation, the rock mass outside the borehole on the far side away from the free face would be undisturbed after splitting. This limitation is regarded as a major restraint towards being able to model the entire tunnel face, because results would gradually be more inaccurate for each splitting cycle due to consequential overestimations of the damage zone. This would lead to wrongful estimations of necessary spacing between splitting boreholes, which in turn makes it impossible to optimize a borehole configuration accurately from this modelling.

8.4 Stress sensitivity

In order to assess the splitting performance under the influence of an external stress field, sensitivity analysis with respect to both magnitude and orientation are performed. To isolate the magnitude as a single variable, two separate hydrostatic stress analysis with different absolute magnitude (5 and 10 MPa) were calculated under otherwise identical conditions. The plotted yield curves from this analysis appear to converge toward linearity after a certain amount of initial yielding. For the later linear portion, a constant spacing between the curves is observed. This suggests that there is proportionality between the magnitude of surrounding field

stress and easiness of yielding. Furthermore, this can be regarded as proportionality between magnitude of confinement stress and easiness of the splitting process.

Two separate measurements of the in-situ stresses at the Follo line shows that different stress states occur within the contract area. It is believed that 3-D measurements conducted inside the Ekeberg halls are less affected by fault movement and stress redistribution than 2-D measurements from inside the Ekeberg road tunnels. Consequently, the 3-D measurements were chosen for the in-situ stress analysis. This measured in-situ stress field is then adapted to an in-plane stress field according to the tunnel orientation relative to in-situ stresses.

The measured in-situ minor stress caused a few problems for the analysis that needed addressing:

- A low mean value (1.9 MPa) in relation to the major in-situ stress (9.9 MPa) caused a very anisotropic stress state that gave immediate yielding in the modelled tunnel face
- A relative high standard deviation (± 2.8 MPa) gives a unrealistic high range of variation that affects the analysis too much
- Minor stress had a non-perpendicular angle to the major principal stress
- With a dip angle of 61° , it comprises most of the vertical stress component. Consequently, it is assumed that it can be reasonably expressed by theoretical vertical stress

Due to the combined effect of the issues mentioned above, the minor in-plane stress (σ_3 in *Phase*²) was recalculated based upon estimated overburden in the area. The standard deviation range was also limited from 2.8 MPa (~150% of the original mean value), to 1 MPa (~30% of mean value). By doing this, total yielding of the tunnel face was avoided, and it was possible to perform sensitivity analysis of the different stress components.

Despite adjusting the in-plane Sigma 3, the stresses still forms an anisotropic stress situation at the tunnel face, with the major in-plane stress being 3 times bigger than the minor stress. The results suggest that induced tensile fracturing occur parallel to the major stress direction (in-plane sigma 1). This is caused by easier expansion in the perpendicular direction, because the magnitude of the minor stress (in-plane sigma 3) acting in this direction is smaller than stresses in other directions. The results of this analysis is expected, as less force is needed to open the joints in this direction because of lower magnitude in the confinement stress.

Sensitivity analysis of the contributing components Sigma 1, Sigma 3 and the dip angle of Sigma 1 reflects the same trend, as a variation of the minor in-plane stress affects yielding most.

Varying the major in-plane stress has also a noticeable effect, while altering the angle has limited influence. Assessing the accumulated effect of combining the standard deviations for σ_1 , σ_3 and the dip angle of σ_1 reveals that the ideal combination with regard to splitting (most yielded elements) comprises a situation of high major stress and low minor stress. This situation represents the most anisotropic situation possible within the range defined by the assumed standard deviations. In sum, this result indicates that easiness of yielding in the model strongly depends upon the degree of anisotropy in the stress field.

The anisotropic effect has been assessed earlier in terms of different free face designs, where it was discovered that redistribution of a hydrostatic stress field gave easier yielding for a more anisotropic free face design. This discovery is consistent with results from applying an anisotropic stress field directly, and suggests that with regard to easiness of splitting, it is more desirable with higher degree of anisotropy in the acting stresses. Assuming the effects of anisotropic geometry and anisotropic stress field are combined, scenarios where stresses either accumulate or cancel each other out may occur. This is a recognized feature within rock mechanics, where aligning the longest axis in an elliptical opening parallel to the major stress direction is utilized to constitute a stable situation (Myrvang, 2001). With regard to splitting, it would be most desirable to invert this situation by aligning the longest elliptical axis parallel to the minor stress, resulting in de-tensioned zones prone to yielding.

8.5 Applicability of D&S

Transferred to a real life situation, the situation above would require accurate understanding of the in-situ stress situation and its relative orientation to the tunnel face at all times. It would also require constantly adopting the design based upon the in-situ stresses. This would lead to extra time consumed, and additional costs to the project. The actual gains in terms of reduced borehole spacing remains unknown, so whether it is altogether practically and economically viable to alter free face after in-situ stress conditions is unknown and beyond the scope of this thesis.

It is believed that predominant joint orientations encountered at the tunnel face also has a significant impact on actual fracture propagation, as the fracture propagation will try to follow existing joints. This is because less force is needed to re-open existing joints than initiating new fractures through intact rock matrix. This feature is to some extent accounted for in the *GSI* parameter, but this parameter does not account for dominating joint sets in relation to tunnel face. As previously discussed, the foliation direction is sub-parallel the tunnel alignment. It is believed that if the borehole pattern is able to maximize the use of existing joints, great profit

in terms of easier splitting can be achieved. In turn, this can render it possible to increase spacing between boreholes, and consequently increase productivity. However, natural geological variations renders it impossible to model this scenario realistically, as measurements of joint orientations in relation to the tunnel face is necessary. This situation would vary from one splitting cycle to another, and utilization of existing joints would require accurate borehole drilling in locations specified by personal with adequate geological understanding. In a practical situation, the profit of such a detailed assessments between each cycle is likely undermined by the costs this would present. Consequently, it appears more viable to assign standardized borehole patterns for different sections of the tunnels based upon a combined evaluation of assumed rock mass, predominant joint orientations and assumed stress field.

One way to simplify the necessary mapping in such a manner that it can be done by on-site personal, is to correlate the splitting performance with the assessed Q-value encountered at the tunnel face. By doing this, optimized borehole configurations could be standardized for the different rock classes defined in the Q-system. These standardized borehole designs would act as basic configurations that allows sufficient breaking between boreholes within the assessed rock class. In order to gain a sufficient empirical basis for this, numerous splitting performance assessments in different rock conditions and different in-situ stress fields is required. In this respect, the Follo line project could act as a pilot project for this work that later projects may benefit from.

9 Conclusion

The existing geological understanding of the contract area suggests that it is comprised of generally high strength gneiss and overall good quality rock mass conditions. The authors own assessments of rock mass properties further enhances this belief, as it is believed that the small differences between the measurements originates from natural variations. Given the situation, “Drill & Split” is considered the most viable excavation method because it is the only option known to the author that satisfies the following criteria:

- No vibration except from borehole drilling
- A high degree of flexibility is maintained during construction
- Efficient breaking in hard rock conditions
- Suitable for excavation of relative short distances

Alternative methods such as Drill & Blast, TBM, Roadheader or wire sawing are deemed inappropriate for use at the Follo line project because they fail on one or more of the criteria listed above.

Using the finite element code *Phase²*, several rock mass features are addressed in terms of influence towards the actual splitting process. The conclusions drawn from the numerical analysis are summarized below:

- Splitting process is very sensitive towards the *GSI* parameter.
- The rock compressive strength (*UCS*) and *m_i* parameter has some influence on splitting
- Parameter sensitivity suggest that joint propagation is practically indifferent towards elastic rock properties *E* and *v*
- Increase in absolute magnitude of hydrostatic stress field reduces efficiency of splitting by a proportional amount
- Anisotropy of the field stresses has significant effect upon both splitting ability and the propagating direction of tension fracture
- Depending on the in-situ stress field, great profit in efficiency of splitting can be achieved by altering geometry and orientation of the free face in relation to the major in-situ stress in a manner that induces the most anisotropic stress situation
- Ideal situations with homogeneous rock mass is modelled. In reality, splitting would probably be dictated by existing discontinuities in the rock mass. This situation may be encountered at the Follo tunnels, where foliation direction is sub-parallel to the tunnel alignment

This study shows that several limitations need to be addressed and may be subject for further investigations. Some major restraints were identified during this analysis, and it is believed that these limitations must be solved in order to be able to optimize a borehole configuration at the tunnel face realistically. The major limitations are summarized below:

- *Phase²* does not appreciate that the rock mass outside the spitting hole on the far side from the free face in reality will remain undisturbed after splitting.
- It is not possible to model a maximum expansion of the wedge inside the borehole in *Phase²*. This causes the software to calculate total failure between borehole and free face, which is not realistic
- The splitting job at the Follo line was not initiated at the time of writing, which rendered the author unable to calibrate the numerical model against actual data gained from field.

It is emphasized that additional simplifications to the above mentioned were necessary in order to conduct the analysis. This further enhances the uncertainty of the analysis, which sum renders the analysis meaningless in terms of absolute values. Therefore, this analysis should only be regarded as a basis for comparison between different scenarios regarding stress states, rock parameters and free face designs rather than presenting absolute conclusions. It is likely to assume that by solving the major limitations mentioned above, a more refined model could be constructed that in turn might be able to assess situations in terms of absolute values.

Based upon the numerical analysis and the general assumptions regarding “Drill & Split”, the overall impression is that the method would be suitable for the conditions encountered at the Follo line. Variations in in-situ stress field and joint orientations would dictate the performance to some extent, but given the alternative methods, D&S appear as the most viable solution at the Follo line project. It is also believed that by designing appropriate borehole configurations for different rock mass qualities assessed in the Q-system, more efficient borehole drilling could be achieved.

10 Further work

As this thesis is conducted on an early stage of the Follo line project, a natural continuation of the work would be to follow actual progress of the splitting process. By following the progress and correlate efficiency against encountered rock mass quality, a more realistic numerical model can be built that may enable more sophisticated analysis with respect to borehole configurations in different encountered rock masses. It is also recognized that some of the limitations encountered in this analysis may be reduced with data of actual splitter performance. In this regard, the actual splitting force needed for fracturing is considered a vital input for further analysis, as the model can be calibrated with real life data.

Registration of foliation inclination in relation to the tunnel face is also an interesting parameter, as it can be assigned values for predominant joint sets in relation to the tunnel face in *Phase²*. With field registrations of strength and infill characteristics of the foliation joints, this could be modelled and its influence investigated in numerical analysis. Monitoring of actual splitting performance under different stress situations and varying free face designs would also be of interest, as it makes it possible to compare against the results gained in the numerical analysis undergone by the author.

Another grand task would be to correlate the splitting performance against established rock mass classification systems, such as the Q-method. This would require a lot of fieldwork, as the candidate would have to evaluate appropriate borehole configurations against several different rock mass qualities in order to create a sufficient empirical basis for conclusions. If successful, this could lead to an empirical based recommendation system for borehole configurations for the “Drill & Split” method.

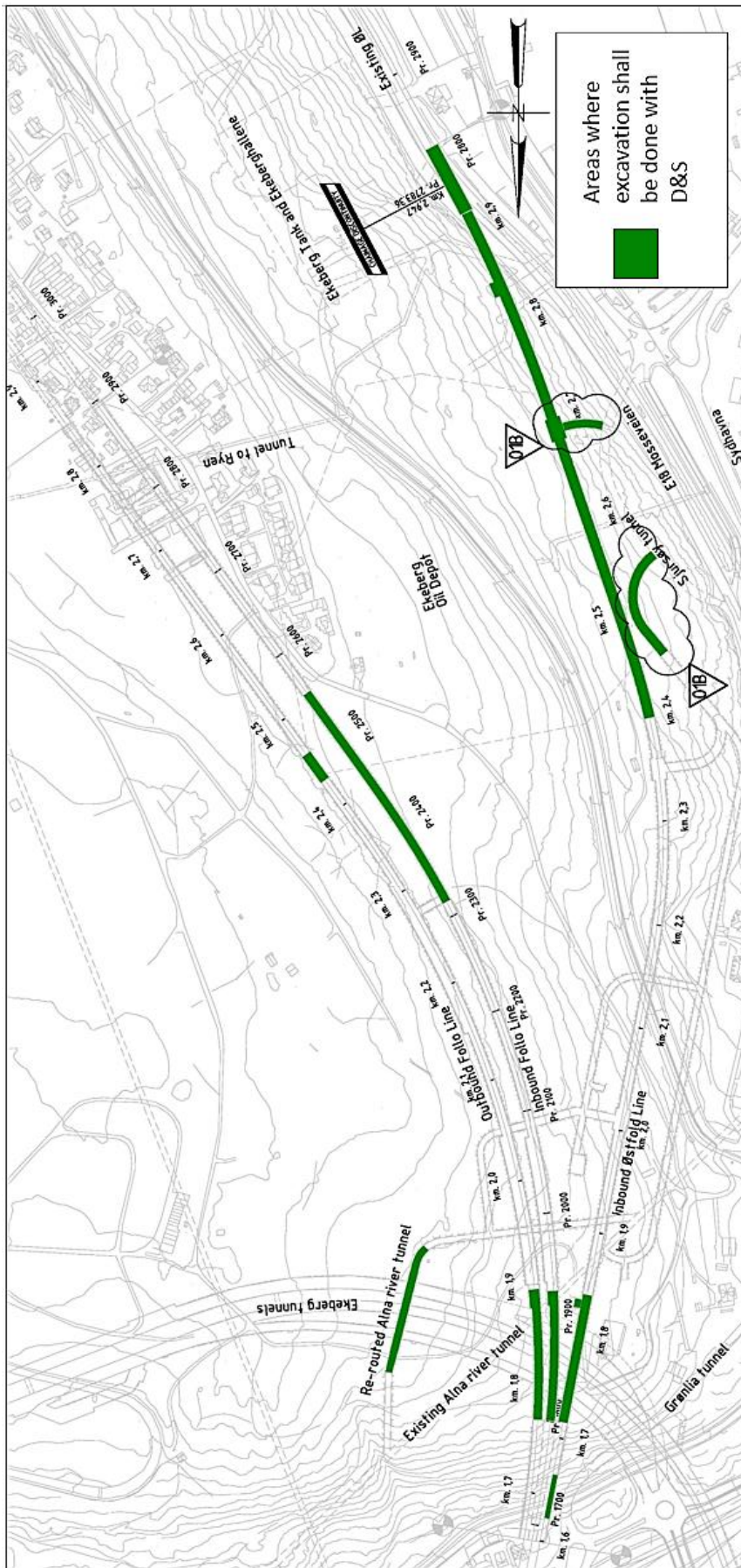
11 References

- Bruland, A. (2013). *Anleggsteknikk GK - kompendie*. Trondheim: Department of Civil and Transport Engineering, NTNU.
- Cai, M. (2010). Practical Estimates of Tensile Strength and Hoek–Brown Strength Parameter of Brittle Rocks. *Rock Mechanics and Rock Engineering Vol.43*, pp. 167-184.
- Darda. (1999). *Hydraulic Rock and Concrete splitters - Application Notes*. Retrieved September 10, 2014, from STM - Construction Equipment: http://www.stm-ce.com/darda_splitters.html
- Føsker, A. (2007). Ekeberg petroleum storage facility Experience from the Ekeberg oil storage and Ekeberg tank. *Norwegian Tunneling Society Publication no. 16 - Underground constructions for the Norwegian oil and gass industry*, pp. 153-159.
- Graversen, O. (1984). Geology and Structural evolution of the Precambrian Rocks of the Oslofjord-øyeren area, Southeast Norway. *NGU Bulletin 398*, pp. 1-50.
- Hoek, E. (2007). *Practical Rock Engineering*. Available from Rocscience.com.
- Hoek, E., Carranza-Torres, C., & Corkum, B. (2002). Hoek-Brown failure criterion. *Proc. NARMS-TAC Conference* (pp. 267-273). Toronto: Rocscience.com.
- Hoek, E., Carter, T., & Diederichs, M. (2013). Quantification of the Geological Strength Index chart. *47th US Rock Mechanics / Geomechanics Symposium*. San Francisco: American Rock Mechanics Association.
- Hoek, E., Marinos, P., & Marinos, V. (2005). The geological strength index: applications and limitations. *Bulletin of Engineering Geology and the Environment Vol.64*, pp. 55-65.
- Hwacheon Engineering Co.,Ltd. (2014). *Hydraulic Rock Splitter*. Retrieved from HRD Rock Splitter: <http://www.hrd-tech.com/hydraulic-rock-splitter>
- ISRM. (1977, October). Suggested methods for the quantitative description of discontinuities in rock masses. *International Journal of Rock Mechanics and Mining Sciences & Geomechanics, Vol. 15(16)*, pp. 319-368.
- ISRM. (1979a). Suggested methods for determining the uniaxial compressive strength and deformability of rock materials. *International Journal of Rock Mechanics and Mining Sciences & Geomechanics, Vol. 16*, pp. 137-140.

- ISRM. (1979b). Suggested methods for determining water content, porosity, density, absorption and related properties and swelling and slake-durability index properties. *International Journal of Rock Mechanics and Mining Sciences & Geomechanics*, Vol. 16, pp. 143-151.
- Jaeger, J., Cook, N., & Zimmerman, R. (1969). *Fundamentals of Rock Mechanics*. Methuen & co.
- Løset, F., & Lien, R. (1980). *Lagerhaller i Ekebergåsen*. Oslo: NGI.
- Myrvang, A. (2001). *Rock Mechanics*. Trondheim: Department of Geology and Mineral Resources Engineering.
- NGI. (2013, Desember). *Using the Q-system*. Bergmasseklassifisering og bergforsterkning. Oslo: Norges Geologiske Institutt. Retrieved Oktober 2014, from <http://www.ngi.no/>
- Nilsen, B., & Broch, E. (2011). *Ingeniørgeologi-Berg Grunnkurskompendium*. Trondheim: Department of Geology and Mineral Resources Engineering.
- Nilsen, B., & Palmstrøm, A. (2000). *Handbook no 2: Engineering Geology and Rock Engineering*. Oslo: Norwegian group for Rock Mechanics.
- NNRA. (2012). *UFB-30-A-30071_00B_Follobanen, Tunnel, FE-analyse av kryssinger i fjell i Ekebergåsen*. Oslo: internal report, unpublished.
- NNRA. (2013a). *UOS-30-A-30000_02B_Inngående Østfoldbane, Tunnel, Engineering Geology and Hydrology, Discipline report*. Oslo: internal report, unpublished.
- NNRA. (2013b). *UOS-30-A-30001_00B Ingeniørgeologisk rapport - Kryssinger i Ekebergåsen*. Oslo: internal report, unpublished.
- NNRA. (2013c). *FE Analysis - Three track tunnel passing Grønli tunnel*. Oslo: Internal report, unpublished.
- NNRA. (2014a). *UFB-30-A-30063_03B_Inngående Østfoldbane, Tunnel, Geotechnical and Geological Investigations Data Report*. Oslo: Internal report, unpublished.
- NNRA. (2014b). *UOS-30-A-90003_00B_The Follo Line Project - EPC D&B - Re-routing Alna river tunnel, Specification*. Oslo: Internal report, unpublished.
- NNRA. (2014c). General view of inbound Østfold line. *Technical drawing: UOS-30-B-30100_03B*. Oslo: internal drawing, unpublished.

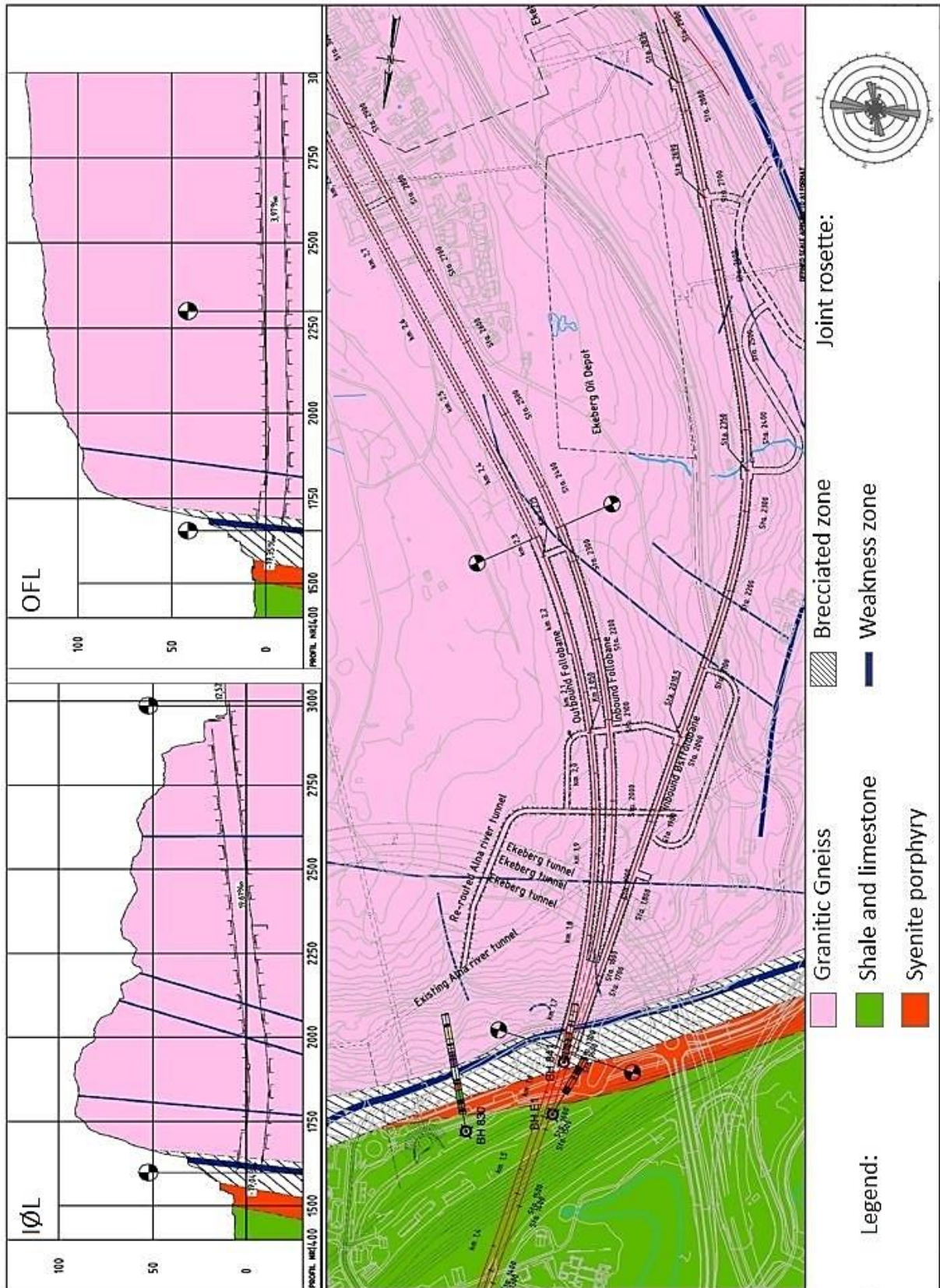
- NNRA. (2014c). *Phase2, 2D FE-analysis: Follo Line crossing of Ekeberg oil Depot cistern no. 9*. Oslo: Internal report, unpublished.
- NNRA. (2015). *The Follo line project -Brochure*. Retrieved from Jernbaneverket: <http://www.jernbaneverket.no/en/startpage1/Projects/New-double-track-Oslo-Ski/>
- Noma, T., & Tsuchiya, T. (2003). Development of low noise and vibration tunneling methods using slots by single hole continuous drilling. *Tunneling and Underground Space Technology, Vol. 18*, pp. 263-270.
- Noma, T., Tsuchiya, T., & Mitsugochi, N. (2009). *Tunneling by rock fracturing method under small cross section area*. Technology development division. Atsugi, Kanagawa: Fujita Corporation.
- Noma, T., Tsuchiya, T., Hada, M., & Nakayama, S. (1991). New Rock-Fracturing Excavation Method for Hard Rock Tunneling by FON Drill and FASE Method. *International Symposium on Automation and Robotics in Construction and Mining, Vol 13*, pp. 851-858.
- Norwegian Public Road Administration. (2009). Engineering geological tunnel mapping. Oslo: Documentation during construction, unpublished.
- Norwegian Public Roads Administration. (1994). *End report Ekeberg tunnel*. Oslo: internal report, unpublished.
- Ramberg, I. B., Bryhni, I., & Nøttvedt, A. (2006). *Landet blir til - Norges geologi*. Trondheim: Norsk Geologiske Forening (NGF).
- Rocscience. (2014). *Phase2 - Support and documentation*. Retrieved from Rocscience: <http://www.rocscience.com/products/3/support>
- SSB. (2015). *Populations projections 2014-2100*. Retrieved from Statistics Norway: <http://www.ssb.no/en/befolkning/statistikker/folkfram/aar/2014-06-17>
- Ståhlbåge, J. (2014). Yamamoto Ultra-large Rock Splitter. *Unpublished presentation received 20. Oct 2014*. Singapore: STM Construction Equipment.
- Volden, J. (2014). *Ingeniørgeologisk vurdering av muligheter og begrensinger for "Drill & Split" og lignende metoder i hardt fjell*. Trondheim: TGB4500 Project work, NTNU.
- Yamamoto Rock Machine CO.,LTD. (2014). Yamamoto Ultra Large Rock Splitter. *Product Brochure*. Tokyo, Japan: STM Construction Equipment.

Appendix A. 2 - Areas where Drill and Split will be used (Drawing UOS-30-B-30400 by NNRA)



12.2 Appendix B - Geology

Appendix B.1 - Engineering geological map (Drawing UOS-30-V-30100 by NNRA)



12.3 Appendix C - Drill and Split method

Appendix C. 1 - Super wedge product brochure (Given by representative from NNRA)

SPECIFICHE TECNICHE TECHNICAL SPECIFICATIONS

pressione d'olio standard standard oil pressure	220 bar
pressione d'olio massima maximum oil pressure	350 bar
forza di rottura splitting power	2400 ton
corsa cuneo wedge stroke	500 mm
diametro dei fori hole diameter	76 mm
profondità dei fori hole depth	1700 mm
interasse tra i fori hole spacing	da 400 x 400 a 750 x 750 mm
pesi weights	SW: 950 kg TW: 1500 kg
peso escavatore excavator weight	over 13 ton



SUPER WEDGE




Ripamonti

Ditta Ripamonti Dr. Gianni S.a.s.
Strada Romana di Sotto - 28877Ornavasso (VB) Italy
Tel. +39 0323 838211
www.ripamonti.net

Ripamonti

PERFORAZIONE DEMOLIZIONE

Fax +39 0323 836147
info@ripamonti.net

Ripamonti SUPER WEDGE

PERFORAZIONE DEMOLIZIONE

IL PRINCIPIO DEL CUNEO SPACCAROCACCIA

Il SUPERWEDGE è stato sviluppato per la demolizione di roccia e cemento in modo economico e nel rispetto dell'ambiente.

I metodi tradizionali di demolizione prevedono l'utilizzo di esplosivi e martelli idraulici che creano sempre problematiche di rumore, vibrazioni e polveri.

Con l'utilizzo del SUPERWEDGE, che è basato sul principio del cuneo spacca roccia, si possono eliminare tutti questi problemi.

Il Superwedge è stato ideato per essere montato su escavatori.

Con il comando remotato è lo stesso operatore che controlla sia escavatore che Superwedge.

Il cuneo ed i due controconei vengono inseriti in fori già eseguiti con apposite macchine da perforazione e immediatamente si spinge il cuneo verso il fondo del foro creando così delle fratture nella roccia e/o cemento.

THE PRINCIPLE OF THE ROCK BREAKING WEDGE

SUPERWEDGE is designed to break rock and concrete economically and environmental-free.

The traditional methods are based on blasting and hydraulic breakers, but they bear serious problems of vibrations, noise and dust. The demolition by Superwedge can be free of them.

Superwedge has been developed to be used as an excavator attachment. Using it's remote control the operator can control both the excavator and the wedge.

The wedges and the counter wedges are inserted in pre drilled holes and the rock is demolished splitting the wedge down.



VANTAGGI PRINCIPALI MAIN FEATURES

- 1 Assenza totale di rumore e vibrazioni durante la rottura della roccia
Vibration and noise free during rock breaking
- 2 Facile sistema di comando
Easy and simple control
- 3 Utilizzo in tutte le condizioni climatiche
Possible to use in any weather conditions
- 4 Facile montaggio su escavatore
Easy to install on excavator
- 5 Grande sicurezza dell'operatore che può lavorare in cabina
Operator is very safe using the remote control in the cabin

MODELLI DISPONIBILI AVAILABLE MODELS SW: ideale per la demolizione in verticale/ ideal for vertical demolition TSW: ideale per la demolizione in galleria/ideal for tunnel demolition

METODOLOGIA DI SCAVO EXCAVATION PROCEDURE

PERFORAZIONE: DRILLING: effettuare fori di diametro 76 mm con apposite macchine to drill holes diam.76mm. In case of tunnel excavation is very important to drill extra affrontino lavori in galleria è necessario effettuare fori di grande diametro o tagli continui.

DEMOLIZIONE: REMOVE: utilizzare il SUPERWEDGE per frantumare la roccia e/o cemento.

SMARINO: rimuovere la roccia frantumata con l'utilizzo di un secondo escavatore dotato di benna o di martello idraulico secondario.



DEMOLIZIONE CEMENTO ARMATO REINFORCED CONCRETE DEMOLITION



SCAVO DI TUNNEL TUNNEL EXCAVATION



SBANCAMENTO ROCCIA OPEN ROCK EXCAVATION



SCAVO DI POZZO SHAFT EXCAVATION



SCAVO DI TRINCEA TRENCH EXCAVATION

12.4 Appendix D - Field mapping

Appendix D. 1 – Parameters for classification in the Q-system (NGI, 2013)

1 RQD (Rock Quality Designation)			RQD
A	Very poor	(> 27 joints per m ²)	0-25
B	Poor	(20-27 joints per m ²)	25-50
C	Fair	(13-19 joints per m ²)	50-75
D	Good	(8-12 joints per m ²)	75-90
E	Excellent	(0-7 joints per m ²)	90-100

Note: i) Where RQD is reported or measured as ≤ 10 (including 0) the value 10 is used to evaluate the Q-value
 ii) RQD-intervals of 5, i.e. 100, 95, 90, etc., are sufficiently accurate

2 Joint set number		J _n
A	Massive, no or few joints	0.5-1.0
B	One joint set	2
C	One joint set plus random joints	3
D	Two joint sets	4
E	Two joint sets plus random joints	6
F	Three joint sets	9
G	Three joint sets plus random joints	12
H	Four or more joint sets, random heavily jointed "sugar cube", etc	15
J	Crushed rock, earth like	20

Note: i) For tunnel intersections, use $3 \times J_n$
 ii) For portals, use $2 \times J_n$

3 Joint Roughness Number		J_r
a) Rock-wall contact, and b) Rock-wall contact before 10 cm of shear movement		
A	Discontinuous joints	4
B	Rough or irregular, undulating	3
C	Smooth, undulating	2
D	Slickensided, undulating	1.5
E	Rough, irregular, planar	1.5
F	Smooth, planar	1
G	Slickensided, planar	0.5
Note: i) Description refers to small scale features and intermediate scale features, in that order		
c) No rock-wall contact when sheared		
H	Zone containing clay minerals thick enough to prevent rock-wall contact when sheared	1
Note: ii) Add 1 if the mean spacing of the relevant joint set is greater than 3 m (dependent on the size of the underground opening) iii) $J_r = 0.5$ can be used for planar slickensided joints having lineations, provided the lineations are oriented in the estimated sliding direction		

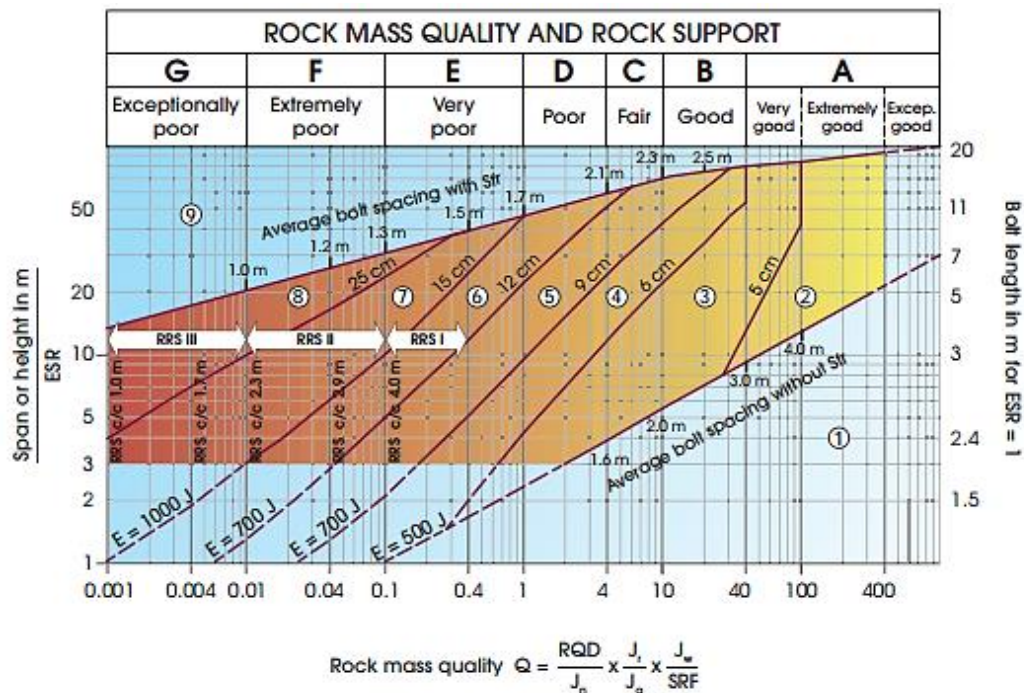
4 Joint Alteration Number		Φ_r approx.	J_a
a) Rock-wall contact (no mineral fillings, only coatings)			
A	Tightly healed, hard, non-softening, impermeable filling, i.e., quartz or epidote.		0.75
B	Unaltered joint walls, surface staining only.	25-35°	1
C	Slightly altered joint walls. Non-softening mineral coatings; sandy particles, clay-free disintegrated rock, etc.	25-30°	2
D	Silty or sandy clay coatings, small clay fraction (non-softening).	20-25°	3
E	Softening or low friction clay mineral coatings, i.e., kaolinite or mica. Also chlorite, talc gypsum, graphite, etc., and small quantities of swelling clays.	8-16°	4
b) Rock-wall contact before 10 cm shear (thin mineral fillings)			
F	Sandy particles, clay-free disintegrated rock, etc.	25-30°	4
G	Strongly over-consolidated, non-softening, clay mineral fillings (continuous, but <5mm thickness).	16-24°	6
H	Medium or low over-consolidation, softening, clay mineral fillings (continuous, but <5mm thickness).	12-16°	8
J	Swelling-clay fillings, i.e., montmorillonite (continuous, but <5mm thickness). Value of J_a depends on percent of swelling clay-size particles.	6-12°	8-12

c) No rock-wall contact when sheared (thick mineral fillings)			
K	Zones or bands of disintegrated or crushed rock. Strongly over-consolidated.	16-24°	6
L	Zones or bands of clay, disintegrated or crushed rock. Medium or low over-consolidation or softening fillings.	12-16°	8
M	Zones or bands of clay, disintegrated or crushed rock. Swelling clay. J_w depends on percent of swelling clay-size particles.	6-12°	8-12
N	Thick continuous zones or bands of clay. Strongly over-consolidated.	12-16°	10
O	Thick, continuous zones or bands of clay. Medium to low over-consolidation.	12-16°	13
P	Thick, continuous zones or bands with clay. Swelling clay. J_w depends on percent of swelling clay-size particles.	6-12°	13-20

5 Joint Water Reduction Factor		J_w
A	Dry excavations or minor inflow (humid or a few drips)	1.0
B	Medium inflow, occasional outwash of joint fillings (many drips/"rain")	0.66
C	Jet inflow or high pressure in competent rock with unfilled joints	0.5
D	Large inflow or high pressure, considerable outwash of joint fillings	0.33
E	Exceptionally high inflow or water pressure decaying with time. Causes outwash of material and perhaps cave in	0.2-0.1
F	Exceptionally high inflow or water pressure continuing without noticeable decay. Causes outwash of material and perhaps cave in	0.1-0.05
Note: i) Factors C to F are crude estimates. Increase J_w if the rock is drained or grouting is carried out ii) Special problems caused by ice formation are not considered		

6 Stress Reduction Factor			SRF
a) Weak zones intersecting the underground opening, which may cause loosening of rock mass			
A	Multiple occurrences of weak zones within a short section containing clay or chemically disintegrated, very loose surrounding rock (any depth), or long sections with incompetent (weak) rock (any depth). For squeezing, see 6L and 6M		10
B	Multiple shear zones within a short section in competent clay-free rock with loose surrounding rock (any depth)		7.5
C	Single weak zones with or without clay or chemical disintegrated rock (depth \leq 50m)		5
D	Loose, open joints, heavily jointed or "sugar cube", etc. (any depth)		5
E	Single weak zones with or without clay or chemical disintegrated rock (depth $>$ 50m)		2.5
Note: i) Reduce these values of SRF by 25-50% if the weak zones only influence but do not intersect the underground opening			
b) Competent, mainly massive rock, stress problems			SRF
		σ_c / σ_1	σ_θ / σ_c
F	Low stress, near surface, open joints	>200	<0.01
G	Medium stress, favourable stress condition	200-10	0.01-0.3
H	High stress, very tight structure. Usually favourable to stability. May also be unfavourable to stability dependent on the orientation of stresses compared to jointing/weakness planes*	10-5	0.3-0.4
J	Moderate spalling and/or slabbing after $>$ 1 hour in massive rock	5-3	0.5-0.65
K	Spalling or rock burst after a few minutes in massive rock	3-2	0.65-1
L	Heavy rock burst and immediate dynamic deformation in massive rock	<2	>1
Note: ii) For strongly anisotropic virgin stress field (if measured): when $5 \leq \sigma_1 / \sigma_3 \leq 10$, reduce σ_c to $0.75 \sigma_c$. When $\sigma_1 / \sigma_3 > 10$, reduce σ_c to $0.5 \sigma_c$, where σ_c = unconfined compression strength, σ_1 and σ_3 are the major and minor principal stresses, and σ_θ = maximum tangential stress (estimated from elastic theory)			
iii) When the depth of the crown below the surface is less than the span; suggest SRF increase from 2.5 to 5 for such cases (see F)			
c) Squeezing rock: plastic deformation in incompetent rock under the influence of high pressure			SRF
		σ_θ / σ_c	
M	Mild squeezing rock pressure	1-5	5-10
N	Heavy squeezing rock pressure	>5	10-20
Note: iv) Determination of squeezing rock conditions must be made according to relevant literature (i.e. Singh et al., 1992 and Bhasin and Grimstad, 1996)			
d) Swelling rock: chemical swelling activity depending on the presence of water			SRF
O	Mild swelling rock pressure		5-10
P	Heavy swelling rock pressure		10-15

Appendix D. 2 – Rock mass classification and support scheme for Q-system (NGI, 2013)



Support categories

- ① Unsupported or spot bolting
- ② Spot bolting, **SB**
- ③ Systematic bolting, fibre reinforced sprayed concrete, 5-6 cm, **B+Sfr**
- ④ Fibre reinforced sprayed concrete and bolting, 6-9 cm, **Sfr (E500)+B**
- ⑤ Fibre reinforced sprayed concrete and bolting, 9-12 cm, **Sfr (E700)+B**
- ⑥ Fibre reinforced sprayed concrete and bolting, 12-15 cm + reinforced ribs of sprayed concrete and bolting, **Sfr (E700)+RRS I +B**
- ⑦ Fibre reinforced sprayed concrete >15 cm + reinforced ribs of sprayed concrete and bolting, **Sfr (E1000)+RRS II+B**
- ⑧ Cast concrete lining, **CCA** or **Sfr (E1000)+RRS III+B**
- ⑨ Special evaluation

Bolts spacing is mainly based on Ø20 mm

E = Energy absorption in fibre reinforced sprayed concrete

ESR = Excavation Support Ratio

Areas with dashed lines have no empirical data

RRS - spacing related to Q-value

- I** **Si30/6 Ø16 - Ø20 (span 10m)**
D40/6+2 Ø16-20 (span 20m)
- II** **Si35/6 Ø16-20 (span 5m)**
D45/6+2 Ø16-20 (span 10m)
D55/6+4 Ø20 (span 20m)
- III** **D40/6+4 Ø16-20 (span 5m)**
D55/6+4 Ø20 (span 10 m)
D70/6+6 Ø20 (span 20m)







Si30/6 = Single layer of 6 rebars, 30 cm thickness of sprayed concrete

D = Double layer of rebars

Ø16 = Rebar diameter is 16 mm

c/c = RSS spacing, centre - centre

Appendix D. 3 GSI classification scheme (Hoek, Marinos, & Marinos, 2005)

<p>GEOLOGICAL STRENGTH INDEX</p> <p>From the description of structure and surface conditions of the rock mass, pick an appropriate box in this chart. Estimate the average value of the Geological Strength Index (GSI) from the contours. Do not attempt to be too precise. Quoting a range of GSI from 36 to 42 is more realistic than stating that GSI = 38. It is also important to recognize that the Hoek-Brown criterion should only be applied to rock masses where the size of the individual blocks or pieces is small compared with the size of the excavation under consideration. When individual block sizes are more than approximately one quarter of the excavation dimension, failure will generally be structurally controlled and the Hoek-Brown criterion should not be used.</p> <p>STRUCTURE</p>		<p>SURFACE CONDITIONS</p> <p>VERY GOOD Very rough, fresh unweathered surfaces</p> <p>GOOD Rough, slightly weathered, iron stained surfaces</p> <p>FAIR Smooth, moderately weathered and altered surfaces</p> <p>POOR Slickensided, highly weathered surfaces with coatings or fillings of angular fragments</p> <p>VERY POOR Slickensided, highly weathered surfaces with soft clay coatings or fillings</p> <p>DECREASING SURFACE QUALITY →</p>				
 <p>INTACT OR MASSIVE – intact rock specimens or massive in situ rock with very few widely spaced discontinuities</p>	90	80	N/A	N/A	N/A	
 <p>BLOCKY - very well interlocked undisturbed rock mass consisting of cubical blocks formed by three orthogonal discontinuity sets</p>	70	60				
 <p>VERY BLOCKY - interlocked, partially disturbed rock mass with multifaceted angular blocks formed by four or more discontinuity sets</p>	50					
 <p>BLOCKY/DISTURBED - folded and/or faulted with angular blocks formed by many intersecting discontinuity sets</p>	40					
 <p>DISINTEGRATED - poorly interlocked, heavily broken rock mass with a mixture of angular and rounded rock pieces</p>	30					
 <p>FOLIATED/LAMINATED – Folded and tectonically sheared foliated rocks. Schistosity prevails over any other discontinuity set, resulting in complete lack of blockiness</p>	N/A	20		10	5	

Appendix D. 4 Estimated parameters from field mapping

<i>Location</i>	<i>A</i>	<i>B</i>	<i>C</i>	<i>D</i>	<i>E</i>
<i>RQD</i>	80	75	90	90	90
<i>J_n</i>	4	4	4	6	9
<i>J_r</i>	2	1,5	1,5	3	4
<i>J_a</i>	1	1	1	1	1
<i>J_w</i>	1	1	1	1	1
<i>SRF</i>	1	1	2,5	2,5	2,5
<i>Q-value</i>	40	28,1	13,5	18	16

Appendix D. 5 - Joint registrations

Joint set	1	1	1	-	2	2	2	2	3	3
Strike (°)	80	85	85	20	120	108	115	120	155	145
Dip (°)	82	73	63	60	78	75	76	80	25	40
Dip direction	S	S	S	SE	NE	SW	SW	NE	SW	SW

12.5 Appendix E - Laboratory testing

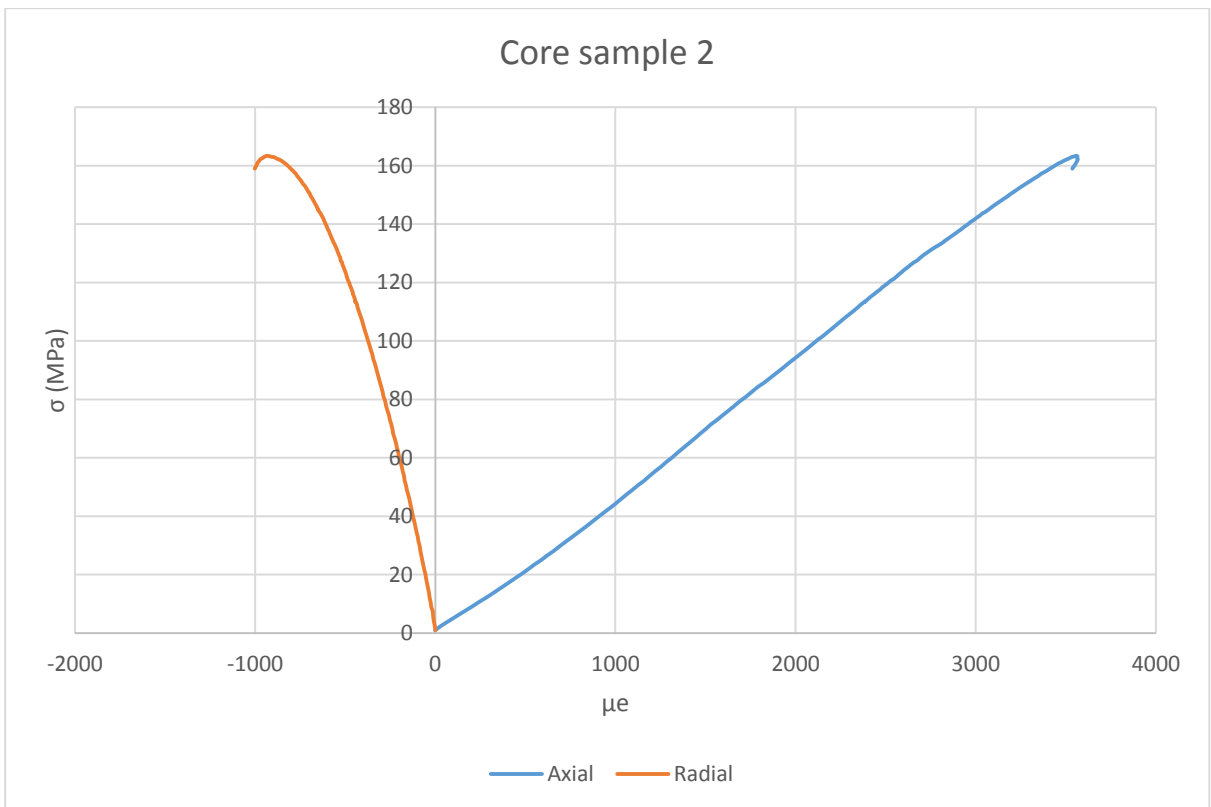
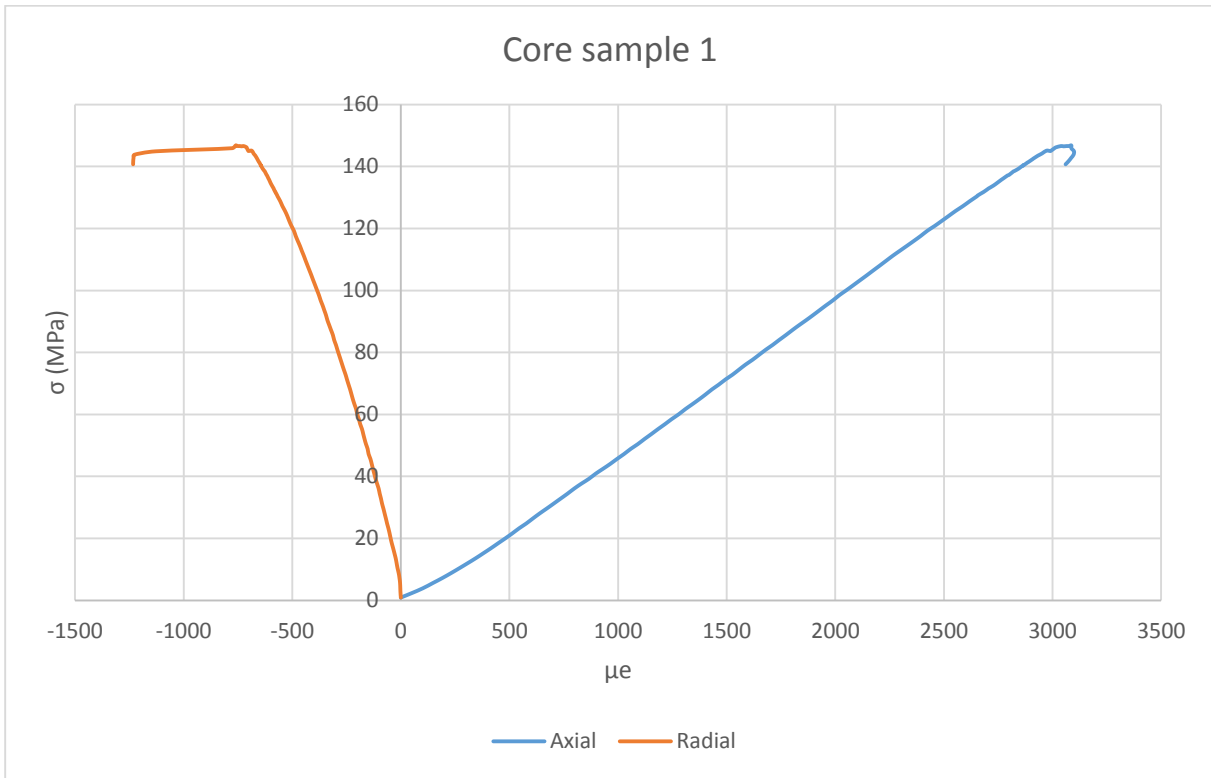
Appendix E. 1 – Rock sample 1 after drilling

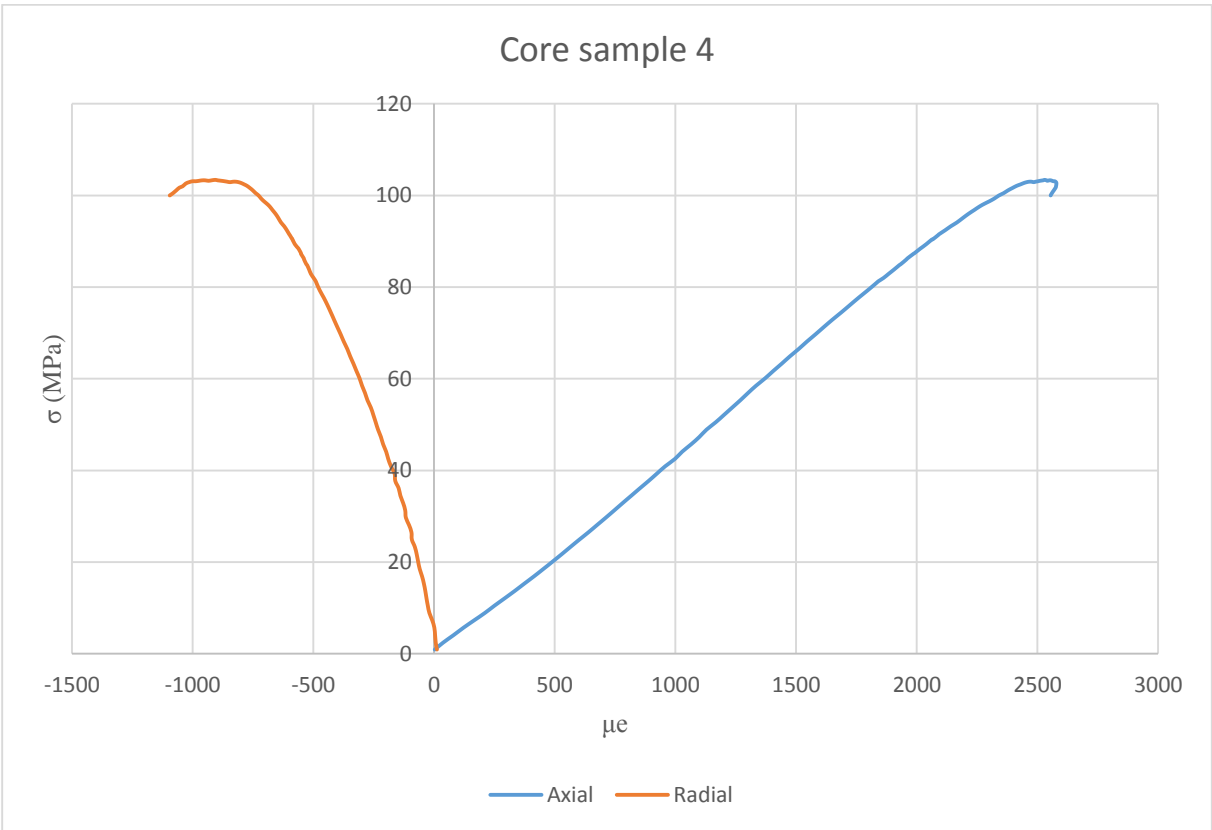
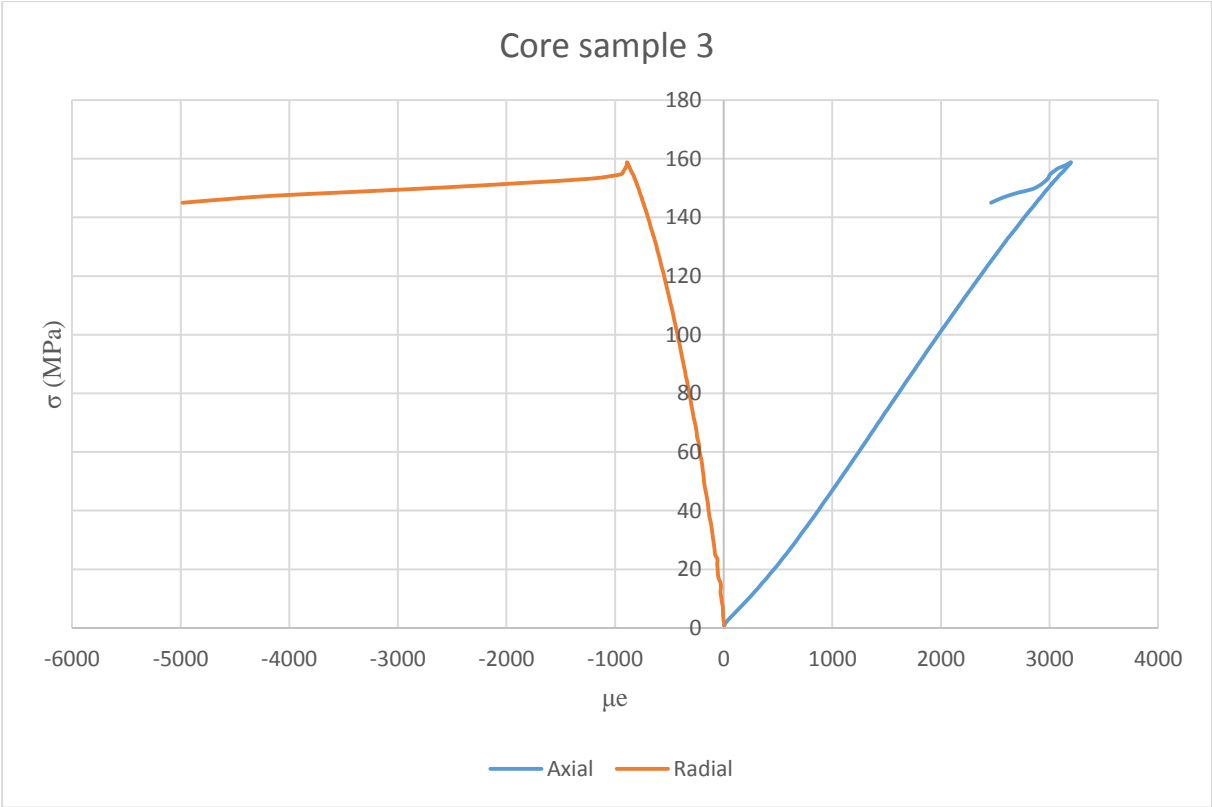


Appendix E. 2 - Rock sample 2 after drilling



Appendix E. 3 - Stress-strain curves from UCS testing





Appendix E. 4 - Failure modes for core sample 1 to 4



12.6 Appendix F - Numerical analysis

12.6.1 - Analysis assumptions






Appendix F. 1 - scheme for m_i classification (Hoek E. , 2007)

Rock type	Class	Group	Texture			
			Coarse	Medium	Fine	Very fine
SEDIMENTARY	Clastic		Conglomerates* (21 ± 3)	Sandstones 17 ± 4	Siltstones 7 ± 2	Claystones 4 ± 2
			Breccias (19 ± 5)		Greywackes (18 ± 3)	Shales (6 ± 2) Marls (7 ± 2)
	Non-Clastic	Carbonates	Crystalline Limestone (12 ± 3)	Sparitic Limestones (10 ± 2)	Micritic Limestones (9 ± 2)	Dolomites (9 ± 3)
		Evaporites		Gypsum 8 ± 2	Anhydrite 12 ± 2	
	Organic				Chalk 7 ± 2	
METAMORPHIC	Non Foliated		Marble 9 ± 3	Hornfels (19 ± 4) Metasandstone (19 ± 3)	Quartzites 20 ± 3	
	Slightly foliated		Migmatite (29 ± 3)	Amphibolites 26 ± 6		
	Foliated**		Gneiss 28 ± 5	Schists 12 ± 3	Phyllites (7 ± 3)	Slates 7 ± 4
IGNEOUS	Plutonic	Light	Granite 32 ± 3 Granodiorite (29 ± 3)	Diorite 25 ± 5		
		Dark	Gabbro 27 ± 3 Norite 20 ± 5	Dolerite (16 ± 5)		
	Hypabyssal		Porphyries (20 ± 5)		Diabase (15 ± 5)	Peridotite (25 ± 5)
	Volcanic	Lava		Rhyolite (25 ± 5) Andesite 25 ± 5	Dacite (25 ± 3) Basalt (25 ± 5)	Obsidian (19 ± 3)
		Pyroclastic	Agglomerate (19 ± 3)	Breccia (19 ± 5)	Tuff (13 ± 5)	

* Conglomerates and breccias may present a wide range of m_i values depending on the nature of the cementing material and the degree of cementation, so they may range from values similar to sandstone to values used for fine grained sediments.

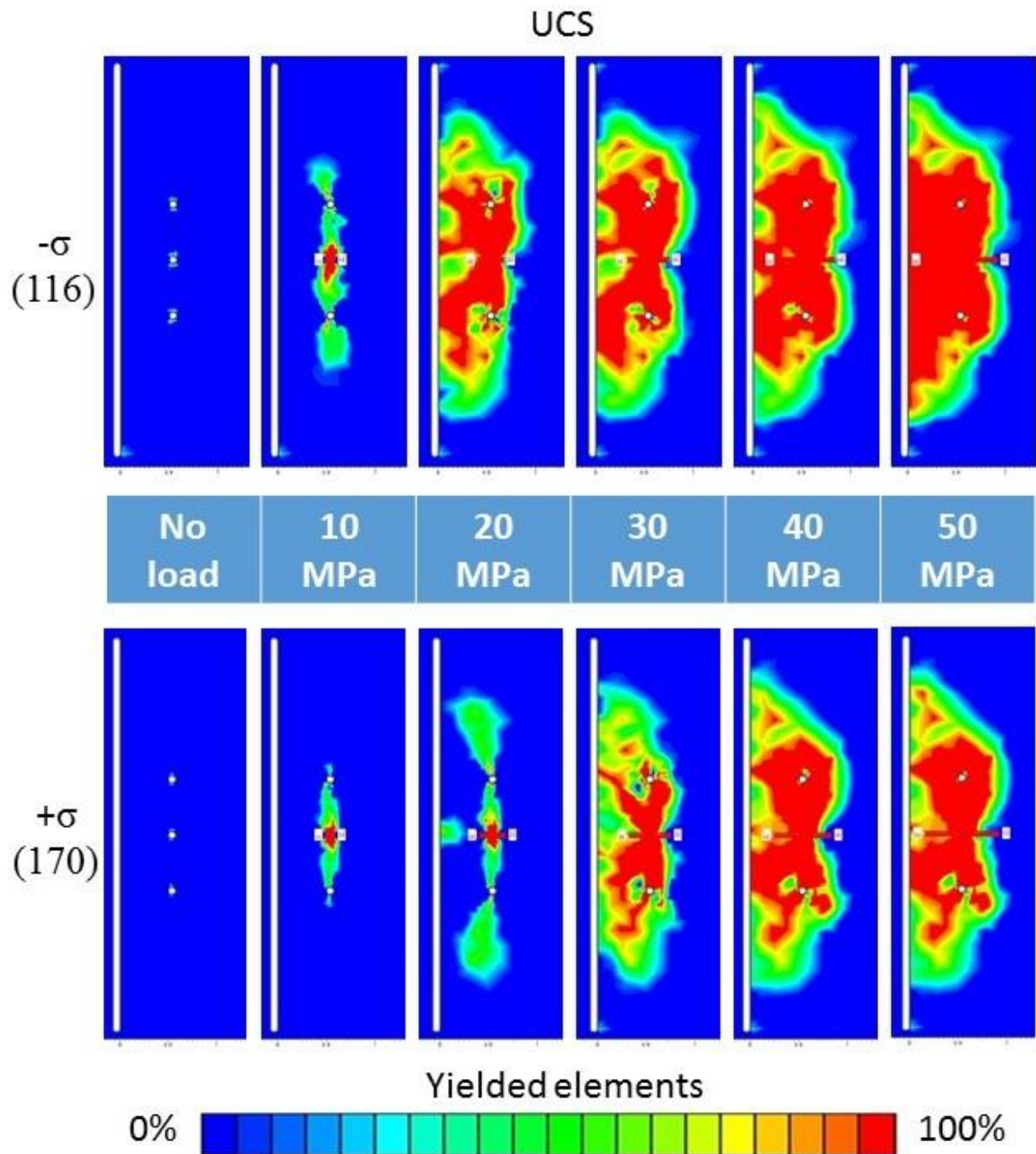
** These values are for intact rock specimens tested normal to bedding or foliation. The value of m_i will be significantly different if failure occurs along a weakness plane.

Appendix F. 2 - Scheme for estimating disturbance factor, D (Hoek E. , 2007)

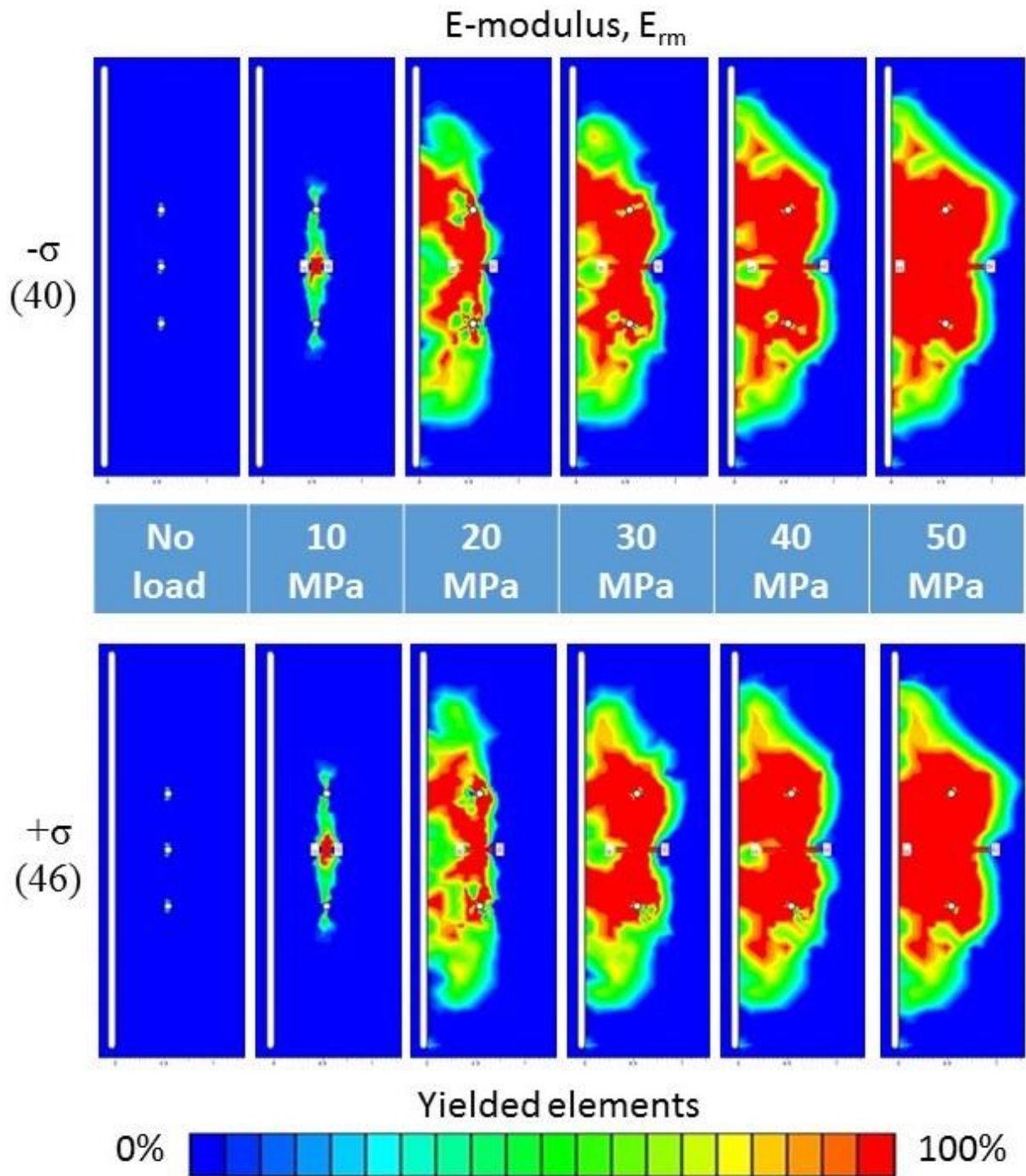
Appearance of rock mass	Description of rock mass	Suggested value of D
	Excellent quality controlled blasting or excavation by Tunnel Boring Machine results in minimal disturbance to the confined rock mass surrounding a tunnel.	D = 0
	Mechanical or hand excavation in poor quality rock masses (no blasting) results in minimal disturbance to the surrounding rock mass. Where squeezing problems result in significant floor heave, disturbance can be severe unless a temporary invert, as shown in the photograph, is placed.	D = 0 D = 0.5 No invert
	Very poor quality blasting in a hard rock tunnel results in severe local damage, extending 2 or 3 m, in the surrounding rock mass.	D = 0.8
	Small scale blasting in civil engineering slopes results in modest rock mass damage, particularly if controlled blasting is used as shown on the left hand side of the photograph. However, stress relief results in some disturbance.	D = 0.7 Good blasting D = 1.0 Poor blasting
	Very large open pit mine slopes suffer significant disturbance due to heavy production blasting and also due to stress relief from overburden removal. In some softer rocks excavation can be carried out by ripping and dozing and the degree of damage to the slopes is less.	D = 1.0 Production blasting D = 0.7 Mechanical excavation

12.6.2 - Individual rock parameter sensitivity

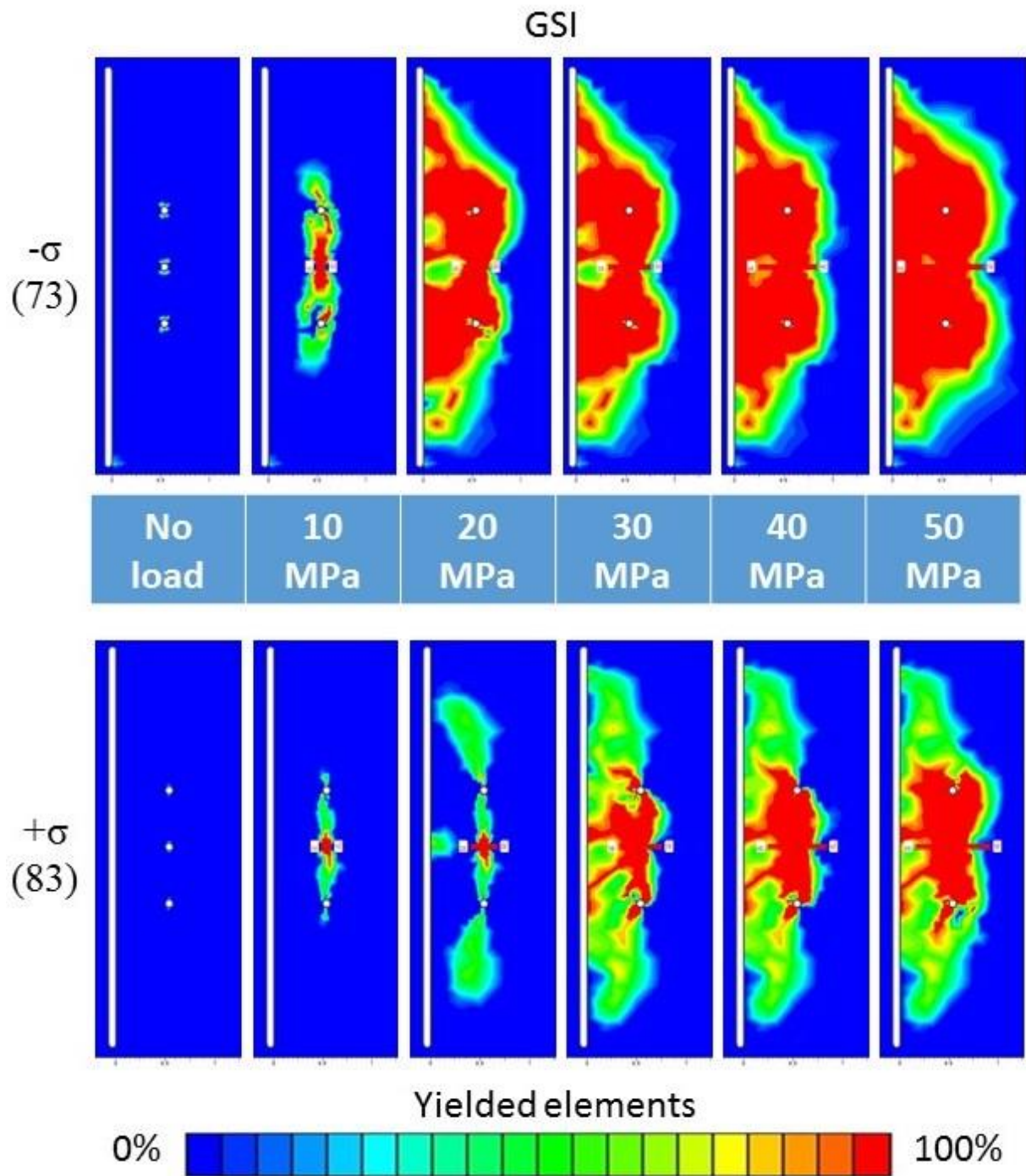
Appendix F. 3 – UCS fracture propagation



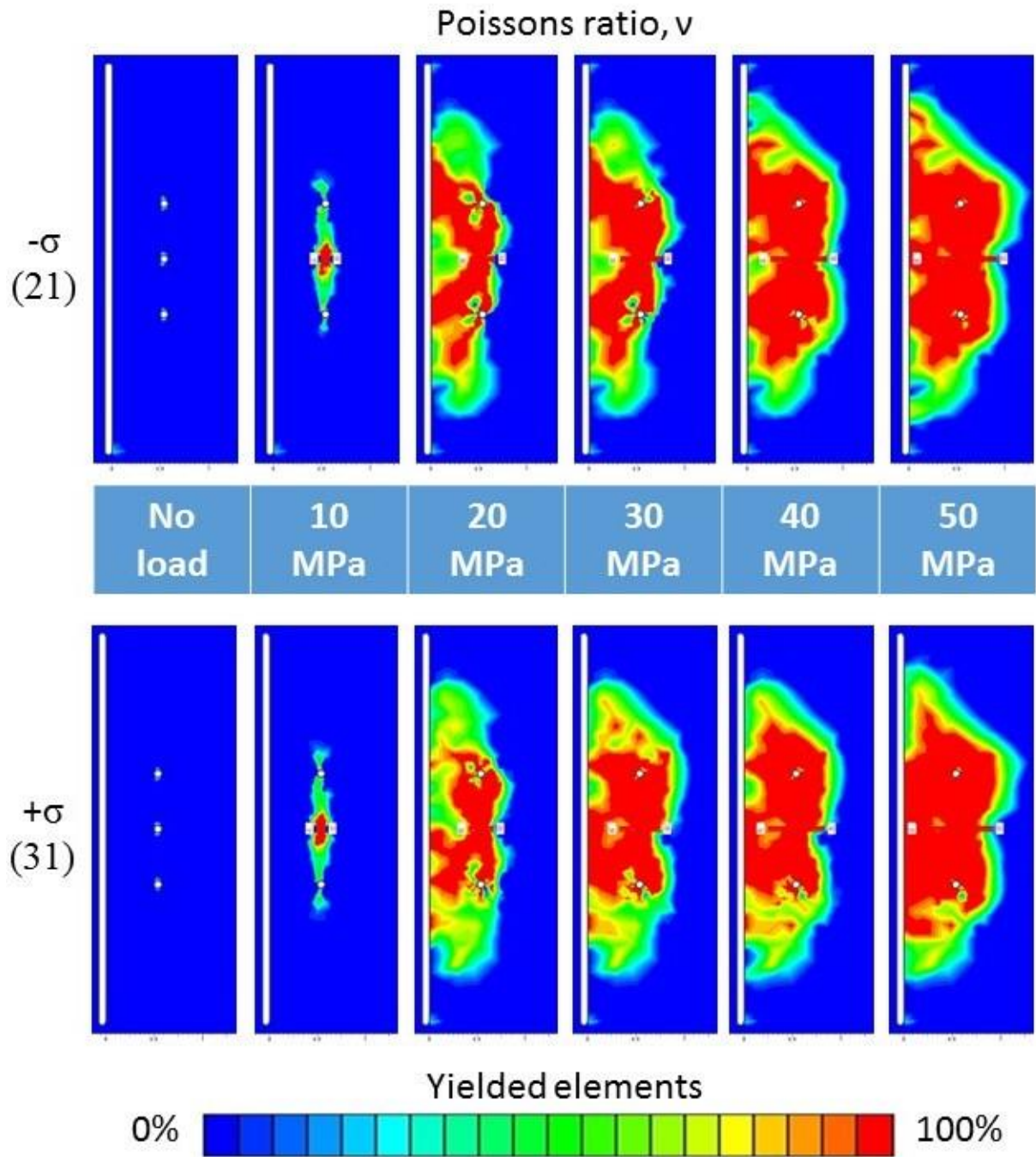
Appendix F. 4 - E-module fracture propagation



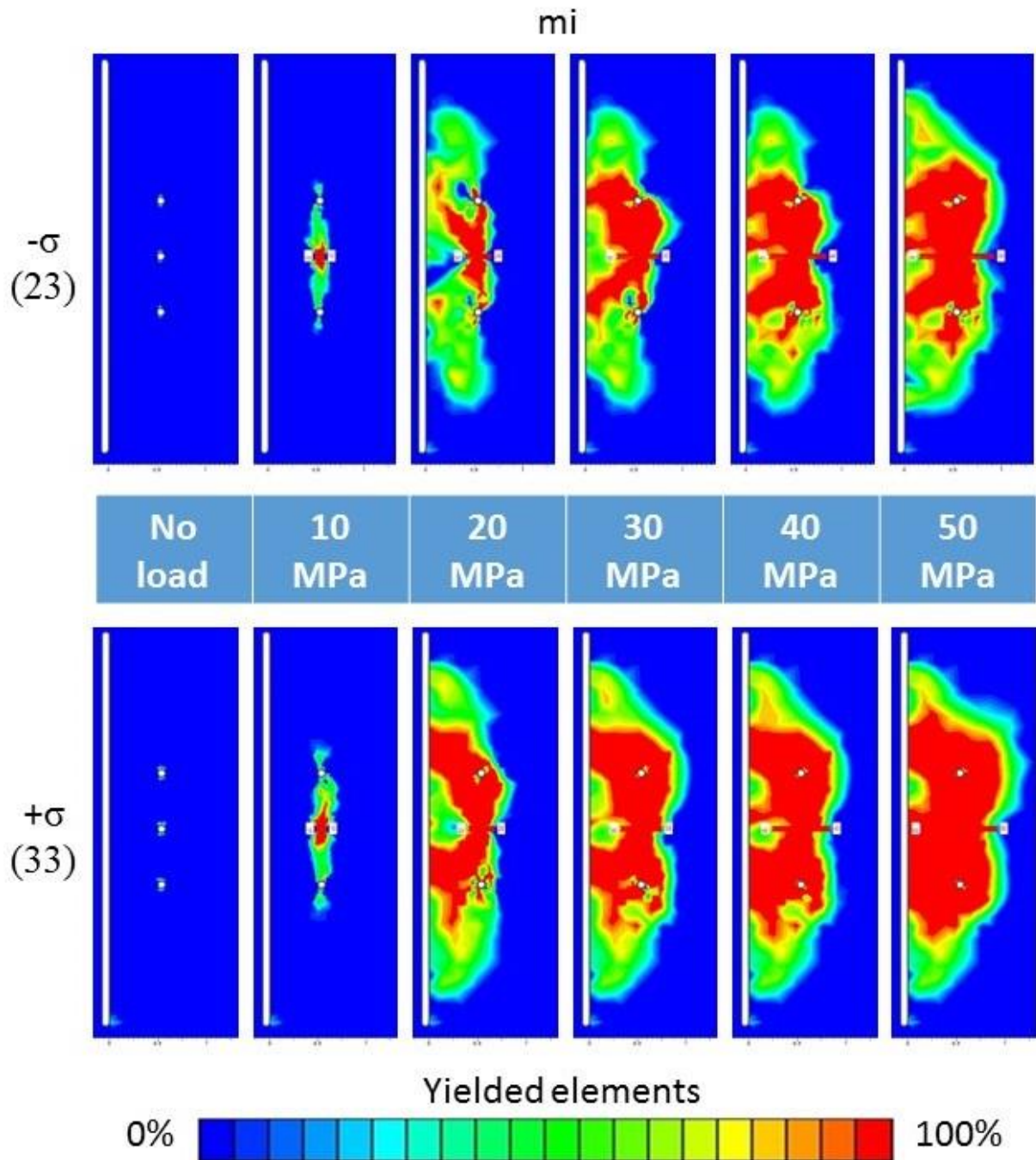
Appendix F. 5 - GSI fracture propagation



Appendix F. 6 - Poisson's ratio fracture propagation



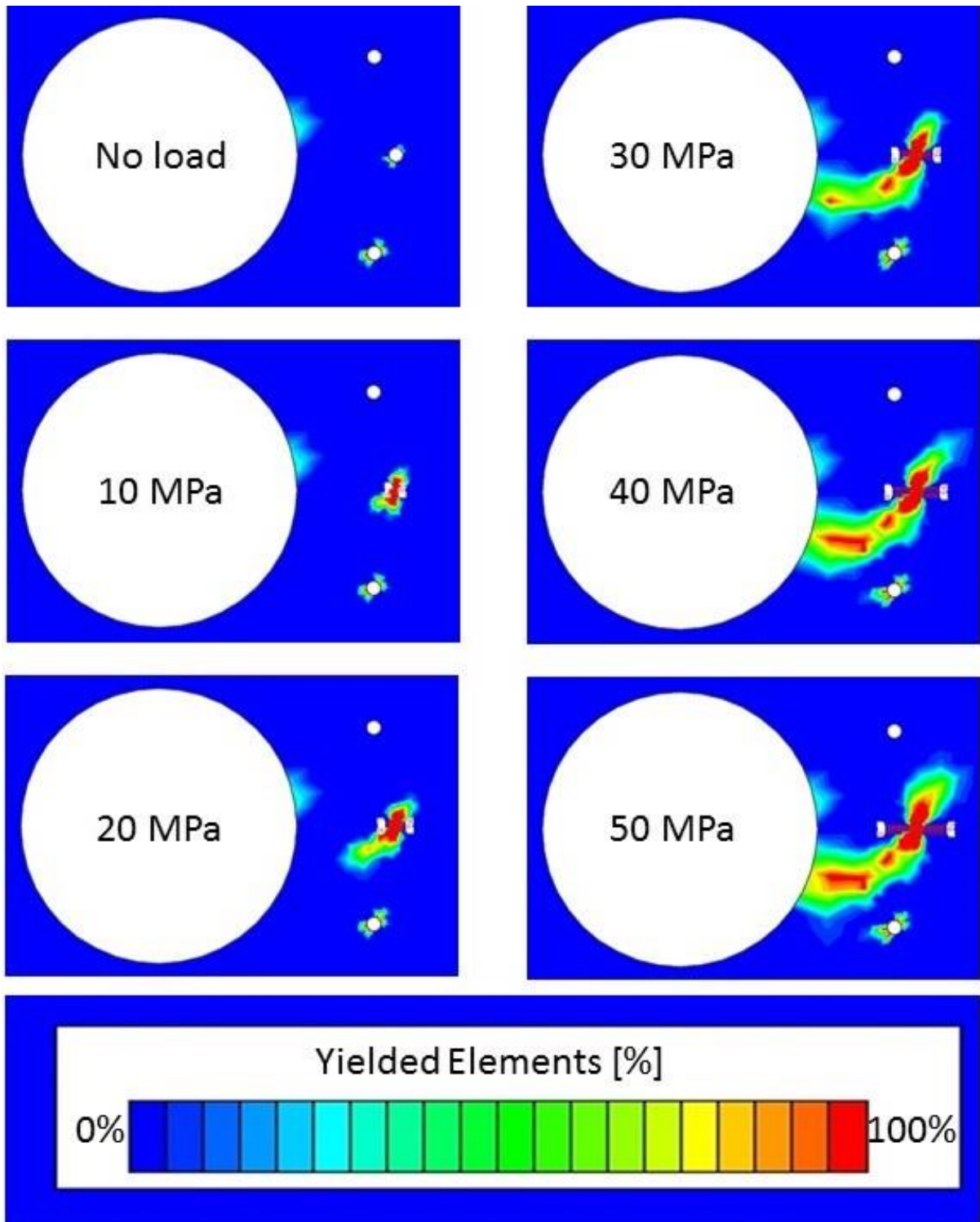
Appendix F. 7 - mi fracture propagation



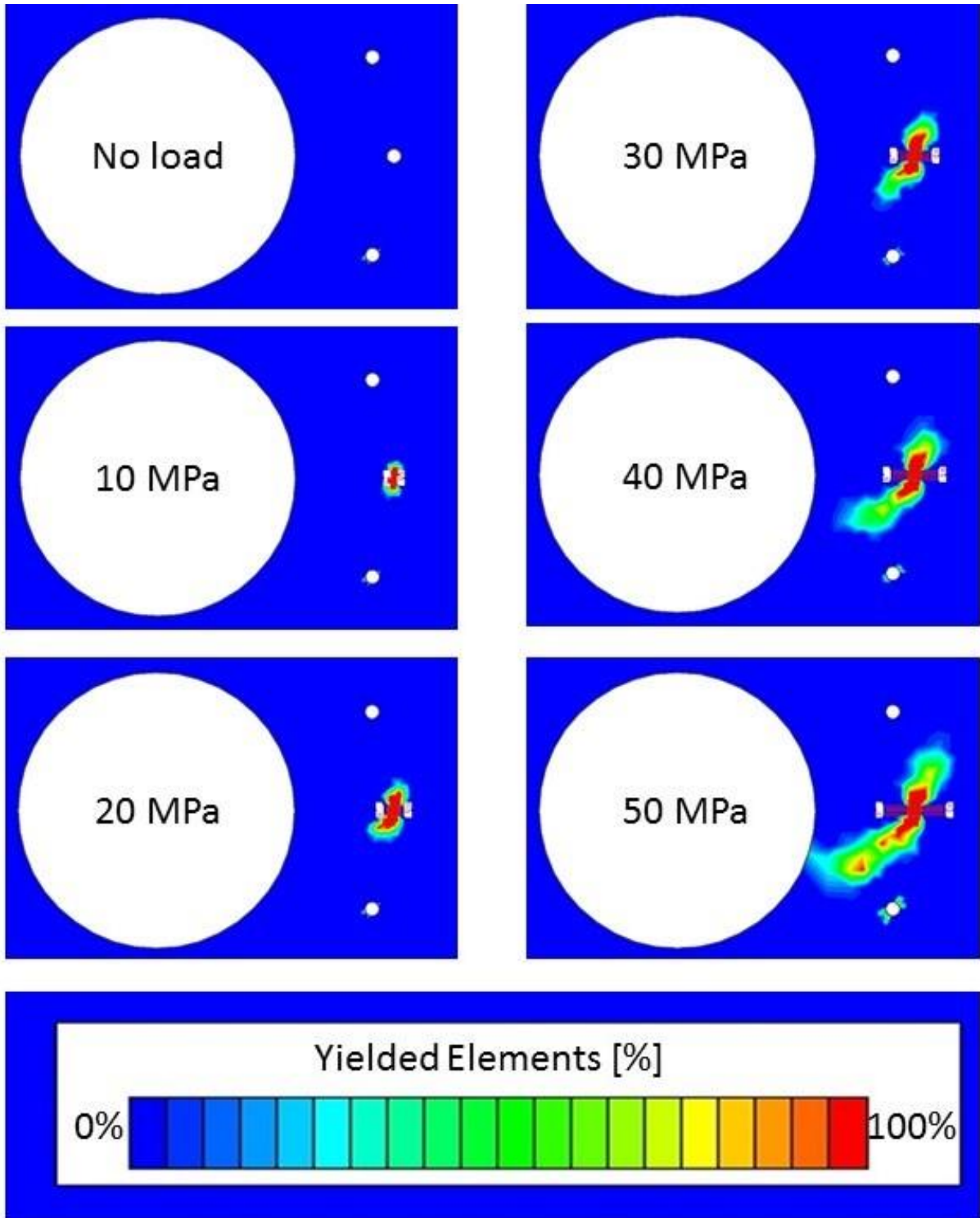
12.6.3 - Individual stress sensitivity analysis

Sigma 1:

Appendix F. 8 - Sigma 1 = 11.8 MPa

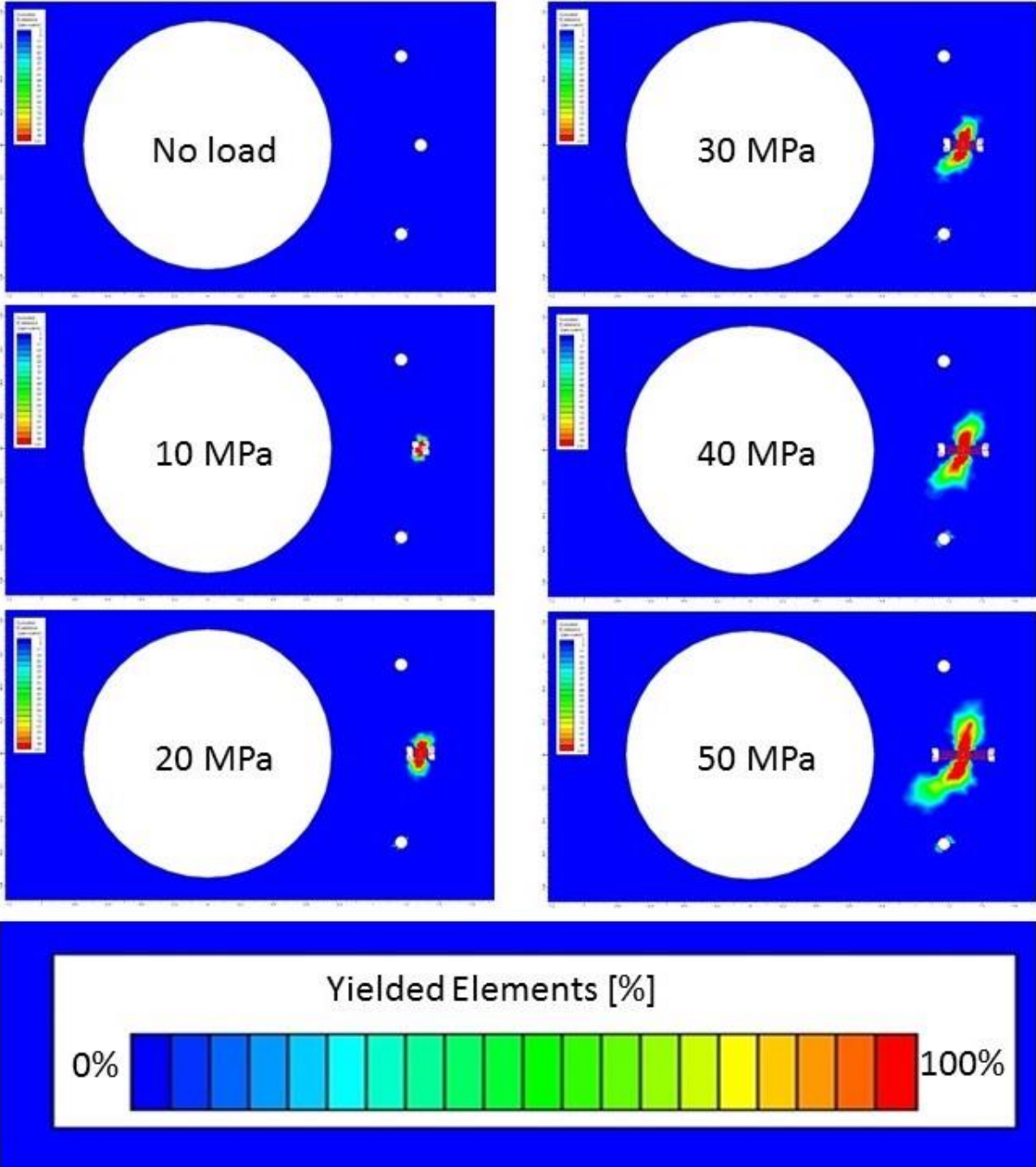


Appendix F. 9 - $\sigma_1 = 8 \text{ MPa}$

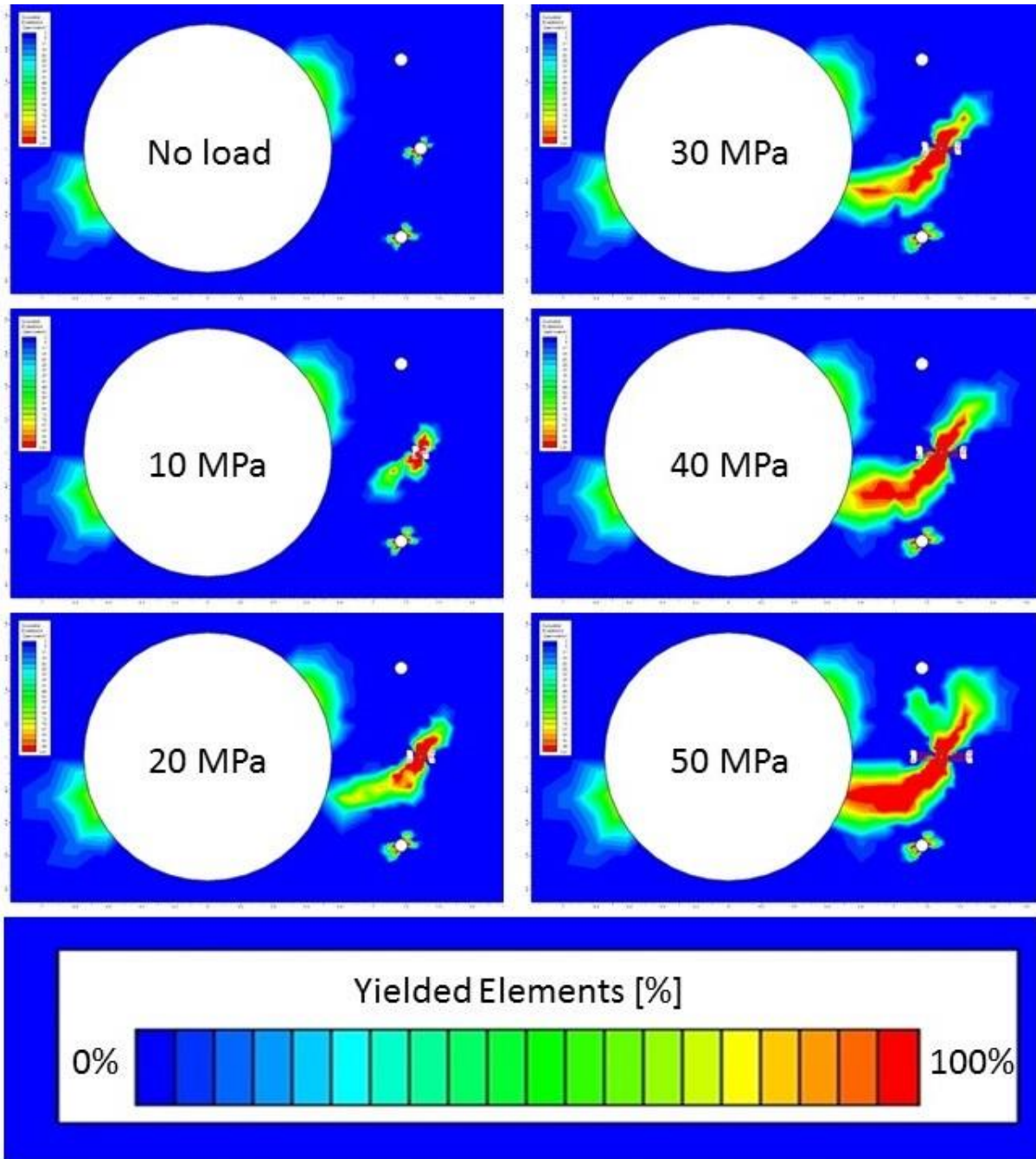


Sigma 3:

Appendix F. 10 - Sigma 3 = 4.2 MPa

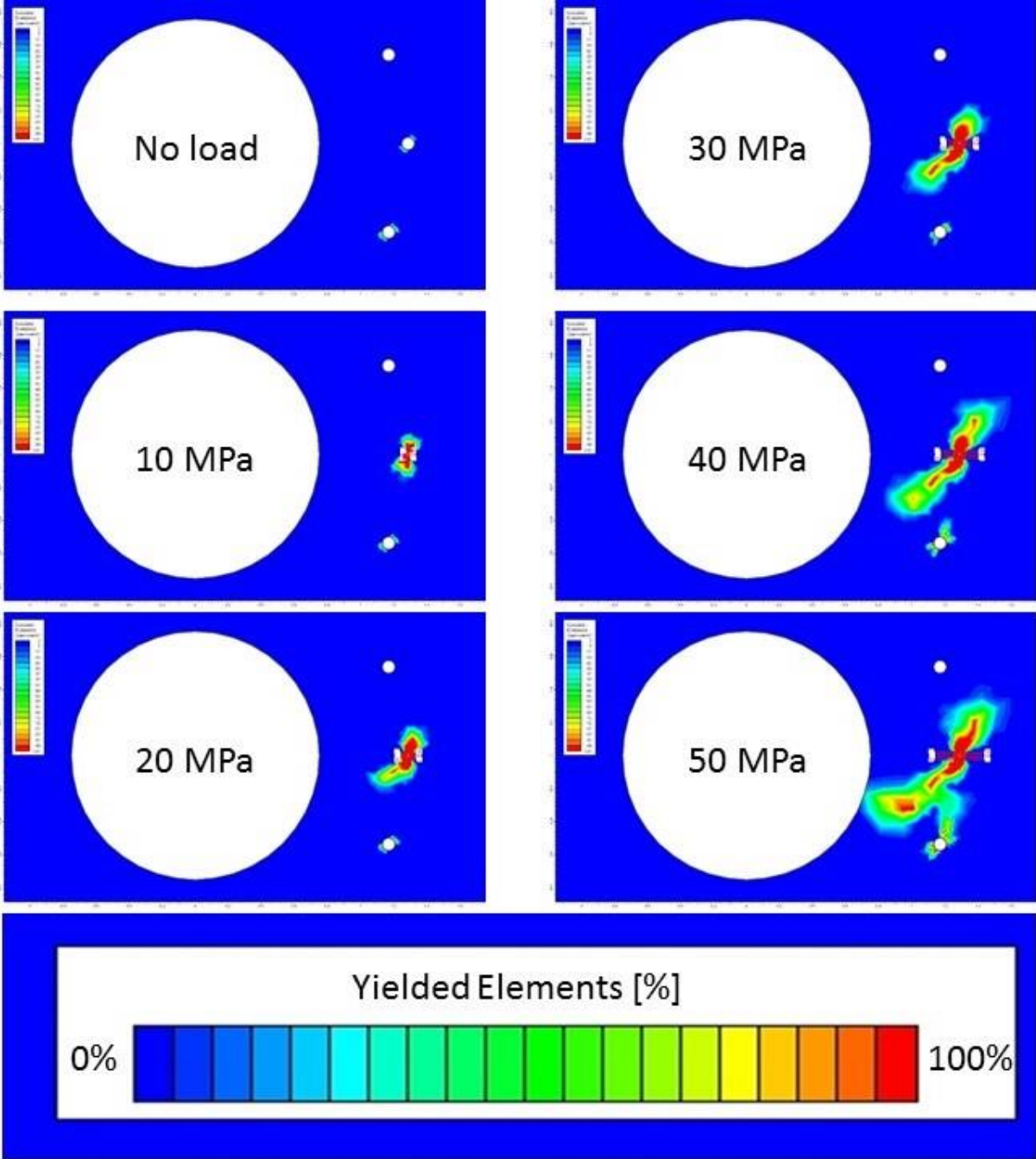


Appendix F. 11 - $\sigma_3 = 2.2 \text{ MPa}$



Angle between Sigma 1 and horizontal:

Appendix F. 12 - Angle = 29°



Appendix F. 13 - Angle = 19°

